CHARACTERIZATION OF THE FXYD PROTEIN FAMILY

IN THE REGULATION OF INSULIN EXOCYTOSIS

APPROVED BY SUPERVISORY COMMITTEE

Michael Roth, Ph.D. (Chair)_____

Melanie Cobb, Ph.D. _____

Kosaku Uyeda, Ph.D. _____

Christopher J. Rhodes, Ph.D. _____

DEDICATION/ACKNOWLEDGMENTS

This dissertation is dedicated to my husband, Brian, whose love and support provided me the strength and perseverance I needed to achieve my goals; and to my son, Ryne, whose innocence and happiness taught me the beauty of life and the patience to live it.

Throughout my academic experiences, there are several people who deserve credit and appreciation for their role in making this dissertation possible. First and foremost, my mentor, Dr. Christopher J. Rhodes for guiding, teaching, and inspiring the research in this dissertation. Dr. James C. Hu, who inspired my initial interest in research, suggested my pursuit of a doctoral degree. My dissertation committee members: Dr. Christopher Newgard, Dr. Melanie Cobb, Dr. Michael Roth, and Dr. Kosaku Uyeda, who believed in my research and kept me focused. All the postdoctoral fellows and technicians in the Rhodes' laboratory provided me with technical advice and friendship throughout my experiences in the lab, particularly Dr. Barton Wicksteed and Jill McCuaig for their invaluable assistance obtaining adenoviral reagents. Assistance in formatting this dissertation manuscript was possible thanks to the assistance of Cynthia Cousen-Jacobs. Dr. J. Michael Edwardson, Dr.

Robert Chow, and Dr. Louis H. Philipson collaborated on experiments and provided insightful discussion. Reagents, including INS-1 [832/13] cells from Dr. Christopher Newgard, secreted alkaline phosphatase adenovirus from Dr. Philippe Halban, and anti-syncollin antibodies from Dr. J. Michael Edwardson were an integral part of this research.

This dissertation would not be possible without the support, camaraderie, and assistance of friends and family. To my parents, Melvin and Carol Shilling, who raised an independent, driven child, and never doubted my abilities. To my brother, Randy Shilling, who always pushed me to excel, and his wife, Kimberely, whose perseverance battling stomach cancer gave me the strength I needed to finish my thesis. To my husband's family especially, Kervyn, Barbara, Greg, Sean, and Krista Hays, whose love and acceptance allowed me to believe in myself. Dr. Jennifer Klem, Dr. Isabelle Briaud, Jill McCuaig, and Dr. Deirdre Brekken listened and advised me throughout my dissertation and remain some of my dearest friends.

Each and everyone listed above and others who have not been named directly, but whose friendship remains important to me, deserve my gratitude and my admiration for supporting me through this portion of my life and career.

CHARACTERIZATION OF THE FXYD PROTEIN FAMILY IN THE REGULATION OF INSULIN EXOCYTOSIS

by

LORI BETH HAYS

DISSERTATION

Presented to the Faculty of the Graduate School of Biomedical Sciences

The University of Texas Southwestern Medical Center at Dallas

In Partial Fulfillment of the Requirements

For the Degree of

DOCTOR OF PHILOSOPHY

The University of Texas Southwestern Medical Center at Dallas

Dallas, Texas

February, 2004

CHARACTERIZATION OF THE FXYD PROTEIN FAMILY

IN THE REGULATION OF INSULIN EXOCYTOSIS

Publication No. _____

Lori Beth Hays, Ph.D.

The University of Texas Southwestern Medical Center at Dallas, 2004

Supervising Professor: Christopher J. Rhodes, Ph.D.

Insulin exocytosis is a complex, regulated process involving numerous exocytotic proteins to coordinate the release of insulin. Syncollin has been implicated in zymogen granule exocytosis in acinar cells. It was hypothesized that either syncollin or a 'syncollin-like' protein may be expressed in β-cells and influence insulin exocytosis. Adenoviral-mediated expression of either long or short forms of syncollin in isolated islets and INS-1 cells showed both forms underwent N-terminal signal peptide cleavage to yield the same 14kD mature protein. Immunofluorescence revealed that adenovirally-expressed syncollin was specifically targeted to the ß-granule lumen. In perifused islets, syncollin expression

significantly inhibited first-phase glucose-induced insulin secretion compared to AdV-GFP infected islets. GLP-1 and glyburide potentiation of insulin secretion was inhibited; whereas constitutive secretion and insulin content were normal in syncollin-infected islets indicating syncollin-mediated inhibition of insulin secretion was not due to inadequate insulin production or secondary stimulus-coupling signals. Thus, syncollin likely inhibited the distal stages of insulin exocytosis providing the first evidence that an intragranular protein is capable of influencing regulated insulin secretion.

Syncollin fluorescent fusion proteins were localized to ß-granules, but did not influence insulin secretion implicating these chimeras as ß-granule specific markers for emerging imaging technology. Real-time confocal microscopy demonstrated syncollin-GFP could be used to examine spatiotemporal dynamics of exocytosis. Furthermore, consecutive infection of syncollin-GFP and syncollin-dsRFP labeled distinct pools of β-granules.

Expression of syncollin was not identified in β-cells; however, a 10Kd 'syncollin-like' protein was expressed, which when sequenced corresponded to FXYD6. Comparison of syncollin and FXYD6 protein structure revealed several conserved domains, indicating syncollin is likely a pseudo-FXYD family member. FXYD6 was the only FXYD protein endogenously expressed in β-cells, which localized to distinct regions of the plasma membrane. Overexpression of FXYD6-Myc enhanced β-granule transport to distinct regions of the plasma membrane that also expressed FXYD6; however, there was no significant effect on glucose-stimulated insulin secretion in isolated islets. SiRNA-mediated reduction of FXYD6 resulted in no obvious changes in β-granule distribution; however, β-granule movement during glucose stimulation was erratic and misdirected. These data implicate

FXYD6 as a molecular beacon on the plasma membrane guiding β-granules to the active site of exocytosis.

TABLE OF CONTENTS

PRIOR PUBLICATIONS

Hays LB, Wicksteed B, Wang Y, McCuaig JF, Philipson LH, Edwardson JM, Rhodes CJ.

An Intragranular Factor Influences Regulated Insulin Exocytosis in Pancreatic β-cells.

In preparation.

Ma L, Bindokas VP, Kuznetsov A, Rhodes C, **Hays L**, Edwardson JM, Ueda K, Steiner DF, Philipson LH.

Optical discrimination of exocytosis and endocytosis in insulin secreting cells.

Submitted to J. Cell Biology

Wäsle B., **Hays LB**, Rhodes CJ, Edwardson JM.

Syncollin inhibits regulated ACTH secretion from AtT-20 cells through a reduction in the secretory vesicle population.

Biochem J. 2004 Mar 24 [Epub ahead of print]

Yaekura K, Julyan R, Wicksteed BL, **Hays LB**, Alarcon C, Sommers S, Poitout V, Baskin DG, Wang Y, Philipson LH, Rhodes CJ.

Insulin secretory deficiency and glucose intolerance in Rab3A null mice.

J Biol Chem. 2003 Mar 14:278(11): 9715-21.

Donelan MJ, Morfini G, Julyan R, Sommers S, **Hays L**, Kajio H, Briaud I, Easom RA, Molkentin JD, Brady ST, Rhodes CJ.

Ca2+-dependent dephosphorylation of kinesin heavy chain on beta-granules in pancreatic β-cells. Implications for regulated β-granule transport and insulin exocytosis.

J Biol Chem. 2002 Jul 5; 277(27):24232-42.

Hays LB, Chen YS, Hu JC.

Two-hybrid system for characterization of protein-protein interactions in *E. coli*.

Biotechniques. 2000 Aug; 29(2):288-90, 292, 294 passim.

LIST OF FIGURES

LIST OF TABLES

LIST OF APPENDICES

LIST OF ABBREVIATIONS

ACTH– ADRENOCORTICOTROPHIC HORMONE

ADV– ADENOVIRUS

AMP– ADENOSINE MONOPHOSPHATE

ARG– ARGININE

ATP– ADENOSINE TRIPHOSPHATE

ATG– ADENONINE, THYMADINE, AND GUANINE (START SITE)

AUG– ADENONINE, URACIL, AND GUANINE (START CODON)

BSA– BOVINE SERUM ALBUMIN

CaM– CALMODULIN

cAMP– CYCLIC ADENOSINE MONOPHOSPHATE

cAMP-GEF–cAMP GUANINE EXCHANGE FACTOR

cDNA– COMPLEMENTARY DEOXYRIBONUCLEIC ACID

C-PEPTIDE – CONNECTING PEPTIDE

CP-E– CARBOXYPEPTIDASE E

CP-H– CARBOXYPEPTIDASE H

CPT1– CARNITINE PALMITOYL TRANSFERASE 1

CYS– CYSTEINE

DiD– DIALKYLCARBOCYANINE

DNA – DEOXYRIBONUCLEIC ACID

dsRFP– RED FLUORESCENT PROTEIN

EDTA– ETHYLENE DIMETETRA ACETIC ACID

ELISA– ENZYME-LINKED IMMUNOABSORBANT ASSAY

GABA– GAMMA AMINOBINTURIC ACID

GFP– GREEN FLUORESCENT PROTEIN

GIP– GLUCOSE-DEPENDENT INSULINOTROPIC POLYPEPTIDE

GLP-1 – GLUCAGON-LIKE PEPTIDE 1

GSIS– GLUCOSE-STIMULATED INSULIN SECRETION

GTP– GUAOSINE TRIPHOSPHATE

HEPES– N-2-HYDROXYETHYLPIPERAZINE-N'-2-ETHANESULPHURIC ACID

HIS– HISTIDINE

HRP– HORSE RADISH PEROXIDASE

IB– IMMUNOBLOT

IF– IMMUNOFLUORESCENCE

K_{ATP}– POTASSIUM CHANNEL

KLH– KEYHOLE LIMPET HEMOCYANIN

KRB– KREBS RINGER BUFFERED

LC-CoA– LONG CHAIN FATTY ACYL COENZYME A

LDCV– LARGE DENSE-CORE VESICLE

LYS– LYSINE

MET– METHIONINE

mM– MILIMOLAR

mRNA – MESSENGER RIBONUCLEIC ACID

NADH– NICOTINAMIDE ADENINE DINUCLEOTIDE

NEDH– NEW ENGLAND DEACONESS HOSPITAL

NSF– N-ETHYLMALEAMIDE SENSITIVE FACTOR

NZW– NEW ZEALAND WHITE

PBS– PHOSPHATE BUFFERED SALINE

PC2– PROINSULIN CONVERTASE 2

PC3– PROINSULIN CONVERTASE 3

PEG– POLYETHYLENE GLYCOL (8,000)

PFK– PHOSPHOFRUCTOKINASE

PFU– PLAQUE FORMING UNITS

PI3K– PHOSPHATIDYLINOSITOL 3-KINASE

PI4K– PHOSPHATIDYLINOSITOL 4-KINASE

PKA– PROTEIN KINASE A

PKB– PROTEIN KINASE B

PKC– PROTEIN KINASE C

PLC– PHOSPHOLIPASE C

PMSF– PHENYLMETHYLSULFONYL FLUORIDE

PNRI– PACIFIC NORTHWEST RESEARCH INSTITUTE

POLY-A – POLYADENYLATION

PP– PANCREATIC POLYPEPTIDE

PP2B– PROTEIN PHOSPHATASE 2 B

RER – ROUGH ENDOPLASMIC RETICULUM

RNAi– RNA INTERFERENCE

RT-PCR– REVERSE TRANSCRIPTASE POLYMERASE CHAIN REACTION

S.E.– STANDARD ERROR

sAP– SECRETED ALKALINE PHOSPHATASE

siRNA– SMALL INTERFERING RNA

SNAP-25– SYNAPTIC ASSOCIATED PROTEIN 25

SNARE–SYNAPTIC ASSOCIATED RECEPTOR

SNLV– SNYAPTIC-LIKE VESICLE

SRP – SIGNAL RECOGNITION PARTICLE

SYNC– SYNCOLLIN

TCA– TRICARBOXYLIC ACID

TGN– TRANS GOLGI NETWORK

TIRF– TOTAL INTERNAL REFLECTIVE FLUORESCENT MICROSCOPY

tRNA-TRANSFER RIBONUCLEIC ACID

t-SNARE– TARGET SNARE PROTEIN

VAMP2– VESICLE ASSOCIATED MEMBRANE PROTEIN 2 (SYNAPTOBREVIN)

v-SNARE– VESICLE ASSOCIATED SNARE PROTEIN

CHAPTER ONE

Introduction

1.1. Diabetes Mellitus

1.1.1. Definition of Diabetes

Currently in the United States, an estimated 16 million individuals are thought to have diabetes (Gerich 2003). By 2030, that number is expected to increase to approximately 32 million people, making diabetes a major health problem of increasing proportions (Gerich 2003). Diabetes Mellitus is an endocrine disease characterized by hyperglycemia and osmotic diuresis. In patients with diabetes, control of glucose homeostasis, which occurs predominantly by the hormone insulin, whose production, storage, and secretion in response to stimulus emanates from the β-cell of the endocrine pancreas, is lost. Clinical diagnosis of diabetes requires a fasting plasma glucose concentration of $\geq$ 7.8mM (140mg/dL) on two separate occasions and plasma glucose concentrations of $\geq$ 11.1mM (200mg/dL) at two times during a 2-hour oral glucose tolerance test (Foster 1998).

Diabetes can be classified into two general categories, type-1 or autoimmune diabetes mellitus and type-2 or non-autoimmune diabetes mellitus, the latter of which accounts for 85-90% of diabetes cases (Gerich 2003). Typically, type-1 diabetes affects patients under the age of 20 resulting from autoimmune destruction of β-cells leading to a lack of insulin production and consequently elevated blood glucose. Patients with type-2 diabetes are usually older and most commonly obese with a familial history of the disease and typically exhibit abnormal insulin secretion and loss of glucose responsiveness in islets, impaired suppression of hepatic glucose output, and insulin resistance in target

tissues (Foster 1998). Type-2 diabetes can also develop in the absence of insulin resistance with a primary defect in insulin secretion, as with maturity-onset diabetes of the young (MODY), which only occurs in 2-4% of adult diabetes cases (Bergman Finegood 2002).

1.1.2. Etiology of Diabetes

Despite the overwhelming research efforts, the actual causes of diabetes remain elusive. Origins of autoimmune β-cell destruction, typical of the pathogenesis of type-1 diabetes, are not completely clear. The genetic basis for susceptibility to this disease involves primarily the major histocompatability complex (MHC) locus, particularly the DQ locus in class II MHC genes (Todd, Mijovic et al. 1989). The pathophysiology of most forms of type-2 diabetes involves both insulin resistance and defects in β-cell function, which are influenced by both genetic and environmental factors; such as, obesity, age, ethnicity, gender, diet, smoking, and physical fitness (Bergman, Finegood et al. 2002; Kahn 2003). Although there is evidence supporting inherited genetic susceptibility for type-2 diabetes, no single gene has been implicated to date; however, polygenic defects, as well as, environmental and cultural influences have not been ruled out (Kahn, Vicent et al. 1996). Genetic modes of inheritance for MODY, a more rare form of type-2 diabetes; however, seem to be linked to mutations in glucokinase, PDX-1, and hepatic nuclear factors 1α and 4α genes (Shih and Stoffel 2002). Regardless, studies with high-risk populations, such as the Pima Indians, have identified insulin resistance and/or insulin secretory defects prior to onset of impaired glucose tolerance suggesting

that either an alteration in insulin sensitivity or insulin secretion is the primary genetic factor contributing to the pathophysiology of type-2 diabetes (Bennett, Burch et al. 1971).

The pathogenesis of type-2 diabetes is likely due to decreased β-cell mass and/or acquired β-cell dysfunction, which results from an inability to cope with the insulin demand in an insulin resistant setting (Gerich 2003; Kahn 2003). Although not well understood, the regulation and plasticity of β-cell mass, which is predominantly controlled by growth factor induced signal transduction via the insulin receptor substrate-2/PI3K/PKB pathway, seems to play a pivotal role in the etiology of type-2 diabetes (Dickson *In press*). Factors contributing to β-cell dysfunction include impairments in insulin secretion and abnormal insulin production (Bergman, 2002). Defects in insulin exocytosis have not been directly implicated in the pathogenesis of type-2 diabetes in humans; however, recent evidence from rab3A null mouse and munc18 transgenic mouse studies suggest that preservation of the exocytotic machinery is an important element to maintaining insulin secretory function in β-cells (Rorsman and Renstrom 2003; Spurlin, Thomas et al. 2003; Yaekura, Julyan et al. 2003). The entire mechanism of insulin exocytosis, especially the regulation of this process is not well established, suggesting other unidentified or uncharacterized exocytotic proteins should be considered as possible factors in facilitating insulin secretion in type-2 diabetic patients. The purpose of this research is to elucidate these other factors involved in the regulation of insulin exocytosis in the β-cell in an effort to understand the distal stages of insulin secretion under normal conditions.

1.2. Pancreatic Islets of Langerhans

The pancreas is composed of exocrine acinar cells and the endocrine islets of Langerhans, which comprise 1-2% of the total pancreatic volume(Lacy 1967). Each islet consists of approximately 3,000-5,000 cells that are classified into five types including α-cells, which secrete glucagon, β-cells, which secrete insulin, δ-cells, which secrete somatostatin, pancreatic polypeptide containing cells (PP), and the newly identified ε-cells, which secrete ghrelin (Lacy 1967; Prado 2004). The architecture of the islet consists of α-, δ-, PP, and ε-cells located predominantly on the periphery of the islet; whereas, β-cells localize to the interior core of the islet and comprise 65-75% of the total cellular content of islets (Orci, Vassalli et al. 1988).

Islets are highly vascularized with a glomerular-like capillary network. The β-cells of an islet typically have two capillary faces (one venal and one arterial), of which the venal capillary face corresponds to sites of β-granule accumulation indicating the likelihood of β-cell polarity within the islet (Bonner-Weir 1988). Recent evidence with two-photon confocal imaging reported most exocytotic events occurred in specific regions of the islet confirming islet polarity (Takahashi, Kishimoto et al. 2002). This polarity allows secreted insulin to enter the blood stream to exert its effects on insulin-sensitive tissues and cells (Orci, Vassalli et al. 1988; Liu, Guth et al. 1993).

The circulation of blood flow within an islet emanates from the interior core, implicating a physiological role for β-cell mediated paracrine effects on α-cell secretion (Orci, Vassalli et al. 1988; Liu, Guth et al. 1993). The dynamics of this putative paracrine relationship were supported by experiments with streptozotocin-treated rats, where the contribution of insulin secretion from endogenous β-cells was negligible. In

these animals, insulin infusion significantly inhibited glucagon secretion, suggesting insulin secretion from β-cells may influence glucagon secretion (Zhou *In press*). The complexity of intra-islet communication is an intense area of research, although the mechanistic details remain unresolved. Gap junctions, which are regions through which small molecules might be passed, have been identified in islets implicating these regions in cell-to-cell communication and seem to be important in the regulation of islet hormone secretion (Halban, Wollheim et al. 1982).

1.3. Insulin Production

Insulin is produced, stored, and secreted in a regulatory manner by the β-cells in the islets of the endocrine pancreas (Orci, Vassalli et al. 1988). The biologically active insulin molecule is composed of two polypeptide chains bound together by two disulfide bridges resulting in a protein with a molecular weight of 6,000 Daltons. The structure of insulin consists of a 21 amino acid A chain and a 30 amino acid B chain joined by two interchain cysteine disulfide bridges at A-Cys^{7}/B-Cys^{7} and A-Cys^{20}/B-Cys^{19}, as well as an intrachain disulfide bridge from A-Cys^{6}/A-Cys^{11}. Insulin is synthesized as an inactive precursor preproinsulin, consisting of an N-terminal hydrophobic signal peptide, the B chain of insulin, an Arg-Arg sequence, a connecting peptide (C-peptide), a Lys-Arg sequence, and the A chain of insulin (Rhodes 2000).

1.3.1. The Preproinsulin Gene

The preproinsulin gene is highly conserved among species. The human preproinsulin gene is localized to chromosome 11 (Owerbach, Bell et al. 1980) and

contains two introns, one in the 5' untranslated region and the other within the coding region for C-peptide; however, other species only include one intron (Rhodes 2000). In most species the insulin gene exists as a single gene, however the mouse and rat genomes contain two non-allelic insulin genes (Lomedico, Rosenthal et al. 1980).

Transcription of the preproinsulin gene is stimulated predominantly by glucose; however, other nutrients and hormones influence insulin gene transcription, including mannose, leucine, ketone bodies, non-esterified fatty acids, glucagon-like peptide 1 (GLP-1), leptin, growth hormone, and prolactin (Docherty and Clark 1994). The transcriptional regulation of preproinsulin mRNA by glucose is complex and occurs over long time periods (>18 hours) of glucose stimulation; therefore, it is only relevant to prolonged hyperglycemia and refeeding after periods of stimulation (Rhodes 2000). Regulation of insulin gene transcription occurs in the 5' promoter and enhancer regions upstream of the ATG start site (Ohneda, Ee et al. 2000). In this 5' flanking region the insulin gene contains conserved DNA *cis* elements, to which specific regulatory transcription factors (e.g. PDX-1, NeuroD, NKX6.1, BETA2, and MafA) bind (Docherty and Clark 1994; Ohneda, Ee et al. 2000; Melloul, Marshak et al. 2002). Following transcription, the introns are spliced to yield preproinsulin mRNA that is further modified with a 5' 7-methylguanosine cap and a 3' poly-A tail (Bell, Swain et al. 1979)

1.3.2. Proinsulin Biogenesis

1.3.2.1. Cell Biology

Following transcription, preproinsulin mRNA is translocated from the nucleus to the cytosol where the translation initiation complex, consisting of 40S and 60S ribosomal

subunits and methionyl-tRNA bound to the AUG initiation codon, begins translation of the mRNA (Orci, Vassalli et al. 1988). During the elongation phase of translation, the signal peptide of preproinsulin is exposed and interacts with the signal recognition particle (SRP) resulting in cotranslational transfer from the cytosol to the rough endoplasmic reticulum (RER), where the SRP binds to the SRP receptor. Upon receptor binding the SRP is released from the signal peptide and ribosome via GTP hydrolysis resulting from the intrinsic GTPase activity of SRP. The signal peptide of preproinsulin then interacts with the signal sequence receptor, which is proposed to be a component of a protein translocation pore. In the intraluminal space of the RER the signal peptide is cleaved by a signal peptidase to yield proinsulin (Rhodes 2000). Proinsulin is folded in the RER in a process likely catalyzed by a disulfide isomerase and the molecular chaperone, BiP, which is thought to prevent nonspecific aggregation of incompletely folded proteins (Goodge and Hutton 2000; Rhodes 2000). Once correctly folded, proinsulin is transported through the *cis* Golgi without post-translational modifications, such as N- or O-linked glycosylation or other post-translational additions, to the *trans* Golgi network (TGN) where proinsulin is sorted to the regulated secretory pathway (Rhodes 2000).

1.3.2.2. Regulation

Modulation of insulin levels results from both transcriptional and translational events; however, translational regulation occurs within 20 minutes after glucose stimulation, whereas transcriptional effects require longer time periods (Docherty and Clark 1994; Rhodes 2000). Although both transcription of preproinsulin and translation

of proinsulin are regulated in islets, proinsulin translation is maximally amplified >10-fold by glucose within one hour, whereas, transcriptional stimulation by glucose requires approximately twenty-four hours, suggesting translational regulation is the predominant means of maintaining insulin content and replenishment of intracellular pools depleted by regulated secretion (Rhodes 2000). The stimulation of proinsulin biosynthesis by glucose (>10-fold) is significantly higher than general protein synthesis (<3-fold), indicating proinsulin biosynthesis displays an additional level of specific regulation (Alarcon, Leahy et al. 1995; Rhodes 2000). Wicksteed *et al* identified a conserved primary sequence between 40-48 bases upstream of the AUG start site in the 5' untranslated region of preproinsulin mRNA seems to be important in the regulation of proinsulin translation, while a polypyrimidene track and a conserved sequence (UUGAA) in the 3' untranslanted region is proposed to be involved in the stability of the RNA (Wicksteed, Herbert et al. 2001).

Glucose is the predominant effector of proinsulin biosynthesis; however, other hormones, neurotransmitters and nutrients also regulate proinsulin biosynthesis. The threshold of proinsulin biosynthesis occurs at 2-4mM glucose and is enhanced at glucose concentrations lower than required for stimulation of insulin secretion (4-6mM), but also follows a sigmoidal glucose dose response curve, with maximal biosynthesis occurring at 10-12mM (Goodge and Hutton 2000). Translational regulation of proinsulin biosynthesis requires glucose metabolism; however, the precise metabolic secondary signals leading to stimulation of proinsulin biosynthesis remains unresolved. Regardless, the stimulus-coupling mechanism promoting proinsulin biosynthesis is likely distinct from that of glucose-stimulated insulin secretion (GSIS) as suggested by 1.) The lower threshold

concentration to stimulate proinsulin biosynthesis, 2.) Extracellular calcium is not required for proinsulin biosynthesis, but necessary for GSIS, and 3.) Certain pharmacological agents, nutrients, and neurotransmitters that influence insulin secretion have little or no effect on the regulation of proinsulin biosynthesis (Rhodes 2000). Recent evidence suggests that mitochondrial export of succinate and accumulation of succinate and/or succinyl-CoA in the cytosol appears to be a key intermediate signal in glucose-induced proinsulin biosynthesis (Alarcon, Wicksteed et al. 2002).

1.3.2.3. Processing

The processing of proinsulin occurs in the secretory granule (β-granule). During the maturation of the β-granule, proinsulin is processed within the immature β-granule to the biologically active hormone, insulin, with >90% efficiency (Rhodes 2000). Two endopeptidases, PC2 and PC3 cleave the dibasic Arg^{31}, Arg^{32} (PC3) and Lys^{64}, Arg^{65} (PC2) sites within proinsulin (Hutton and Rhodes 1991). In humans, the sequential processing of proinsulin at Arg^{31}, Arg^{32} by PC3 (followed by processing at Lys^{64}, Arg^{65} by PC2) is the predominant cleavage event suggesting PC3 is likely the key enzyme regulating proinsulin processing, which is substantiated by the abundance of PC3 compared to PC2 in β-cells (Rhodes 2000). Carboxypeptidase H (CP-H) is responsible for the removal of the basic amino acids following PC2/PC3 endopeptidic cleavage, accelerating the proinsulin proteolytic maturation to insulin. PC2, PC3, and CP-H require an acidic pH (5.5) and calcium (1-10mM) for optimal activity. During β-granule maturation, the β-granule undergoes acidification allowing processing of proinsulin to occur within the appropriate cellular compartment (Hutton 1982; Hutton and Rhodes

1991). The acidification of the β-granule involves H^+-ATPase pumps localized on the β-granule membrane, which likely participate in the regulation of proinsulin processing (Hutton 1982). The intragranular environment also has high calcium concentrations (1-10mM) that is important in endopeptidase and CP-H activities and likely constitutes another regulatory component of proinsulin processing (Orci, Vassalli et al. 1988; Rhodes 2000). Additional levels of regulation may also occur at the proteolytic maturation of PC2 and PC3 through their chaperone molecules 7B2 and proSAAS. Proteolytic cleavage of the chaperones by the endopeptidases (7B2/PC2 and proSAAS/PC3) alleviates inhibition of the pro protein forms of PC2 and PC3 resulting in maturation and activation of the endopeptidases (Rhodes 2000). Once processed, insulin is stored in the mature β-granules as hexameric crystals.

1.3.3. β-Granule Trafficking/Maturation

Generally, vesicle-mediated secretion encompasses three types of secretory vesicles including constitutive secretory vesicles, large-dense core vesicles (LDCV), and small synaptic-like vesicles (SNLV). Constitutively secreted vesicles are secreted in an unregulated manner and primarily contain plasma membrane proteins. LDCV and SNLV vesicles undergo regulated secretion in response to stimuli and typically contain hormones or other proteins which may be required at larger quantities when stimulated (Bauerfeind and Huttner 1993). The precise sorting of proteins to their respective pathways is unclear; however, proteins sorted to the constitutive secretory pathway, which likely occurs through a bulk-flow mechanism, may be a default to those not actively sorted to the regulated pathway (Rhodes 2000).

Proinsulin is sorted through the *trans* Golgi network to β-granules with >99% efficiency and maintained in large-dense core vesicles (β-granules) prior to secretion (Easom 2000; Rhodes 2000). Although the mechanism of proinsulin sorting to β-granules is predominantly unclear, one hypothesis suggests that proinsulin aggregation in the TGN, due to mild acidity and high calcium concentrations, occurs through interactions with membrane lipids leading to reorganization of cholesterol-rich microdomains and the budding of the immature granule (Tooze, Martens et al. 2001). A study showing that a mutant form of proinsulin incapable of hexamerization was efficiently sorted to granules in the neuroendocrine AtT-20 cell line, suggests that proinsulin sorting is not necessarily dependent upon self-aggregation (Quinn, Orci et al. 1991). However, the proinsulin conversion endoprotease (PC2) displays aggregation properties and may facilitate proinsulin sorting by binding proinsulin to the TGN in accordance with the aggregation/membrane rearrangement model. Structurally, disulfide Ω loops have been linked to prohormone sorting in other cell types (e.g. proopiomelanocortin (POMC) secretion); however, this mechanism is not likely for proinsulin sorting (Rhodes 2000). Alternatively, it is hypothesized that certain proteins may act as "sorting receptors" to facilitate protein sorting to the regulated secretory pathway, although the identity of such receptors are undetermined in β-cells. It has been suggested that carboxypeptidase E (CP-E) may be a candidate sorting receptor in β-cells; however, this is not likely since proinsulin was efficiently sorted in CP-E deficient mice (Irminger, Verchere et al. 1997).

Additional sorting of β-granule components also occurs in the immature secretory granule in accordance with 'sorting for retention' or 'sorting for exit' models (Orci,

Vassalli et al. 1988; Rhodes 2000). Clathrin-coated regions of the immature granule bud from maturing granules, taking proteins bound to receptors (sorting for exit) and retaining those unbound proteins in the maturing granule (sorting by retention) (Kuliawat and Arvan 1994). These 'post-edited' granules that bud from the maturing β-granules are hypothesized to constitute constitutive-like secretory vesicles that may function to remove unwanted lysosomal proteases from β-granules, although this pathway is very minor in the β-cell and likely does not significantly result in proinsulin sorting, since only <1% of proinsulin is released according to this pathway (Arvan and Halban 2004). The mechanism and proteins involved in facilitating the removal of budding vesicle and its components is unknown. Regardless of the mechanism for proinsulin sorting to the β-granule, it is likely that both granule refinement/maturation and TGN sorting contribute to sorting proinsulin to β-granules (Kuliawat and Arvan 1994; Rhodes 2000).

Mature β-granules contains the biologically active hexameric crystalline form of insulin, which consists of three insulin dimers interacting at B-His^{10} of the insulin molecules around an axis of two zinc atoms (Rhodes 2000). The vast majority of mature β-granules are amassed in a storage pool within the cytosol, awaiting stimulation to trigger transport to the plasma membrane for eventual exocytosis (Easom 2000). The stimulus-coupling and exocytotic mechanisms controlling insulin secretion are discussed in detail in sections 1.4 and 1.5. It is established that newly synthesized β-granules are preferentially secreted; however, the mechanism and regulation of preferential release of β-granules is still unknown in β-cells (Rhodes and Halban 1987).

1.4. Insulin Secretion

Insulin is secreted in a regulated manner in response to stimulation from various secretagogues including certain nutrients, hormones, neurotransmitters, and pharmacological agents (MacDonald 1990). Some secretagogues such as glucagon-like peptide-1 (GLP-1), sulfonylureas, acetylcholine, certain amino acids, and fatty acids augment basal and/or glucose-stimulated insulin secretion (MacDonald 1990; Holz, Kuhtreiber et al. 1993; Prentki, Tornheim et al. 1997; Deeney, Gromada et al. 2000; MacDonald, El-Kholy et al. 2002); whereas, other agents such as the neurotransmitters norepinephrine and epinephrine, can inhibit glucose-induced insulin secretion (Chey and Chang 2001).

1.4.1. Nutrients

1.4.1.1. Glucose

Among the several secretagogues that stimulate insulin secretion from β-cells the most physiologically relevant nutrient to stimulate insulin secretion is glucose (Lang 1999). The threshold for glucose to initiate insulin secretion is between 4-6mM with stimulation following a sigmoidal curve and maximal stimulation occurring at 15mM glucose concentrations. The kinetics of glucose-stimulated insulin secretion are biphasic, where the first phase represents a brief and rapid peak at 2-5 minutes that falls within 5-10 minutes and a second, more sustained, phase of insulin secretion that is maximal at one hour (Straub and Sharp 2002). The first phase of insulin secretion is thought to correspond to secretion of the readily-releasable pool of β-granules that are morphologically docked and competent for exocytosis upon stimulation; whereas, the

second phase likely represents those β-granules that must be transported, docked, and primed prior to secretion (Bratanova-Tochkova, Cheng et al. 2002).

Glucose metabolism is necessary for the stimulation of insulin secretion, which occurs in a pulsatile manner (Cunningham, Deeney et al. 1996). In patients with type-2 diabetes and their close relatives, the pulsatility of insulin secretion is lost, suggesting that abnormal pulsatility of insulin secretion may be an early phenomenon in the etiology of the disease (Foster 1998). Phosphofructokinase (PFK), the enzyme that catalyzes the phosphorylation of fructose-6-phosphate to fructose 1, 6-bisphosphate, is an early step in glycolysis and the rate-limiting enzyme of glucose metabolism (MacDonald 1990; Gylfe, Ahmed et al. 2000). Glycolytic metabolism upstream of PFK is out-of-phase with insulin secretion, however, the oscillatory nature of PFK is responsible for subsequent glycolytic and mitochondrial ATP oscillations in-phase with insulin secretion (Gylfe, Ahmed et al. 2000). Glycolytic oscillations in NADH, O_2 consumption, and the ATP/ADP ratio have been demonstrated in β-cells. These glycolytic oscillations occur in glucose-stimulated islets with the same periodicity as calcium and insulin secretion, further demonstrating glycolytic oscillations are correlated to oscillations in intracellular $[Ca^{2+}]_i$ (Prentki, Tornheim et al. 1997). Intracellular $[Ca^{2+}]_i$ oscillations have been demonstrated in intact islets and individual β-cells with both fast and slow oscillations, the latter likely constituting the physiological oscillations of β-cells and the pulsatility of insulin secretion (Bergsten, Grapengiesser et al. 1994). These intracellular $[Ca^{2+}]_i$ oscillations result from oscillations in the cytosolic ATP/ADP ratio, which influences calcium influx by facilitating the closure of K_{ATP} channels with subsequent membrane depolarization

and the opening of voltage-dependent calcium channels (Deeney, Kohler et al. 2001; Fridlyand, Tamarina et al. 2003).

The proximal signals of glucose-stimulated insulin secretion are relatively well defined. Together, the GLUT2 transporter and glucokinase, the enzyme responsible for phosphorylating glucose to yield glucose-6-phosphate, are thought to function as a "glucose sensing apparatus" and to maintain glucose homeostasis in the β-cell (Schuit, Huypens et al. 2001). Glucose is rapidly transported into the β-cell by the GLUT2 transporter, due to its low affinity for glucose (K_m=40mM) (Figure 1.1). This allows for transport of glucose into the β-cell that is proportional to plasma glucose concentrations (Brown 2000). Glucokinase also has a low affinity for glucose (K_m= 17mM) and is the rate-limiting reaction of glycolysis, making the rate of glucose conversion to glucose-6-phosphate proportional to the extracellular glucose concentration. The low affinity of glucokinase for glucose allows β-cells to detect a range of circulating blood glucose levels, such that under stimulatory conditions, insulin is secreted proportional to the relative glucose concentrations (Matschinsky 2002).

The β-cell is distinct from other cells in that glucose must be metabolized to stimulate insulin secretion (MacDonald 1990). Metabolism of glucose through glycolysis and the Kreb's cycle results in enhanced energy production via an increased cytosolic ATP/ADP ratio, which facilitates closure of ATP-sensitive K^+ channels (K_{ATP} channels) (Lang 1999). The K_{ATP} channel in β-cells is composed of four subunits Kir6.2, which comprises the pore of the channel for potassium ion permeation, and four SUR1 regulatory subunits(Bryan 2000). Typically under glucose stimulation, ATP and ADP bind to different sites of the Kir6.2 subunit causing a conformational change in the

channel to prevent potassium efflux. The SUR1 subunit modulates this ATP/ADP effect on the Kir6.2 subunit (Bryan 2000). Closure of these K_{ATP} channels inhibits potassium efflux resulting in plasma membrane depolarization (Doyle and Egan 2003). Voltage-gated L-type calcium channels subsequently open culminating in an increase in cytosolic $[Ca^{2+}]_i$ levels (Lang 1999). Although closure of the K_{ATP} channel is the predominant mechanism leading to calcium-dependent insulin secretion, a K_{ATP} channel-independent pathway through cAMP-mediated insulin secretion (Figure 1.1) is also involved, albeit to a lesser degree, as evidence from SUR1 null mice demonstrated (Nakazaki, Crane et al. 2002). The increase in cytosolic $[Ca^{2+}]_i$ is a critical secondary signal to trigger insulin secretion; although, other secretagogues, such as glucagon-like peptide-1 (GLP-1), acetylcholine, and fatty acids, also augment Ca^{2+}-dependent insulin secretion (Figure 1.1) (Holz, Kuhtreiber et al. 1993; Prentki, Tornheim et al. 1997; Deeney, Gromada et al. 2000; MacDonald, El-Kholy et al. 2002).

1.4.1.2. Fatty Acids

Long-chain fatty acyl-CoA (LC-CoA) can also enhance insulin secretion either through circulating fatty acids from the bloodstream or by glucose metabolism in the β-cell; however, potentiation of insulin secretion likely occurs via glucose metabolism (Prentki, Tornheim et al. 1997). Glucose metabolism results in increased malonyl-CoA production, which inhibits carnitine palmitoyl transferase I (CPT1), the mitochondrial fatty acid transporter; thereby reducing LC-CoA availability for mitochondrial β-oxidation of fatty acids causing an increase in the cytosolic levels of LC-CoA (Bjorklund, Yaney et al. 1997; Yaney and Corkey 2003). Although the precise mechanism of LC-

CoA stimulation of insulin secretion is not determined, studies indicate LC-CoA may regulate atypical and/or novel PKC activation by an unknown mechanism causing PKC-mediated stimulation of insulin secretion (Figure 1.1) (Yaney, Korchak et al. 2000). Alternatively, acylation of proteins involved in the mechanism of exocytosis likely contribute to the stimulation of insulin secretion; however, the identity of these acylated proteins is unknown (Yaney and Corkey 2003).

1.4.1.3. Amino Acids

Amino acids, such as leucine, glutamine, arginine, and alanine also potentiate insulin secretion; however, it is not entirely evident as to how the different amino acids influence insulin secretion. Leucine, in the presence of glutamine, may either stimulate insulin secretion by transamination to α-ketoisocaproate, which then undergoes mitochondrial oxidation, and/or by allosteric activation of glutamate dehydrogenase, which results in the oxidation of glutamate to α-ketoglutarate. Metabolism of glutamate to α-ketoglutarate would then increase the available Kreb's cycle metabolite; thereby enhancing the metabolic generation of ATP and increasing the cytosolic ATP/ADP ratio (MacDonald 1990). As previously discussed, augmentation of the ATP/ADP ratio facilitates closure of K_{ATP} channels and ultimately stimulation of insulin secretion (Doyle and Egan 2003). Alanine enhances the glutamate-induced insulin release by increasing glutamate deamination in the mitochondria (Fahien, MacDonald et al. 1988). The mechanism of arginine stimulation of insulin secretion is unclear, but may involve three mechanisms: 1.) The depolarization of the plasma membrane due to L-arginine uptake leading to calcium influx; 2.) The metabolism of arginine through ornithine to increase

the Kreb's cycle metabolite α-ketoglutarate; 3.) Nitric oxide stimulation of insulin secretion where nitric oxide is derived from L-arginine metabolism (Blachier, Mourtada et al. 1989; Malaisse, Blachier et al. 1989; Schmidt, Warner et al. 1992).

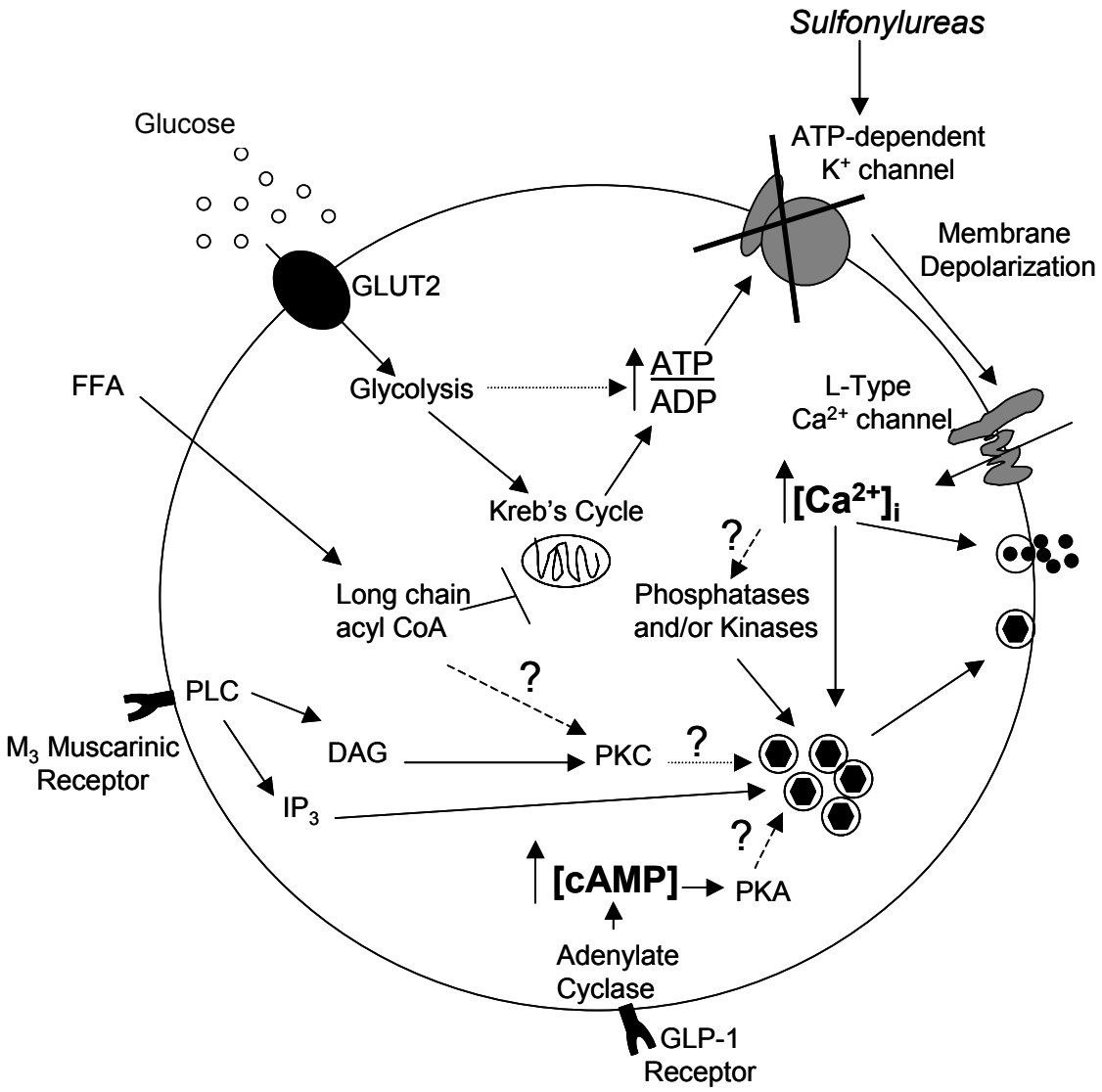

Figure 1.1: Schematic diagram of insulin secretion in the β-cell. Glucose is transported into the cell by the GLUT2 transporter and is metabolized through glycolysis and the Kreb's cycle resulting in increased ATP/ADP, which closes ATP-dependent K+ channels. Closure of K+ channels causes membrane depolarization which opens voltage-gated calcium channels and increases intracellular calcium. The subsequent regulation of β-granule exocytosis by calcium is unknown (?). Other secretagogues, FFA, GLP-1, and acetylcholine, and their effects on insulin secretion are also depicted.

1.4.2. Hormones

GLP-1 is an incretin hormone produced and secreted from the L-cells of the distal ileum and colon upon food ingestion. GLP-1 binds to GLP-1 receptors on β-cells and initiates a $G_{\alpha}s$-protein coupled activation of adenylate cyclase, which results in increased cyclic AMP levels (cAMP) and activation of protein kinase A (PKA). PKA phosphorylation has been implicated in the regulation of K_{ATP} channel and the docking and fusion of β-granules as putative mechanisms in the augmentation of GSIS (Figure 1.1) (MacDonald, El-Kholy et al. 2002).

Glucose-dependent insulinotropic polypeptide, GIP, is a gastrointestinal incretin hormone secreted by K-cells of the duodenum. GIP stimulates insulin secretion in response to dietary stimulation of GIP secretion by PKA-dependent pathways, as described for GLP-1. GIP stimulation of insulin secretion is also mediated by PKA-independent pathways, which involve cAMP-GEF, a putative regulator of low molecular weight G-proteins involved in β-granule transport and/or exocytosis (Mayo, Miller et al. 2003).

1.4.3. Pharmacological Agents

Sulfonylureas, including glyburide (also known as glibenclamide), stimulate insulin secretion by binding to the SUR1 subunit of the K_{ATP} channel; thereby, facilitating closure of the channel independent of glucose metabolism (Figure 1.1) (Bryan 2000). As previously described, closure of the K_{ATP} channel results in an influx of calcium through voltage gated L-type calcium channels; thereby stimulating insulin secretion (Doyle and Egan 2003).

1.4.4. Neurotransmitters

The pancreas is an innervated organ allowing neurotransmitter access to islets for stimulation of insulin secretion (Kirchgessner and Gershon 1991; Foster 1998). The parasympathetic neurotransmitter, acetylcholine, is released from intrapancreatic nerves in response to the absorptive stages of feeding (Kirchgessner and Gershon 1991; Chey and Chang 2001). Acetylcholine binds to M3 muscarinic receptors on β-cells and activates phospholipase C-β (PLC) through $G_{\alpha}q$ -mediated activation (Chey and Chang 2001). Activation of PLC hydrolyzes phosphatidylinositol 4,5-bisphosphate (PIP_2) to generate diacylglycerol (DAG) and inositol phosphate (IP_3). DAG subsequently activates PKC, which enhances glucose-stimulated insulin secretion through an undetermined substrate (Figure 1.1) (Konturek, Zabielski et al. 2003). The role of IP_3 in the regulation of insulin secretion may ensue through mobilization of intracellular calcium stores, although the significance of intracellular calcium stores on the stimulation of insulin secretion likely occurs subsequent to the initial stimulation from L-type calcium channel activation (Roe, Lancaster et al. 1993).

Catecholamines, such as norepinephrine and epinephrine, inhibit glucose-stimulated insulin secretion, although the mechanism of this inhibition is not well understood. The sympathetic neurotransmitters produced from the adrenal medulla inhibit insulin secretion through α2-adrenergic receptor activation resulting in the inhibition of adenylate cyclase by $G_{\alpha}i$-mediated inhibition (Mayo, Miller et al. 2003). The decrease in adenylate cyclase activity reduces the cAMP levels in the cell, which as discussed previously influences insulin secretion.

1.5. Exocytosis

Like synaptic vesicle exocytosis in neurons and zymogen granule exocytosis in acinar cells, exocytosis in β-cells is both a calcium and ATP-dependent process (Easom 2000; Rhodes 2000). The mechanism as to how increases in $[Ca^{2+}]_i$ evoke components of the insulin exocytotic machinery is not as well defined as the details regarding the generation of stimulus-coupling signals (Wollheim, Lang et al. 1996). Although the increase in cytosolic $[Ca^{2+}]_i$ is a requirement to trigger glucose-stimulated insulin secretion, it is not clear how calcium and other factors link to the exocytotic machinery to elicit the tight control of insulin secretion. This is further complicated by the complexity of exocytosis, which consists of multiple steps each likely regulated in a comprehensive manner. The only insight to date as to putative effectors of the calcium signal includes proteins such as calmodulin and synaptotagamin; however, other proteins are probably involved to mediate the calcium-dependent facilitation of insulin secretion (Easom 2000).

1.5.1. Cell Biology

Exocytosis can be subdivided into five stages: transport, pre-docking, docking, priming, and membrane fusion (Figure 1.2) (Schweizer, Betz et al. 1995).

1.5.1.1. Transport

The transport of granules from the cytosolic storage pool is calcium and ATP-dependent involving transport proteins, as well as protein kinases and phosphatases (Easom 2000; Sim, Baldwin et al. 2003). It has been estimated that there might be as many as 10,000 β-granules in a β-cell maintained in a storage pool in the cytosol until

stimuli initiate their transport to the plasma membrane along microtubules and subsequently along microfilament networks of the cytoskeleton (Figure 1.2) (Easom 2000; Rorsman and Renstrom 2003; Sim, Baldwin et al. 2003). Evidence supporting microtubule involvement in β-granule transport has been demonstrated both *in vitro* and *in situ* in which interactions between β-granules and microtubules have been observed (Malaisse, Malaisse-Lagae et al. 1975; Dentler and Suprenant 1986). Furthermore, mitotic spindle inhibitors, which function by disrupting or stabilizing microtubule polymers suppress 2nd phase insulin secretion, implicating microtubules in β-granule transport (Malaisse, Malaisse-Lagae et al. 1975).

The mechanism of β-granule transport involves the ATP-dependent motor protein kinesin I (consisting of two heavy and two light chains), rab3A, calmodulin, and calcium/calmodulin-dependent protein kinases/phosphatases (CaM kinase II and PP2B) (Easom 2000). A proposed model for the role of these proteins in the regulation of β-granule exocytosis is as follows. The function of kinesin in β-cells is to attach β-granules to microtubules and mediate their transport along the cytoskeletal network in response to calcium (Easom 2000; Donelan, Morfini et al. 2002). Under basal conditions, calmodulin-mediated activation of CaM kinase II leads to the phosphorylation of kinesin, resulting in its inactivation. However, during stimulatory conditions calmodulin is proposed to bind PP2B to promote the dephosphorylation and activation of kinesin resulting in transport of the β-granules to the plasma membrane (Donelan, Morfini et al. 2002). Other proteins proposed to regulate β-granule transport include rab3A, which is a small GTPase that is transiently associated with the cytosolic face of the β-granule membrane via a post-translationally attached polyisoprenoid group (Rorsman and

Renstrom 2003). At basal glucose concentrations when cytosolic $[Ca^{2+}]_i$ levels are low, rab3A transiently binds calmodulin through a low affinity interaction (K_d=18-22μM) compared to the binding affinity of other calmodulin interacting proteins keeping calmodulin in the vicinity of the granule membrane. Upon increased cytosolic $[Ca^{2+}]_i$, calmodulin binding is likely transferred from rab3A to a different calmodulin-binding protein (Kajio, Olszewski et al. 2001).

1.5.1.2. Pre-docking

Once the β-granule is transported from the cytosolic storage pool to the plasma membrane, munc18/nSec1 plays a critical role in mediating granule docking and is likely a regulatory step in the mechanism of exocytosis. Munc18 is expressed in β-cells; however, its involvement in insulin secretion has yet to be established (Katagiri, Terasaki et al. 1995). Munc18 in other cell types is proposed to function as a negative regulator of exocytosis by sequestering syntaxin prior to granule docking (Burgoyne and Morgan 2003). This prohibits the association of syntaxin into the 7S SNARE complex with VAMP and SNAP-25 (Gotte and von Mollard 1998; Hua and Scheller 2001). Upon stimulation, munc18 is released from syntaxin which can then interact with VAMP and SNAP-25 to form the SNARE complex, although the mechanism that promotes munc18 dissociation is unknown (Easom 2000; Burgoyne and Morgan 2003).

1.5.1.3. Docking

Docking is defined as the pool of unprimed β-granules that are initially interacting with the plasma membrane (Easom 2000). Once transported, the granule is docked at the

plasma membrane through the interaction of v-SNARE (vesicle SNARE) and t-SNARE(target SNARE) proteins (Burgoyne and Morgan 2003). β-cells express a full complement of SNARE proteins similar to those expressed in neurons; however the SNAREs implicated in exocytosis include the v-SNARE, VAMP-2, and the t-SNAREs, syntaxin 1A and SNAP-25, which together form a 7S complex (Figure 1.2) (Wheeler, Sheu et al. 1996). Mutation of VAMP-2 in β-cells caused mislocalization of β-granules in addition to inhibition of insulin secretion implying a role for SNARE proteins in docking β-granules at the plasma membrane (Regazzi, Sadoul et al. 1996). However, genetic loss of VAMP or syntaxin, as well as SNARE complex disruption by *clostridial* toxins were unable to prevent vesicle docking to the plasma membrane in neurons (Table 1.1) (Boyd, Duggan et al. 1995). Other studies in yeast indicate that t-SNARE proteins associated with multiple v-SNARE isoforms, suggesting SNARE proteins do not mediate the precision of granule docking (Yang, Gonzalez et al. 1999).

A 19.5S protein complex, called the exocyst, likely mediates the precision of granule docking to the plasma membrane (Hsu 2004). The exocyst consists of eight proteins (Sec3p, Sec5p, Sec6p, Sec8p, Sec10p, Sec15p, Exo70p, and Exo84p) originally identified in yeast; however, mammalian homologues of all eight proteins have been identified (Lipschutz 2002). It is hypothesized that members of the Ras superfamily, such as small GTPases including rab27 in β-cells, may regulate the precision of granule docking to the exocyst (Waselle, Coppola et al. 2003).

1.5.1.4. Priming

After the granule is targeted to the plasma membrane, it is hypothesized that the granule undergoes an ATP-dependent priming phase preparing the granule for subsequent membrane fusion; however, these mechanisms are unclear (Figure 1.2). NSF and α-SNAP have been implicated as essential proteins involved in priming the granule prior to membrane fusion through disassembly of *cis* SNARE complexes (Klenchin and Martin 2000). Evidence supporting this hypothesis in β-cells was demonstrated by capacitance measurements on cells treated with N-ethylmaleamide to inactivate NSF which inhibited Ca^{2+}-induced insulin exocytosis similar to ATP withdrawal (Eliasson, Renstrom et al. 1997). Another putative role for ATP/ADP during β-granule priming is phosphatidylinositol 4-kinase (PI4K). Recent evidence demonstrates ADP-dependent activation of PI4K enhanced the number of β-granules in the ready-releasable pool (Olsen, Hoy et al. 2003).

1.5.1.5. Membrane Fusion

Membrane fusion between the β-granule and plasma membrane is a calcium-dependent process and the final step in exocytosis culminating in the release of intragranular cargo into the extracellular milieu (Figure 1.2) (Burgoyne and Morgan 2003). Morphologically, fusion between the β-granule membrane and the plasma membrane involves the formation of a fusion pore and can be described as either total membrane fusion or transient membrane fusion (Rorsman and Renstrom 2003). Total membrane fusion is the complete incorporation of the β-granule membrane into the plasma membrane (Jahn, Lang et al. 2003). Evidence for total fusion has been described

in neurons through increased capacitance of membranes after stimulation of secretion, suggesting vesicles incorporate into the plasma membrane following fusion (Martin 2003). An alternative hypothesis for membrane fusion is the transient model of membrane fusion, as known as the "kiss and run" hypothesis. Instead of complete membrane fusion between the β-granule and plasma membrane, the β-granule undergoes a transient membrane fusion, which is likely mediated by pore formation and expansion (Rorsman and Renstrom 2003). Following fusion, the pore closes and the entire β-granule is then recycled. Evidence supporting the "kiss and run" hypothesis has been seen in acinar cells by atomic force microscopy. Pore-like structures in acinar cells opened wider upon stimulation, but following stimulation returned to the initial pore size, suggesting the granule was not incorporated into the plasma membrane following fusion (Cho, Quinn et al. 2002). Total internal reflective fluorescent microscopy (TIRF) of isolated islets infected with various β-granule specific markers has suggested the predominance of the transient mechanism of membrane fusion in β-cells (Michael 2003), although total membrane fusion has been demonstrated in β-cells (Michael 2003; Tsuboi and Rutter 2003; Tsuboi and Rutter 2003). It appears that both transient and total membrane fusion exist in the β-cell; however, the functional mechanism and regulation is unclear (Barg 2003). Recently amperometric analysis of individual fusion pores in neuronal PC12 cells transfected with synaptotagmin IV displayed increased frequency and duration of transient membrane fusion events while mutant forms of synaptotamin inhibited this effect, suggesting that synaptotagmin may regulate the choice between total and transient membrane fusion (Wang, Lu et al. 2003).

Biochemically the mechanism of membrane fusion involves the mixing of two lipidic bilayers; however, the facilitation and molecular details of membrane fusion are still under investigation (Jahn, Lang et al. 2003). Integration of two lipid bilayers is thermodynamically unfavorable, suggesting that membrane fusion can only occur once the free energy barrier for fusion is overcome. Evidence suggests that the membrane tension between the granule and plasma membrane and the "zippering" action of the SNARE complex is enough to overcome this free energy barrier for fusion (Gotte and von Mollard 1998). The energetics of fusion pore expansion requires additional deformation of the membranes of which the molecular mechanism is unresolved (Chizmadzhev, Kuzmin et al. 2000).

Clearly fusion pores are an integral part of membrane fusion; however, little is known about the molecular composition of these structures (Jena 2003; Jena, Cho et al. 2003). Existence of pore-like structures in rat islets by freeze-fracture analysis was demonstrated on both the β-granule and plasma membrane (Orci, Perrelet et al. 1977). Other evidence has emerged identifying a 0.47μm geometric fusion pore between the β-granule and plasma membrane; however, the exact composition and regulation of this pore remains to be identified (Takahashi, Kishimoto et al. 2002).

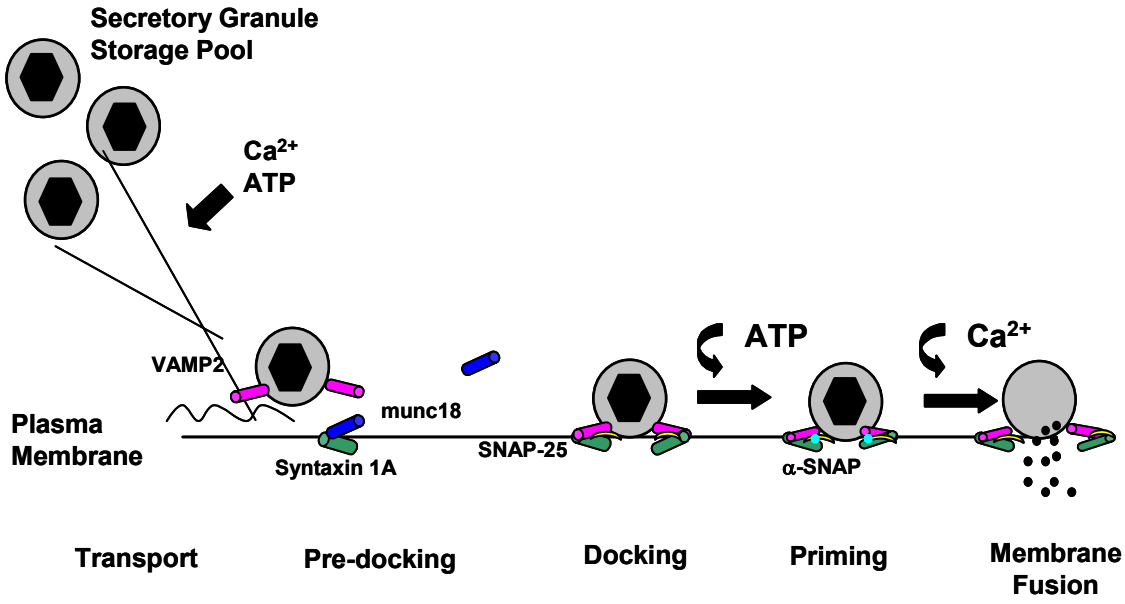

Figure 1.2: Schematic representation of exocytosis in β-cells. β-granules are transported from a storage pool in an ATP and Ca^{2+} -dependent process to the plasma membrane. Prior to docking, munc18 dissociates from syntaxin, allowing docking and 7S SNARE complex formation. Once docked to the plasma membrane, the β-granules are primed and subsequently undergo Ca^{2+} -dependent membrane fusion with the plasma membrane expelling the intragranular contents into the extracellular milieu.

1.5.2. Regulation

The five phases of exocytosis including transport, pre-docking, docking, priming, and membrane fusion are all potential regulatory points. (Easom 2000) Under basal conditions, insulin is maintained and stored in a readily available pool of β-granules (Easom 2000; Rhodes 2000). Upon secretagogue stimulated insulin release (i.e. >6mM glucose), only a small fraction (<2% of total insulin content per hour) of these β-granules are released (Easom 2000; Rorsman and Renstrom 2003). Additionally, the amount of circulating insulin in the blood depends predominantly on the rate of exocytosis (Barg, Ma et al. 2001). Therefore, insulin exocytosis must be tightly regulated.

Interestingly, there is a substantial delay between release of intragranular components and membrane fusion. Capacitance measurements indicate that the peak of exocytosis occurs within 20 ms; however, insulin secretion measurements indicate peak levels of insulin release at 2 min, a discrepancy of approximately 1000-fold. The expansion of the fusion pore to allow the insulin molecule to be released into the extracellular space could account for this discrepancy (Rorsman and Renstrom 2003). Proteins involved in the expansion of the fusion pore and release of β-granule cargo could affect the kinetics of exocytosis and ultimately serve as a possible area for regulation of exocytosis.

1.5.2.1. SNARE Proteins

Mechanistically, SNARE proteins are proposed to facilitate membrane fusion. The SNARE hypothesis suggests that the formation of the SNARE complex, which consists of VAMP, SNAP-25, and syntaxin, in a “zippered” anti-parallel manner

overcomes the free energy barrier for fusion and is; therefore, responsible for facilitation of membrane fusion (Gotte and von Mollard 1998). Data supporting this hypothesis include experiments with *Botulinum* neurotoxins that abolish SNARE complex integrity, which significantly inhibited insulin secretion in β-cells (Table 1.1) (Boyd, Duggan et al. 1995). Recent evidence utilizing extracellular targeted SNARE proteins to fuse two distinct cells reinforces the hypothesis that SNARE complex formation facilitates membrane fusion (Hu, Ahmed et al. 2003). However, contrary evidence from yeast vacuolar fusion indicates that formation of the SNARE complex is necessary for membrane fusion; however, membrane fusion can occur prior to complex formation suggesting SNARE complex formation is not the only requirement to promote membrane fusion (Xu, Rammner et al. 1999). Clearly SNARE complex formation is fundamental to membrane fusion; however, the regulation of membrane fusion cannot be accounted for solely by the function of SNARE proteins.

Toxin	**Target SNARE**	**Effect on Insulin Exocytosis**
Tetanus toxin	VAMP-2/cellubrevin	Inhibits Ca^{2+}-dependent exocytosis; no effect on GTPγS induced exocytosis.
Botulinum toxin A	SNAP-25	Inhibits Ca^{2+}-dependent exocytosis
Botulinum toxin B	VAMP-2/cellubrevin	Inhibits Ca^{2+}-dependent exocytosis
Botulinum toxin C1	Syntaxin/SNAP-25	Inhibits Ca^{2+}-dependent exocytosis; no effect on GTPγS induced exocytosis
Botulinum toxin C2	Actin microfilaments	Inhibition/Stimulation depending on the phase of insulin secretion
Botulinum toxin E	SNAP-25	Inhibits Ca^{2+}-dependent exocytosis
Botulinum toxin F	VAMP-2/cellubrevin	No effect

Table 1.1: Comparison of *Clostridial botulinum* or *Tetanus* toxins on insulin exocytosis.

1.5.2.2. Calcium-dependent proteins

A pivotal area of regulation involves the calcium-dependent aspect of insulin secretion. As previously discussed, both transport and membrane fusion requires calcium to facilitate and regulate these stages of exocytosis. Voltage-gated L-type calcium channels are the predominant calcium channel in β-cells responsible for the influx of calcium in response to membrane depolarization as previously discussed (Roe, Lancaster et al. 1993). Opening of the L-type calcium channel causes an influx of calcium, which reaches total cytosolic concentration of 100nM in β-cells; however, the calcium concentration required to stimulate exocytosis is 10μM, suggesting that exocytosis occurs in regions near calcium channels (Easom 2000; Rorsman and Renstrom 2003). In fact, syntaxin 1A and SNAP-25 interact with L-type calcium channels, coupling the exocytotic machinery in the vicinity of high calcium concentrations (Seagar and Takahashi 1998). This calcium connection suggests the importance of a calcium "sensor" to detect changes in the intracellular $[Ca^{2+}]_i$ and consequently facilitate the calcium-dependent requirement of exocytosis.

The putative calcium "sensor" suggested in both neurons and β-cells is synaptotagmin (Perin, Fried et al. 1990; Gao, Reavey-Cantwell et al. 2000). There are several isoforms of synaptotagmin; however, synaptotagmin III and VII are expressed in islets and co-localize with β-granules (Wheeler, Sheu et al. 1996; Gao, Reavey-Cantwell et al. 2000). The fundamental property of a putative calcium sensor is a calcium-binding domain with the same affinity for calcium as the maximal level of cytosolic $[Ca^{2+}]_i$ concentrations required to stimulate membrane fusion. Indeed, the affinity of synaptotagmin III and VII for calcium is 1-10μm, which correlates to the concentration of

calcium required to elicit insulin secretion (Easom 2000; Rorsman and Renstrom 2003). Furthermore, synaptotagmin interacts with the 7S SNARE complex and the L-type calcium channel, placing it in the appropriate vicinity to detect changes in intracellular calcium (Seagar and Takahashi 1998). Evidence supporting synaptotagmin as the calcium sensor in β-cells was demonstrated by overexpression of synaptotagmin III or VII, which individually increased calcium-dependent insulin secretion (Gao, Reavey-Cantwell et al. 2000). Structurally, the PKC-like C2 domains of synaptotagmin (C2A and C2B) together are responsible for binding calcium (Sorensen, Fernandez-Chacon et al. 2003). Although the mechanism is unresolved, it is hypothesized that once synaptotagmin detects an increase in intracellular $[Ca^{2+}]_i$, it is proposed that synaptotagmin, along with the SNARE complex, represents the driving force necessary to promote membrane fusion, perhaps through formation of a pore. Evidence indicates the N-terminal intragranular region of synaptotagmin oligomerizes in a calcium-dependent manner, and that this oligomerization is important for function of synaptotagmin in neurons (Fukuda and Mikoshiba 2000).

1.5.2.3. Other Proteins

The different stages of insulin exocytosis are all putative regulatory steps that likely entail multiple levels of regulation, which is analogous to exocytosis in other cells containing regulated vesicular release (Burgoyne and Morgan 2003). However, the precise mechanism of regulation at each stage is unresolved. Insulin secretion requires a calcium signal to trigger insulin exocytosis; yet, other secondary signals including cAMP, GTP, and ATP have been implicated in the facilitation of insulin exocytosis (Prentki,

Tornheim et al. 1997). These criteria together suggest other regulatory proteins may be involved in the regulation of insulin exocytosis, apart from calcium-dependent protein regulation. Indeed, non-calcium binding proteins, such as munc18/nSec1 and rab3A, have been implicated in the regulation of insulin exocytosis at the level of β-granule transport, as discussed earlier (sections 1.5.1.1 and 1.5.1.2.). Regardless, the complete regulation of insulin exocytosis remains unclear; therefore, other proteins, not previously examined in β-cells, may play additional roles in the regulation of insulin exocytosis.

1.5.2.3.1 Syncollin

Studies in the exocrine pancreas identified an intragranular protein, syncollin, which may play a role in the regulation of exocrine large dense-core zymogen granule exocytosis, distinct from synaptic vesicle exocytosis. Syncollin was originally cloned as a calcium-dependent syntaxin binding protein, suggesting a role as a putative calcium sensor similar to synaptotagmin. Additionally, fluorescence-dequenching experiments to examine the *in vitro* fusion between zymogen granule membranes loaded with octadecylrhodamine with purified pancreatic plasma membranes demonstrated that increasing concentrations of purified syncollin inhibited membrane fusion (Edwardson, An et al. 1997). However, subsequent examination of purified zymogen granules showed that bis-(sulfosuccinimidyl) suberate, a water-soluble cross-linking reagent impermeable to membranes, could only access syncollin for formation of homo-oligomers in sonicated granule preparations, suggesting syncollin is localized to the lumen of the zymogen granule (An, Hansen et al. 2000). The localization of syncollin to the lumen of the zymogen granule argues that the *in vitro* fusion experiment is not indicative of the

physiological mechanism of syncollin function since addition of recombinant syncollin would have localized to the cytosolic surface of the granule membrane and casts doubt on the physiological significance of the *in vitro* syntaxin binding data based on the inaccessibility of protein-protein interaction across the granule membrane.

Other observations have led to the suggestion that syncollin may participate in the distal stages of regulated exocytosis, perhaps through formation of an exocytotic fusion pore. In zymogen granules, syncollin has been shown to interact directly with membrane lipids and insert into the granule membrane in a cholesterol-dependent manner (Edwardson, An et al. 1997; Hodel, An et al. 2001). Furthermore, the quaternary structure of syncollin is composed of an oligomeric state, which associates with the lipid bilayer in a "doughnut-shaped" structure (Geisse, Wasle et al. 2002). Although syncollin is not essential for exocrine cell exocytosis, as indicated by the mild phenotype of syncollin knockout mice (Antonin, Wagner et al. 2002; Geisse, Wasle et al. 2002), it likely interacts with other cellular proteins to make the exocytotic process more efficient and may consequently contribute to the regulation of exocytosis (Geisse, Wasle et al. 2002).

It has also been hypothesized that syncollin may affect secretory protein transport. Evidence supporting this hypothesis is seen in the syncollin null mouse, which is viable with no defect in acinar cell secretion (Antonin, Wagner et al. 2002). In these animals administration of caerulin resulted in severe pancreatitis, inhibition of protein synthesis and diminished intracellular transport of secretory proteins, as determined by pulse-chase experiments, compared to normal control animals administered caerulin (Antonin, Wagner et al. 2002). However, *in vitro* evidence indicates the homo-oligomeric syncollin

structures do not appear to function in sorting/binding zymogen aggregates (An, Hansen et al. 2000). Other evidence with two-photon confocal analysis of acinar cells from syncollin null mice exhibited a 60% decrease in calcium-stimulated exocytotic events compared to acinar cells from normal control mice [J.M. Edwardson, personal communication], supporting the involvement of syncollin at the level of exocytosis.

1.5.2.3.2. FXYD Proteins

During the course of this research, it was discovered that syncollin might be a pseudo member of the FXYD family of proteins (Chapter 5). The FXYD protein family is a recently categorized group of proteins that display tissue-specific expression, although very little is known about their function (Sweadner and Rael 2000). Most proteins within this family have modulating activity on the Na^+/K^+ ATPase, although modulation is not required for ATPase function (Therien and Blostein 2000). However, other evidence proposes these proteins may function at the level of exocytosis, although the mechanism is unresolved and may include modulation of the Na^+/K^+ ATPase. FXYD1/phospholemman has been demonstrated to promote GLUT4 translocation to the plasma membrane in adipocytes, possibly in a PKC-dependent manner, implicating a role for FXYD proteins in PKC-mediated granule trafficking (Walaas, Horn et al. 1999). The mechanism of GLUT4 translocation, although unresolved, parallels the mechanism β-granule exocytosis particularly with the involvement of SNARE proteins in GLUT4 vesicle association with the plasma membrane, suggesting common exocytotic proteins may mediate both pathways (Simpson, Whitehead et al. 2001). Additionally, FXYD2 (also known as the γ subunit of the Na^+/K^+ ATPase) reconstitution in *Xenopus* oocytes

resulted in the formation of 5nm pores that were large enough to pass inulin, a 5,000 Dalton protein, implicating FXYD protein function in pore formation rather than ion channel activity (Sha, Lansbery et al. 2001).

Regardless of the function of these FXYD proteins, tissue-specific distribution may result in different physiological consequences for the cells (Sweadner and Rael 2000) (Table 1.2). FXDY2 and FXYD4 are expressed in different regions of the kidney and are proposed to modulate Na^+/K^+ ATPase activity resulting in a regulatory role on sodium absorption in the kidney, which is critical to body fluid and electrolyte homeostasis (Farman, Fay et al. 2003). FXYD1, expressed in cardiac muscle, is also proposed to modulate Na^+/K^+ ATPase activity; which influences heart contractility (Zhang, Qureshi et al. 2003). The tissue expression and function of FXYD5 is currently undetermined. FXYD3 is ubiquitously expressed; however, expression of the protein is enhanced in tumors, including human mammary tumor. FXYD7 is a brain-specific isoform proposed to modulate Na^+/K^+ ATPase activity leading to neuronal excitability (Geering, Beguin et al.).

FXYD Isoform	Common Name	Tissue Expression	Function
FXYD1	Phospholemman	Heart, Skeletal muscle, adipocytes	Heart contractility; GLUT4 translocation
FXYD2	γ subunit Na^+/K^+ ATPase	Kidney	Na^+ absorption
FXYD3	Mat-8	Ubiquitous	?
FXYD4	CHIF	Kidney; colon	Na^+ absorption
FXYD5	RIC	?	?
FXYD6	Phosphohippolin	Brain	?
FXYD7	?	Brain	?

Table 1.2: FXYD protein family members including tissue expression and known functional roles within the tissues.

1.6. Project Aims

Regulated insulin secretion is a complex, dynamic process requiring stringent control of β-granule exocytosis in order to achieve the precise secretion of insulin in response to stimulation. As previously discussed, both metabolic substrates and multiple proteins coordinate the regulation of insulin secretion. The mechanism of this regulation is uncertain and other proteins are likely involved. The aim of this research is to examine other putative proteins that may be involved in regulated exocytosis of insulin β-granules in an effort to further elucidate the molecular machinery responsible for the regulation of insulin secretion. Utilizing a candidate-based approach, this research will examine the zymogen granule protein, syncollin, which has been implicated in zymogen granule exocytosis in acinar cells. Due to the similarity of certain aspects of zymogen granule exocytosis in acinar cells and β-granule exocytosis, it is hypothesized that syncollin itself or a syncollin family member could be involved in regulating insulin exocytosis in β-cells. Interestingly, the primary sequence of syncollin contains a modified FXYD domain (DPYYD), suggesting that syncollin may be a pseudo-FXYD family member.

Although the function of FXYD proteins is unresolved, some FXYD isoforms display functional effects on exocytotic events, such as granule transport, or form functional pore structures on the plasma membrane, suggesting a possible role for FXYD proteins in exocytosis. Therefore, FXYD proteins represent another candidate possibly involved in the mechanism of insulin exocytosis. Examination of FXYD protein expression in β-cells as well as functional relevance to insulin exocytosis will be determined to assess the hypothesis of FXYD protein participation in insulin exocytosis.

CHAPTER TWO

Materials and Methods

2.1. Materials

2.1.1.Animals

Isolated pancreatic islets were obtained from male Wistar rats (250-275g) purchased from Charles River Labs (Wilmington, MA). Male/female NEDH rats (~8 weeks old) bred at PNRI were used to propagate insulinoma tumors for the acquisition of enriched β-granule fractions (Chapter 2, Section 1.2.10.2). All animal protocols were approved according to the PNRI Institutional Animal Care and Use Committee.

2.1.2. Antibodies

Antibodies utilized in immunoblot (IB) and immunofluorescence (IF) experiments are listed in Table 2.1. Syncollin polyclonal antiserum 'B' and monoclonal antiserum (87.1) have been described previously (An, Hansen et al. 2000; Hodel and Edwardson 2000) and were kindly provided by Dr. R. Jahn (Max Planck Institute; Göttingen, Germany).

Antibody	Species	Company	Dilution	
PRIMARY ANTIBODIES			**IB**	**IF**
α-β-catenin	Mouse	Transduction Labs	1:1000	-
α-insulin	Guinea Pig	Sigma	-	1:100
α-myc	Mouse	Cell Signaling	1:1000	1:500
α-nSec1/munc18	Mouse	Transduction Labs	1:1000	-
α-syncollin 'B'	Rabbit	R. Jahn, polyclonal	1:500	1:100
α-syncollin (87.1)	Mouse	R. Jahn	1:1000	-
α-syntaxin	Mouse	Upstate	1:1000	-
α-VAMP2	Rabbit	Calbiochem	1:1000	-
SECONDARY ANTIBODIES				
α-rabbit-HRP	Donkey	Jackson Labs	1:5000	-
α-mouse-HRP	Goat	Upstate	1:5000	-
α-rabbit-Cy3	Donkey	Jackson Labs	-	1:300
α-guinea pig-Cy5	Donkey	Jackson Labs	-	1:300
α-mouse-Cy2	Donkey	Jackson Labs	-	1:300

Table 2.1: List of antibodies used in immunoblot and immunofluorescence experiments.

2.1.2.1. Anti-FXYD6 Antibody Generation

The anti-FXYD6 polyclonal antibody was generated from an N-terminal peptide (peptide synthesis by Sigma-Genosys; The Woodlands, TX) portion of FXYD6 (EKEKEKDPFYC). The N-terminal FXYD6 peptide was specific to FXYD6 as determined by BLAST analysis with no specific similarity to other FXYD isoforms. Conjugation of the FXYD6 peptide to keyhole limpet hemocyanin (KLH) was performed according to the manufacturer's instructions for the Pierce (Rockford, IL) Imject Maleimide Activated mcKLH kit. Quantification of FXYD6 conjugation to KLH was assessed by measurement of free sulfhydryl groups with Ellman's reagent (5, 5'- Dithio-bis (2-nitrobenzoic acid)) and compared to pre-conjugated peptide resulting in 95% conjugation of the peptide.

Antibody production in female NZW rabbits was performed by Covance (Denver, PA) according to approved animal guidelines. The conjugated peptide was injected with Freund's adjuvant followed by subsequent injection boosts every 3-4 weeks. Test bleeds from each boost were analyzed by immunoblot on INS-1 lysate and FXYD6-Myc infected INS-1 lysate. Antibody purification by IgG affinity chromatography was performed on the final bleed from rabbit #341 using a HiTrap Protein-A sepharose column (Amersham Biosciences).

ELISA and immunoblot analysis were utilized to characterize the purified antibody. ELISA reagents were used according to manufacturer's protocols from the BioRad alkaline phosphatase substrate EIA kit. FXYD6 peptide-coated 96-well plates were incubated with dilutions of anti-FXYD6 serum or pooled IgG purified fractions followed by incubation with donkey anti-rabbit IgG secondary antibodies (0.25μg/ml) and subsequent development with the EIA chromogen. Immunoreactivity was demonstrated in the final bleeds of rabbits #340 and #341 at dilutions ranging from 1:10-1:500. Pre-immune serum showed no immunoreactivity in this ELISA. IgG pooled fractions demonstrated immunoreactivity at dilutions ranging from 1:10-1:500, indicating recovery of the anti-FXYD6 antibody (Figure 2.1A). Immunoblot analysis of INS-1 and Adv-FXYD6-Myc infected INS-1 lysates indicated the presence of a band at ~16Kd for uninfected INS-1 cells, which migrated slightly higher in FXYD6-Myc infected INS-1 cells, indicative of the Myc-tag extension. Anti-FXYD6 serum from rabbit #341 displayed a more intense signal with no cross-reactivity recognized in the pre-bleed, unlike the immunoblot for antiserum from rabbit #340 (Figure 2.1B). *In vitro* blocking of the anti-FXYD6 antiserum with 10μg or 300μg of FXYD6 N-terminal peptide prior to

immunoblot analysis resulted in reduction of the 16Kd band in uninfected INS-1 lysate for rabbit #341. Although the apparent molecular weight (16Kd) is slightly higher in uninfected INS-1 cells than the predicted molecular weight of FXYD6 (10Kd) (Yamaguchi, Yamaguchi et al. 2001), the inhibition of antibody recognition by the FXYD6 peptide, indicated the anti-FXYD6 antibody specifically recognized FXYD6.

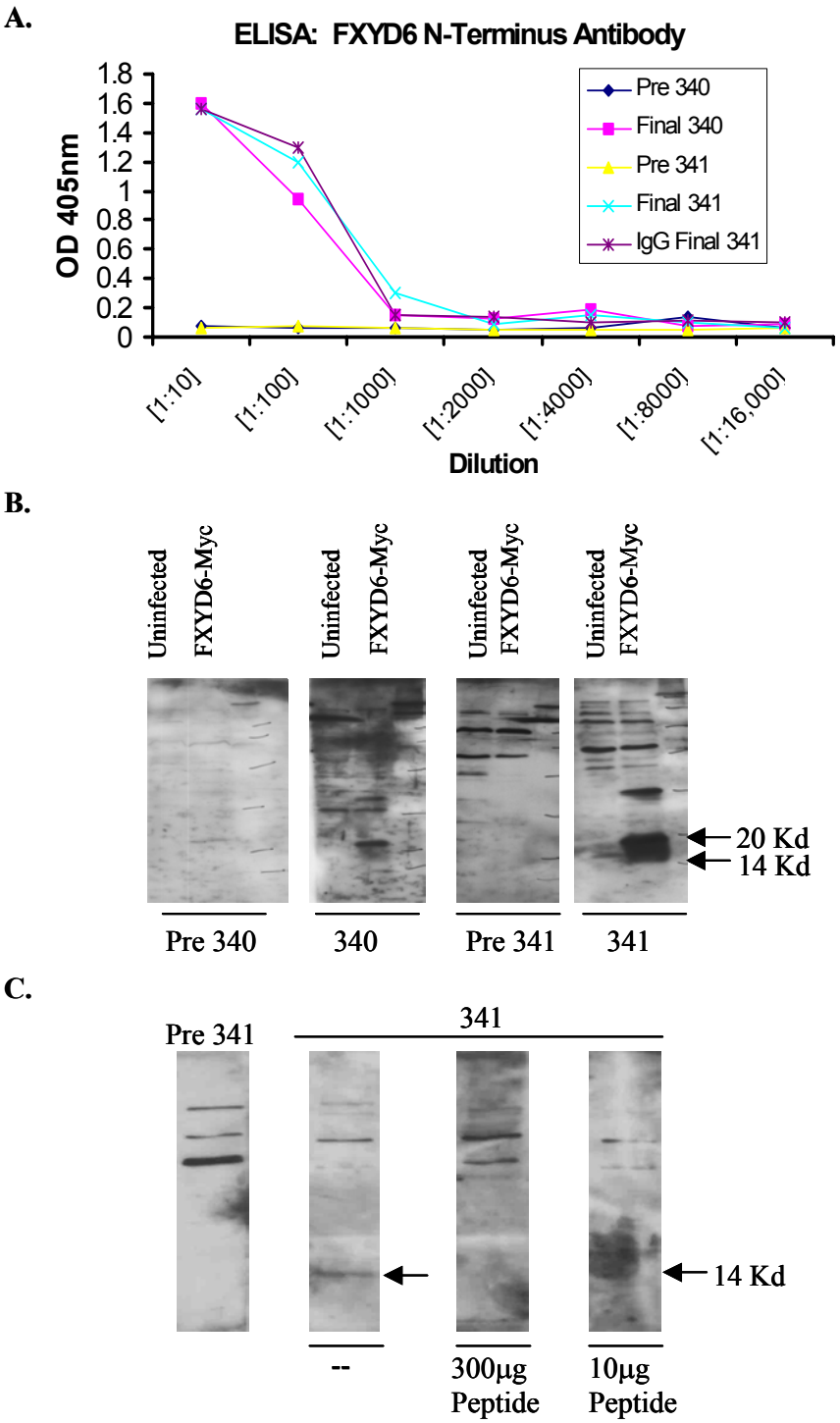

Figure 2.1: Characterization of α-FXYD6 N-terminal antibody. A. ELISA analysis with N-terminal peptide. B. Immunoblot analysis of uninfected INS-1 (832/13) and FXYD6-Myc infected INS-1 with α-FXYD6 N-terminal antibody. 340 and 341 refer to different rabbits identification numbers. C. FXYD6 peptide blocking to determine immunoblot specificity of α-FXYD6 N-terminal antibody on uninfected INS-1.

2.1.3. General Reagents

Fetal bovine serum was obtained from Hyclone Laboratories, Inc. (Logan, UT). Grove, PA). ProMix [^{35}S] protein labeling mix, from Amersham Biosciences (Arlington Heights, IL), containing 75% of L-[^{35}S] Methionine was used for islet protein synthesis radiolabeling. GLP-1_{7-36} was purchased from Bachem Inc. (King of Prussia, PA). Dialkylcarbocyanine was purchased from Molecular Probes (Eugene, OR). Unless otherwise stated, all other chemical reagents were of the highest purity available and purchased from Sigma-Aldrich or Fisher Scientific (Santa Clara, CA).

2.2. Methods

2.2.1.Islet Isolation

Pancreatic islets were isolated from rat pancreas based on the protocol from Lacy and Kostianovsly (Lacy and Kostianovsky 1967). Wistar rats were anesthetized with 0.75ml/kg body weight of a ketamine/xylazine mixture. Inflation of the pancreas via cannulation of the pancreatic duct was achieved with 8ml of M199 media containing 1.5mg/ml collagenase P (Invitrogen) and subsequently incubated for 11-15 minutes at 37°C followed by vigorously shaking to homogenize the pancreas. Digested pancreas was then washed with M199 media supplanted with 10% FBS to inactivate collagenase P digestion. Separation of islets by Histopaque centrifugation gradients and subsequent hand picking resulted in 200-500 islets/rat. Isolated islets were cultured for 16-18 hours with adenovirus in 5.6mM glucose RPMI media containing 10% FBS and 100units/ml penicillin and streptomycin.

2.2.2. INS-1 cell culture

INS-1 cells [832/13] were generously provided by Dr. C.B. Newgard (Duke University; Durham, NC) and were maintained in 11.2mM glucose RPMI 1640 media (Invitrogen; Baltimore, MD) containing 10% FBS, 50μM β-mercaptoethanol, 100units/ml penicillin and streptomycin, 0.5M HEPES (pH 7.4), 102mM glutamine, and 50mM sodium pyruvate (Hohmeier, Mulder et al. 2000).

2.2.3. Cloning

DNA prepared from Qiagen (Valencia, CA) spin columns was subjected to restriction endonuclease digest for 1 hour, electrophoresed and the appropriately sized fragments were excised from an agarose gel and purified with GeneCleanII (BioRad). The purified fragments were then ligated with T4 DNA ligase (Invitrogen) and subsequently ethanol precipitated prior to $CaCl_2$ transformation into DH5α cells. Transformed cells were incubated 1 hour at 37°C to allow for plasmid expression of the antibiotic resistance gene prior to plating to (ampicillin or kanamycin) antibiotic supplanted Luria-Bertani agar plates. All cloning was verified by restriction digest and only candidates with the predicted size were sequenced for final verification by the PNRI sequencing facility.

2.2.4. Recombinant Adenoviruses

Recombinant adenoviruses expressing GFP (Adv-GFP), syncollin-Met1, (Adv-Sync-Met1), syncollin-Met2 (Adv-Sync-Met2), syncollin-GFP (Adv-Sync-GFP), luciferase (Adv-luciferase), syncollin-dsRFP (Adv-Sync-dsRFP), and FXYD6-Myc

(Adv-FXYD6-Myc) were cloned into the appropriate adenoviral vectors as described in each corresponding chapter. Homologous recombination and adenoviral purification was performed by the PNRI Viral Vector Core facility as described (He, Zhou et al. 1998). Cloned adenoviral plasmids were subjected to homologous recombination in *Escherichia coli* with a supercoiled DNA vector (pAdEasy) containing most of the adenoviral genome. Once confirmed by restriction digest, the supercoiled adenoviral DNA was transfected with Superfect lipofectamine reagent (Qiagen) into 293 cells, where cell lysis occurred upon adenoviral propagation. After repeated cell lysis increase the quantity of adenovirus, the adenovirus was purified from 293 crude lysate with PEG 8,000/5M NaCl solution and further concentrated through CsCl ultracentrifugation followed by desalting using Sephadex G-25 columns (PD-10 columns, Pharmacia). The secreted alkaline phosphatase adenovirus (Adv-sAP) was generated as previously outlined and provided by Phillipe Halban (University of Geneva; Geneva, Switzerland) (Molinete, Lilla et al. 2000). For experiments with adenovirus-mediated protein expression, isolated islets were incubated with the adenoviruses for 16-18 hours at $1X10^7$ pfu/islet to $4X10^8$ pfu/islet in 5.6mM glucose RPMI 1640 media prior to analysis. INS-1 cells were incubated with $1X10^7$ pfu/well to $4X10^8$ pfu/well for 2 hours and cultured 16-18 hours in 5.6mM glucose RPMI 1640 media prior to analysis.

2.2.5. RT-PCR

RNA was obtained from cell lines or tissue, as indicated in each experiment, by total RNA extraction with RNAeasy kits (Qiagen) according to the manufacturer's protocol. The RNA was denatured at 65°C for 5 minutes prior to cDNA synthesis using

T-primed cDNA synthesis reactions (Amersham) according to the manufacturer's protocol. PCR amplification was performed using conserved oligonucleotides specific for the target gene. PCR parameters were optimized for each set of oligonucleotides. Oligonucleotides used in PCR experiments are described in Table 2.2.

Gene	5' Oligonucleotide	3' Oligonucleotide
Syncollin	5' acctgccctacctgcc 3'	5' tttgcggtactcttccagtcgagggtag 3'
FXYD1	5' gcatctcccggccacatcctgatt 3'	5' ccgcctgcggtggacagacg 3'
FXYD2	5' aggagctgtcagctaaccat 3'	5' tcttcattgacctgcctatgct 3'
FXYD3	5' aagagtttgctctgagcctgttggt 3'	5' gcagttgtgagcagagcctggtg 3'
FXYD4	5' gagggaataacctgtgcctggagtga 3'	5' ggtactggcagagcctggagtga 3'
FXYD5	5' ctggaattatcatcctcact 3'	5' gaacaggataggcaggatcacagca 3'
FXYD6	5'atggagacggtgctgatcctc 3'	5' gttctctgccttctggggctc 3'
FXYD7	5' ggatcctttgcagatttccac 3'	5' aagctcaagatgtggaccctgagg 3'

Table 2.2: List of primer sequences used in RT-PCR analysis.

2.2.6. *In vitro* Insulin Secretion and Islet Perifusion

Isolated rat islets or INS-1 [832/13] cells were infected with adenovirus as described and analyzed for insulin secretory activity at either basal (2.8mM) or stimulatory (16.7mM) glucose ($^{\pm}$ 10nM GLP-1 or 5μM glyburide as indicated) (Donelan, Morfini et al. 2002). Cells were incubated in Krebs-Ringer buffer (pH 7.4) (20mM HEPES, 25mM KCl, 5mM $MgSO_4$-$7H_2O$, 0.7M NaCl, 5mM $CaCl_2$, 30mM $NaHCO_3$, and 0.1% BSA) at 2.8mM glucose for 1 hour followed by incubation at either basal or

stimulatory glucose (± GLP-1 or glyburide, where indicated) KRB for an additional hour. Cells were lysed in lysis buffer (50mM HEPES, 1% NP-40, 4mM EDTA, 1μM leupeptin, 10μg/ml aprotinin, and 0.1mM PMSF), sonicated (15 watts, 10 seconds), and centrifuged (5min at 16,000xg). Samples of KRB media and cell lysate were analyzed by rat insulin radioimmunoassay according to the manufacturer's protocol (Linco). For perifusion of isolated islets, adenovirally infected isolated islets (125 islets) were placed on 8 μm polycarbonate hydrophilic filters (Whatman) in Swinnex chambers and subsequently perifused at a 1ml/min flow rate with 2.8mM glucose KRB for 30 minutes with 2ml fractions collected the last 10 minutes. The solution was then switched to 16.7mM glucose KRB and fractions were collected at 1-minute and 5 minute intervals. The solution was finally returned to 2.8mM glucose KRB for 10 minutes while 2ml fractions were collected. All solutions and islets were maintained at 37°C. The islets were washed from the hydrophilic filters with lysis buffer and sonicated as described above. Both the secreted fractions and islet lysate were analyzed by rat insulin radioimmunoassay to determine the insulin concentration.

2.2.7. Immunofluorescence and Confocal Microscopy

Adenovirus infected INS-1 cells were grown on glass coverslips and fixed in 4% paraformaldehyde (Polysciences; Warrington, PA). The cells were treated with 0.1% saponin in PBS for 30 minutes, blocked with 10% donkey serum in 5% BSA/PBS for 1 hour, and subsequently probed with appropriate primary antibodies in 5% BSA/PBS for 16-18 hours. Following three 5-minute washes with PBS, secondary antibodies containing the appropriate fluorophores were incubated for 1 hour in 5% BSA/PBS and

the coverslips were mounted to glass slides. The slides were viewed by confocal microscopy (Olympus FV500) with a UPLAPO 60X objective at the appropriate wavelength for the indicated fluorophores (i.e. excitation spectra 488, 595, and 605nm and emission spectra 507, 650, and 670nm) using XYZ series sequential scans at 0.5μm z-sections. The images shown are digitally magnified and the XYZ scans are compressed into one image with Fluoview software (Olympus; Melville, NY).

2.2.8. Alkaline Phosphatase Activity

Isolated islets were incubated 16-18 hours with $1X10^8$ pfu/islet of Adv-sAP. Alkaline Phosphatase activity was measured from both the media and cell lysate as previously described (Molinete, Lilla et al. 2000). Isolated islets were infected with adenovirus and treated as described for *in vitro* insulin secretion experiments over a 1-hour stimulation period with 2.8mM or 16.7mM glucose in KRB and subsequent analysis by radioimmunoassay. For alkaline phosphatase activity, each sample was incubated with substrate buffer (1mg/ml p-nitrophenyl phosphate in 100μM diethanolamine) and measured at 405nm in a 96-well plate for 60 minutes at one-minute intervals. The samples were normalized to lysis buffer without alkaline phosphatase. The slope of each line was determined for the measurement of alkaline phosphatase activity.

2.2.9. Proinsulin Biosynthesis

Isolated rat islets were infected with $4X10^8$ pfu/islet of purified Adv-Sync or Adv-GFP for 16-18 hours and incubated for 1 hour with 2.8mM or 16.7mM glucose in Krebs-Ringer buffer (pH 7.4). Isolated islets were pulse-radiolabeled with [^{35}S]

methionine for 20 minutes and lysed as described in section 1.2.6. Immunoprecipitation of the lysate for proinsulin utilized an anti-insulin antibody (1:50) that was precipitated by Pansorbin and analyzed by alkaline urea gel electrophoresis and subsequent visualization using Optiquant phosphoimaging software, as previously described (Alarcon, Leahy et al. 1995).

2.2.10. Subcellular Fractionation

2.2.10.1. INS-1 cells

Uninfected INS-1 cells were grown on a 10cm plate to 100% confluency and lysed in 10μM ammonium bicarbonate buffer. The lysate was incubated on ice for 30 minutes, sonicated (15 watts, 10 seconds), and centrifuged at 1,000xg for 5 minutes. The supernatant was then centrifuged in a Beckman ultracentrifuge for 1 hour at 115,000xg. The resulting pellet was resuspended in Laemmli buffer and analyzed by electrophoresis and subsequent immunoblot.

2.2.10.2. NEDH Insulinoma tumor

Subcellular fractionation was performed as described previously (Chick, Warren et al. 1977; Hutton 1989; Donelan, Morfini et al. 2002). Insulinoma tumors were removed from NEDH rats and homogenized with a Potter homogenizer. The homogenate was centrifuged at 3,000xg for 5 minutes. The supernatant was layered on a Nycodenz gradient and centrifuged for 90 minutes at 125,000xg and the interface between the 32% and 63% Nycodenz gradients were collected and centrifuged an additional 15 minutes at 20,000xg. The resultant pellet was resuspended in wash buffer (0.25M sucrose and 10mM KMes) and enriched with consecutive percoll (Amersham)

gradient centrifugation. The final pellet, which consisted of 75-80% β-granules, as verified previously by enzyme markers, was resuspended in wash buffer.

2.2.11. Protein Assay

Protein concentrations were measured by bicinchoninic acid (BCA) assay according to the manufacturer's protocol (Pierce; Rockford, IL). Tricarboxylic acid precipitation and subsequent counting in a β-scintillation counter was used to measure total protein synthesis following ^{35}S methionine administration, as described for proinsulin biosynthesis.

2.2.12. Statistics

Where appropriate, data are presented as the mean $\pm$ the S.E. Statistical significance is determined by unpaired Student's t-test where indicated, where $p<0.05$ was considered statistically significant. Accumulated insulin secretion was calculated by determining the area under the curve for the indicated portion of the curve.

CHAPTER THREE

An Intragranular Factor Influences Regulated Insulin Secretion In Pancreatic β–cells

3.1. Introduction

Much of the characterization of β-cell exocytosis has been driven in part by discoveries made in other vesicular transport systems. Particularly, analogies have been made to the mechanism of regulated synaptic vesicle exocytosis for the control of insulin exocytosis of large dense core vesicles (LDCV), and indeed there are similar protein isoforms involved, as discussed in detail previously (Chapter1). Despite these similarities, synaptic vesicle exocytosis and LDCV exocytosis display functional differences. The kinetics of synaptic vesicle exocytosis in neurons (0.1-1 ms) is much faster than LDCV exocytosis in β-cells (85-2000 ms), as determined by capacitance measurements of the readily-releasable pool (Olofsson, Gopel et al. 2002; Martin 2003). In addition, the calcium ion concentrations required to induce membrane fusion are significantly lower in β-cells (1-10μM) than in neurons (100-200μM) (Heidelberger, Heinemann et al. 1994; Easom 2000; Olofsson, Gopel et al. 2002). While common proteins catalyze both processes (*e.g.* members of the SNARE protein family, syntaxins, SNAP-25 and synaptobrevins (Wheeler, Sheu et al. 1996; Linial 1997; Easom 2000; Gao, Reavey-Cantwell et al. 2000)), there are likely unique proteins that contribute to the mechanism of LDCV exocytosis that have yet to be defined.

Comparison between zymogen granule exocytosis of the exocrine pancreas and insulin β-granule exocytosis of the endocrine pancreas reveal more closely associated functional characteristics than that of synaptic vesicle exocytosis. Therefore, zymogen

granule exocytosis may provide additional correlations about large dense core vesicle exocytosis distinct from synaptic vesicle exocytosis. Both zymogen granules and insulin β-granules are large dense core vesicles, which are secreted in a regulatory manner in response to stimulus resulting in calcium-dependent stimulation of exocytosis with a $[Ca^{2+}]_i$ threshold of 1-10μM (Easom 2000; Wasle and Edwardson 2002). The kinetics of zymogen granules exocytosis and insulin β-granule exocytosis consist of a biphasic nature with an initial first phase lasting from 2-5 minutes, followed by a slower, more sustained phase of exocytotic release with only 1-3% of the granule population released in either cell type, suggesting both exocrine and endocrine cells display a complex, stringently controlled regulation of exocytosis (Padfield and Panesar 1998; Wasle and Edwardson 2002; Michael 2003). Based on these characteristics, certain information from zymogen granule exocytosis might be extrapolated for gaining a better insight into the mechanisms of insulin exocytosis.

In pancreatic exocrine cells, the intralumenal zymogen granule protein, syncollin, has been implicated in regulated exocytosis, as previously discussed (Chapter 1.5.2.3.1.). Since syncollin has a potential role in large-dense core vesicle exocytosis, the objective of this study was to determine whether syncollin was expressed in β-cells and examine any functional relevance to the regulation of insulin exocytosis.

3.2. Materials and Methods

Syncollin-Met1, Syncollin–Met2, and Syncollin-GFP adenovirus construction- Cloning, recombination, and adenoviral purification techniques for Adv-Syncollin (Met1 and Met2), and Adv-Sync-GFP were performed as described in Chapter 2. RT-PCR

cloning of syncollin from isolated pancreatic islets was performed in the lab and upon sequencing was found to be equivalent to the published syncollin sequence. The cloned syncollin sequence (Met1) was inserted into pACC-CMV adenoviral vector between EcoRI and SalI with subsequent recombination and viral purification performed as described by a post-doctoral fellow in the lab. Adv-Sync-Met2 was cloned into pADTrac-CMV adenoviral vector between BglII and HindIII. Adv-Sync-GFP was cloned into pShuttle-CMV between BglII and XbaI. The PNRI Viral Vector Core performed recombination and purification of syncollin-Met2 and syncollin-GFP adenoviruses. Adenovirus-mediated syncollin protein expression was determined by immunoblot analysis with a syncollin monoclonal antibody (87.1) on 10μg of protein. Unless otherwise stated, all functional experiments requiring Adv-Sync (Met1 and Met2) and Adv-Syncollin-GFP (expression data not shown) were performed with adenovirus titers at $4X10^8$ pfu/islet, which exhibited good syncollin protein expression (Figure 3.2B) without adverse effects seen on cell viability.

3.3. Results

Syncollin is not endogenously expressed in β-cells - Syncollin is predominantly expressed in the exocrine pancreas, although expression has also been identified in the proximal small intestine (Edwardson, An et al. 1997; Tan and Hooi 2000). Examination of syncollin in the NIH protein database, suggested that syncollin has been identified in islet and insulinoma tissue; however, immunohistochemistry analysis of pancreatic sections indicated that syncollin was not localized to islets (Tan and Hooi 2000).

Syncollin was detected in isolated islets by both RT-PCR and immunoblot analysis (Figure 3.1). However, no detectable expression of syncollin in endocrine pancreatic β-cell lines was found by RT-PCR analysis or immunoblot in insulinoma tissue preparations or INS-1 cells (Figure 3.1). Because INS-1 and insulinoma tissue represent predominantly a homogenous population of β-cells (although some α- and δ-cells are present in insulinoma tissue) (Chick, Warren et al. 1977; Hutton 1989), it is likely that syncollin is not expressed in β-cells. Interestingly in enriched β-granule fractions, a 10Kd band was detected with an anti-syncollin polyclonal antibody (Figure 3.1B). Furthermore, RT-PCR analysis identified a smaller 150bp band in islets, INS-1, and insulinoma tissue (Figure 3.1A). This data suggested the possibility of a 'syncollin-like' protein present in β-cells that will be addressed later (Chapter 5).

Adenoviral-mediated syncollin expression and localization in β-cells – To express syncollin in β-cells, adenoviruses to the two putative isoforms of syncollin (Met1 and Met2) were generated. Initial cloning of syncollin identified a potential start site 31 amino acids upstream of the N-terminus of native syncollin (Met1) (Edwardson, An et al. 1997). However, further characterization of syncollin revealed a second putative start site (Met2) 12 amino acids downstream from the original start site (Figure 3.2A) (Tan and Hooi 2000). At the time of beginning this project, it was unclear which of these syncollin pro-forms led to generation of the soluble 14 Kd native syncollin found in the exocrine pancreas. Unprocessed syncollin (Met1) would result in a protein of a predicted MW of 16Kd, whereas unprocessed syncollin (Met2) would have a predicted MW of 15Kd. Amino terminal sequencing of syncollin and *in vitro* transcription/translation $^{\pm}$

pancreatic microsomes of syncollin (Met2) revealed native syncollin has a MW of 14 Kd, and indicated that the N-terminal hydrophobic sequence is proteolytically cleaved as a signal pre-peptide (An, Hansen et al. 2000). In this study, immunoblot analysis of both Adv-Sync-Met1 and Adv-Sync-Met2 adenoviruses in isolated rat islets indicated that adenoviral-mediated expression of both forms of syncollin yielded the same 14Kd mature protein (Figure 3.2B). Based on the predicted MW of (Met1) and (Met2) syncollins, this suggested that a leader signal peptide was cleaved C-terminally of Gly_{32} in pre-syncollin (Met1) or Gly_{21} in pre-syncollin (Met2) to yield the same mature syncollin protein implying that both leader sequences function as signal peptides placing both Met1 and Met2 in the lumen of the RER/secretory pathway (Figure 3.2A). Subsequent characterization of Met1 and Met2 in exocrine cells revealed that the 5' extension characteristic of Met1 is most likely a cloning artifact (J.M. Edwardson, personal communication).

Immunofluorescence analysis of INS-1 cells infected with either Adv-Sync-Met1 or -Met2 (Figure 3.3) showed that mature syncollin (green) was localized in a punctate pattern with insulin positive (red) β-granules, which measured approximately 0.2-0.5 μm in size. These dimensions are consistent with the size of insulin containing large dense core vesicles in the β-cell. Co-localization of syncollin positive and insulin positive β-granules were depicted by orange/yellow coloration in the merged image (Figure 3.3). Syncollin localization to β-granules was also determined by adenoviral-mediated expression of a syncollin-GFP fusion protein (green; Figure 3.3, panel 7) in INS-1 cells. Syncollin-GFP expression also exhibited a punctate pattern that co-localized with insulin positive β-granules (orange/yellow; Figure 3.3, panel 9) of approximately 0.2-0.5 μm in

size. These data suggest that signal peptide cleavage caused syncollin to enter the secretory pathway at the RER and continue through the Golgi and TGN where syncollin was eventually targeted to the lumen of β-granules in pancreatic β-cells similar to secretory granule localization of syncollin expressed in AtT20 cells, as well as in exocrine cells (Hodel and Edwardson 2000).

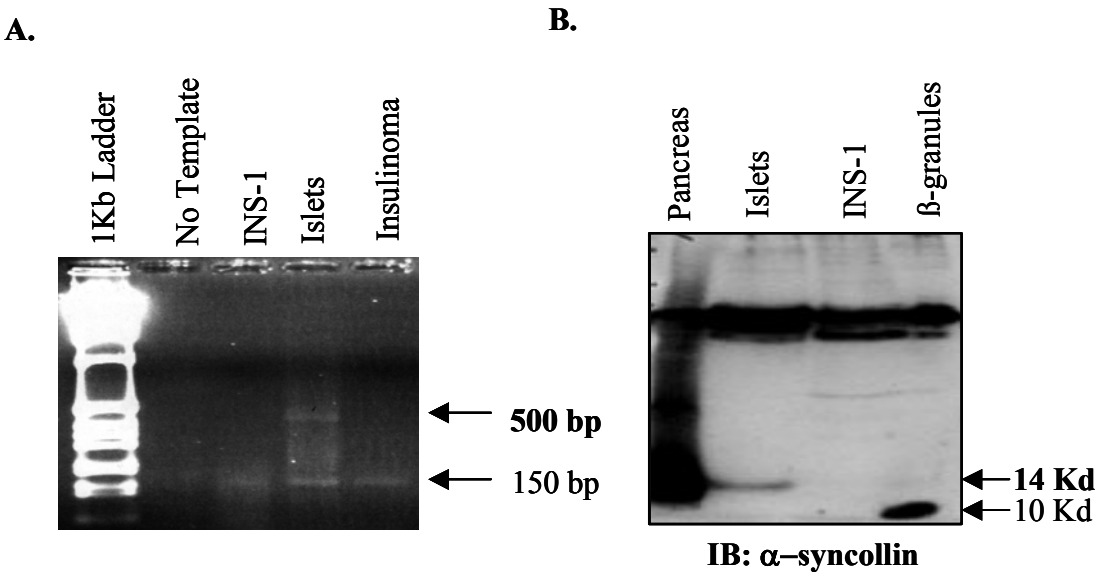

Figure 3.1: Syncollin is not endogenously expressed in β-cells; however, a 'syncollin-like' isoform may be present in β-cells. A. RT-PCR analysis of INS-1, isolated islets, and insulinoma tumor with syncollin-specific primers. The expected 500bp syncollin band is only present in islets. A 150bp 'syncollin-like' band is present in INS-1, islets, and insulinoma. B. Immunoblot analysis with α-syncollin polyclonal antibody on islet, INS-1 and purified β-granule lysates. The 14Kd syncollin band in islets and pancreas lysate; however a 10Kd band is also present in purified β-granules.

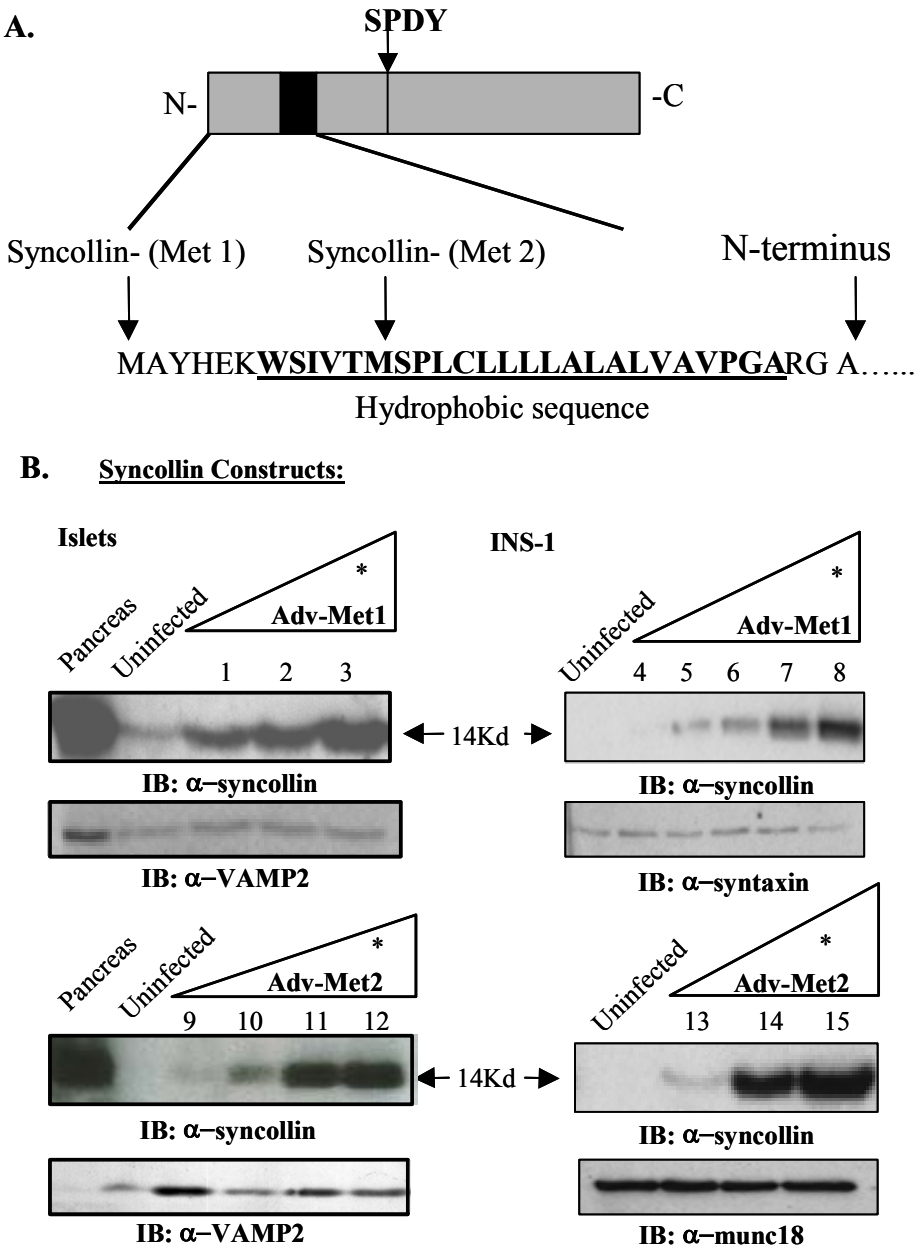

Figure 3.2: Adv-syncollin expression in islets and INS-1 cells. A. Schematic representation of syncollin containing two putative start sites (Met1 and Met2). B. Immunoblot analysis of isolated islets infected with $1X10^7$ (9), $4X10^7$ (1, 10) ,$1X10^8$ (2, 11), or $4X10^8$ (3, 12) pfu/islet and INS-1 cells infected with $5X10^8$ (4), $1X10^9$ (5, 13) , $2X10^9$ (6), $3X10^9$ (7, 14), $4X10^9$ (8, 15) pfu/well. (*) indicates Adv-syncollin infection for subsequent functional experiments.

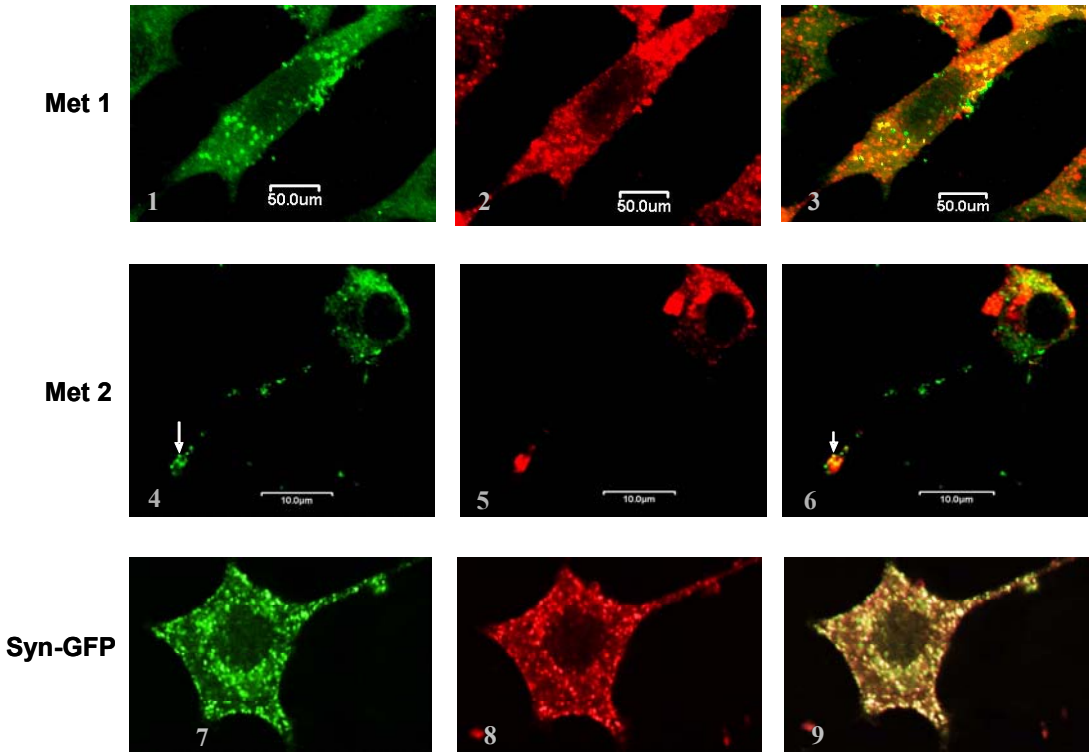

Figure 3.3: Adenoviral expressed syncollin and syncollin -GFP is localized to insulin positive β-granules in INS-1 cells. Immunofluorescence of Adv-Sync Met1 (1-3), Adv-Sync Met2 (4-6) and Adv-Sync GFP (7-9) infected INS-1 cells. Images pictured include syncollin-GFP (green; 7) and staining with anti-syncollin 'B' (green; 1,4), anti-insulin (red; 2,5,8) antibodies. The merged image (orange/yellow; 3,6,9) is an overlay of the digitally compressed images.

Syncollin expression in β-cells inhibits glucose-stimulated insulin secretion –It was investigated whether adenoviral-mediated expression of syncollin in β-granules affected glucose-stimulated insulin secretion from isolated pancreatic rat islets and INS-1 [832/13] cells. Experiments were performed using both Adv-Sync-Met1 and Adv-Sync-Met2 infected cells. Adenoviral-mediated expression of syncollin (Met1) in isolated rat islets significantly inhibited glucose stimulated insulin secretion to $18^{\pm}2.5\%$ ($p<0.05$, n=4) of control Adv-GFP infected islets, while adenoviral expression of syncollin (Met2) inhibited glucose stimulated insulin secretion to $65^{\pm}7.7\%$ ($p<0.05$, n=6) of control Adv-GFP infected islets (Figure 3.4B). Syncollin expression also significantly inhibited glucose-stimulated insulin secretion in INS-1 [832/13] cells to $52^{\pm}9.1\%$ ($p<0.05$, n=3) for Met1 and $40^{\pm}10.6\%$ ($p<0.05$, n=3) for Met2 compared to control Adv-GFP infected cells (Figure 3.4A); however, syncollin-GFP did not affect basal or glucose-stimulated insulin secretion (Figure 3.5). The variability between syncollin-Met1 and -Met2 to inhibit glucose-stimulated insulin secretion was most likely due to differences in syncollin expression level (Figure 3.1B). The longer signal peptide of Met1 may have caused delayed transport through the RER resulting in some degraded or misfolded syncollin (Met1). Alternatively, Met1 contains two AUG start sites, which could affect ribosomal recognition and could slow the synthesis at the translational level.

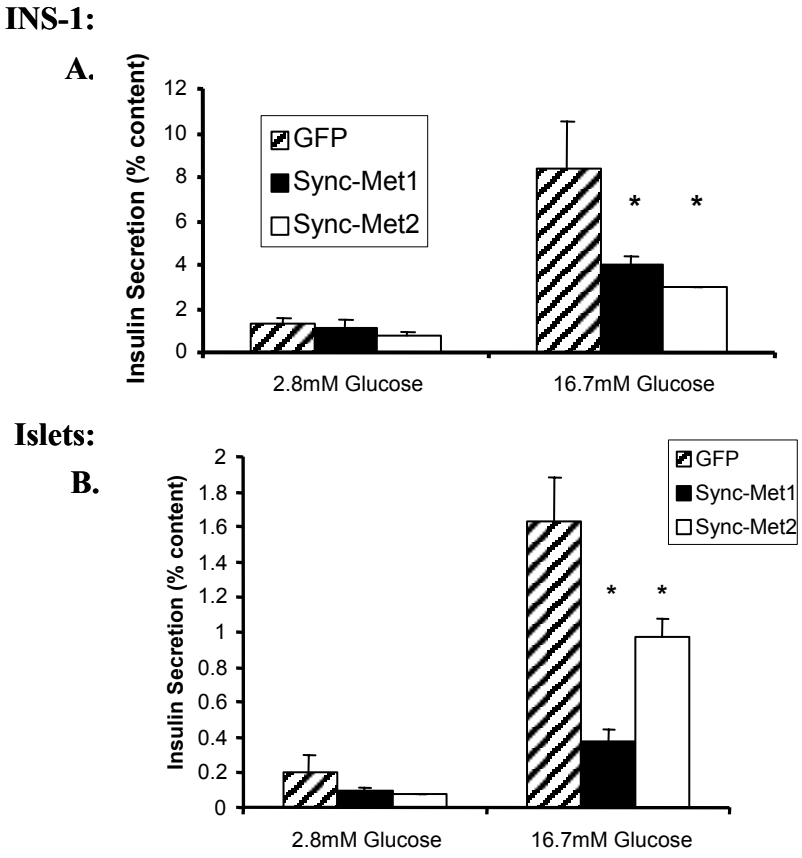

Figure 3.4: Effect of Adv-Sync expression on glucose-stimulated insulin secretion. A. INS-1 cells were infected with $4X10^8$ pfu/well of purified syncollin adenovirus (Met1 and Met2) and analyzed for insulin secretion as previously described. Data are expressed as % of insulin content (secreted/content) for n=6 experiments. B. Isolated rat islets were infected with $4X10^8$ pfu/islet of purified syncollin adenovirus(Met1 and Met2) and analyzed for insulin secretion as previously described. Data are expressed as % of insulin content (secreted/content) for n=6 experiments.

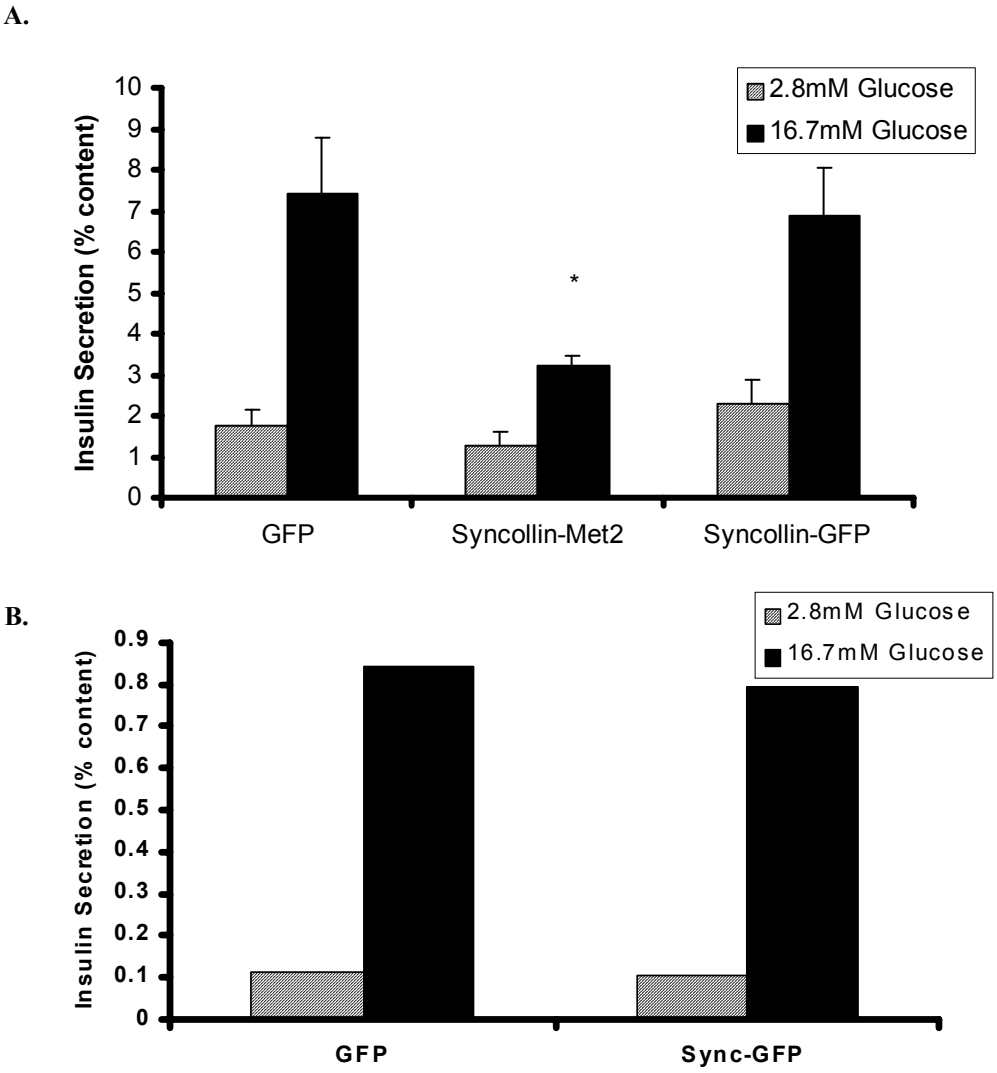

Figure 3.5: Syncollin-GFP does not affect glucose-stimulated insulin secretion in INS-1 [832/13] cells and isolated islets. A.Static glucose-stimulated insulin secretion of syncollin Met2 ($4X10^9$ pfu/well) and syncollin-GFP ($4X10^9$ pfu/well) in INS-1 cells; n=3. B. Static glucose stimulated insulin secretion of syncollin-GFP ($5X10^7$ pfu/islet); n=1.

To examine the kinetics of glucose-stimulated insulin secretion in Adv-Sync infected islets perifusion studies were conducted. In control Adv-GFP infected islets there was a typical biphasic insulin secretory response to glucose stimulation, consisting of a rapid first phase of insulin secretion over ten minutes, followed by a more sustained second phase of insulin release, as previously observed (Figure 3.6A) (Daniel, Noda et al. 1999). In contrast, perifusion of Adv-Sync-Met2 infected isolated islets revealed that the first phase of glucose-stimulated insulin secretion was significantly blunted to $53.4^{\pm}12.4\%$ ($p<0.05$, $n=5$; Figure 3.6A and 3.6B) of control Adv-GFP infected islets. Although the second phase of glucose-stimulated insulin secretion in Adv-Sync-Met2 infected islets was not significantly affected, there was a reduction in the accumulated insulin values compared to control Adv-GFP infected islets (Figure 3.6A and 3.6B). Perifusion of Adv-Sync-Met1 also displayed significantly blunted first phase to $32^{\pm}15.4\%$ ($p<0.05$, $n=5$) compared to Adv-GFP control infected islets. The second phase of Adv-Sync-Met1 was also significantly blunted to $44^{\pm}23.3\%$ of control Adv-GFP infected islets ($p<0.05$, $n=5$; Figure 3.6A and 3.6B). Basal insulin secretion was unchanged in Adv-Sync-Met1 or -Met2 infected islets compared to control Adv-GFP infected islets (Figure 3.6A and 3.6B).

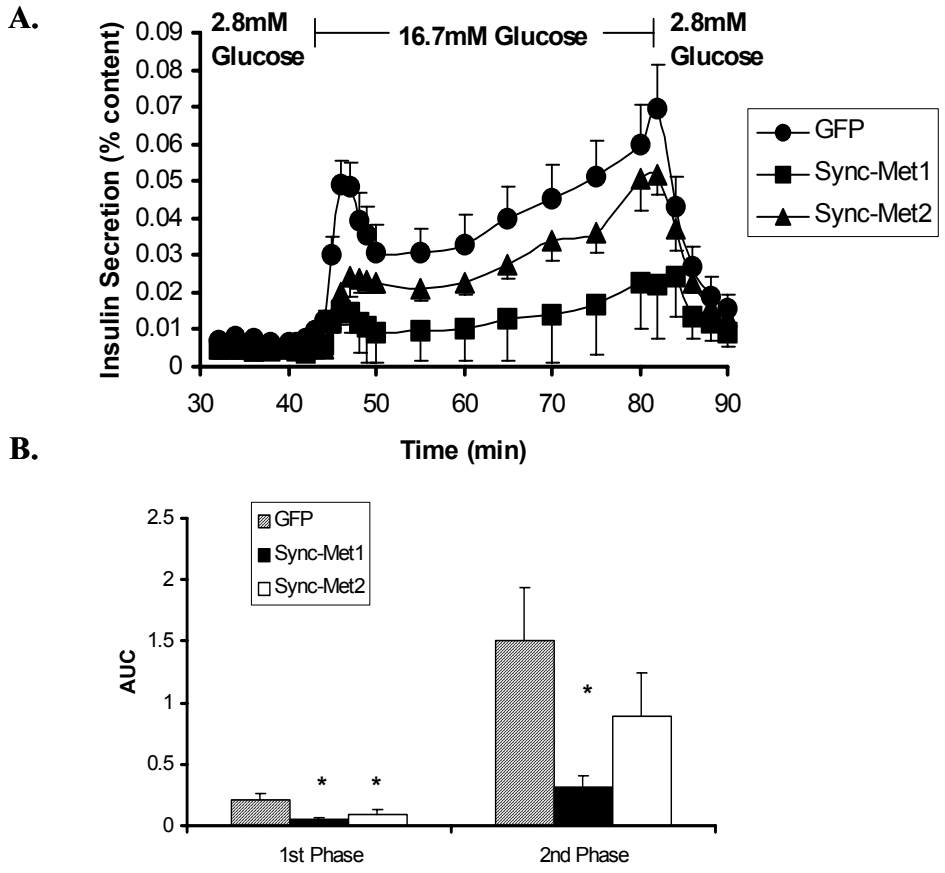

Figure 3.6: Syncollin expression inhibits the 1st phase of glucose-stimulated insulin secretion. A. Isolated rat islets were infected with $4X10^8$ pfu/islet and perifused as described. Data are expressed as % of insulin content for n=5 experiments. B. Calculated accumulated insulin release from the data in A. Accumulated insulin is the area under the curve for each phase and are then used to calculate the mean and S.E. Statistical significance (*) compared to GFP is $p<0.05$; n=5.

Glucose-stimulated insulin secretion can be potentiated by pharmacological agents, such as GLP-1 and glyburide, through different secondary signaling mechanisms (Boyd, Aguilar-Bryan et al. 1991; MacDonald, El-Kholy et al. 2002). The sulfonylurea, glyburide, augments insulin secretion by inhibiting the K_{ATP} channel thereby depolarizing the β-cell causing L-type Ca^{2+} channels to open instigating a rise in cytosolic $[Ca^{2+}]_i$ (Boyd, Aguilar-Bryan et al. 1991). Glyburide increased basal insulin secretion, as demonstrated previously in Adv-GFP infected islets (Boyd, Aguilar-Bryan et al. 1991). Since both forms of syncollin were processed to mature syncollin and glucose stimulated insulin secretion was similar for both forms, only syncollin-Met2 was used to examine the effect of other secretagogues on insulin secretion. Adenoviral-mediated expression of syncollin (Met2) significantly inhibited glyburide enhanced secretion to $60^{\pm}18.8\%$ (stimulatory) and $81^{\pm}16.9\%$ (basal) of control Adv-GFP infected islets ($p<0.05$, $n=4$; Figure 3.7). GLP-1 potentiates glucose-stimulated insulin secretion via augmentation of cAMP levels (MacDonald, El-Kholy et al. 2002). Potentiation of glucose-induced insulin secretion by GLP-1 was significantly enhanced at stimulatory glucose concentrations, as previously demonstrated in Adv-GFP infected islets (MacDonald, El-Kholy et al. 2002); however, adenoviral-mediated expression of syncollin-Met2 inhibited this potentiation to $54^{\pm}4.3\%$ of control Adv-GFP infected islets (Figure 3.7). These data suggest that expression of syncollin in β-granules inhibits regulated insulin secretion induced by other secretagogues and not only by glucose. Hence, syncollin likely mediates its inhibitory effect downstream of glucose metabolism.

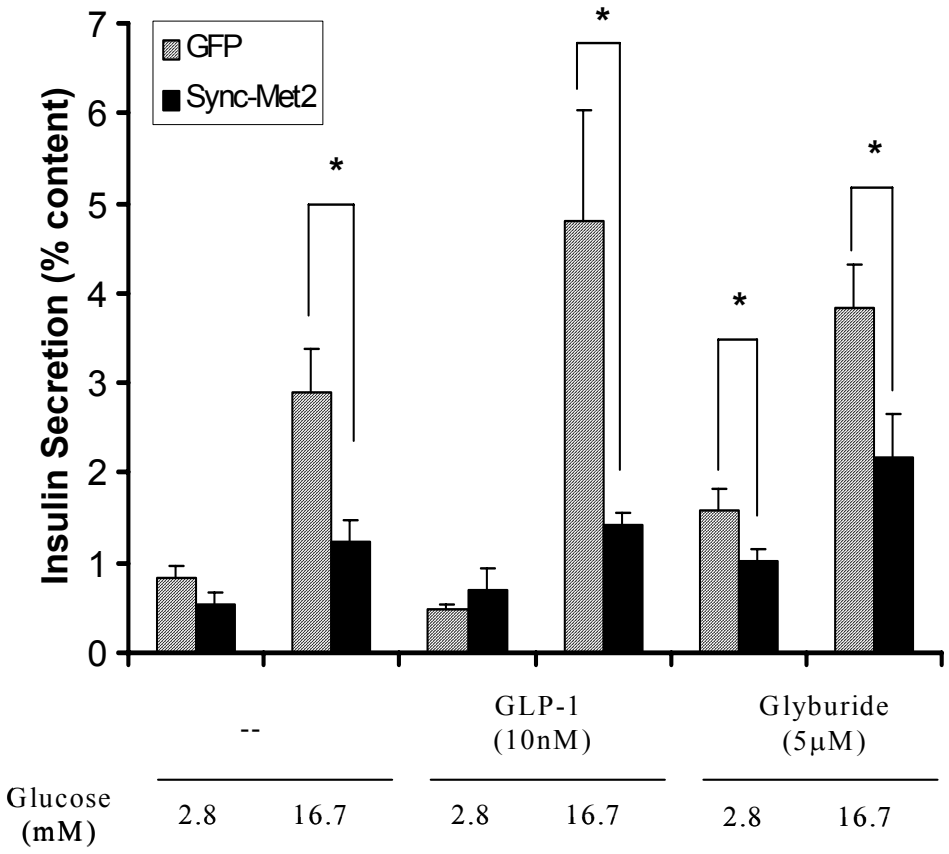

Figure 3.7: Effect of Adv-Sync (Met2) expression on stimulus-coupling mechanisms. Isolated rat islets were infected with $4X10^8$ pfu/islet of purified Adv-Sync-Met2 and Adv-GFP and analyzed for insulin secretion as described. Data are presented as the % of insulin content (secreted/content) for n=4 experiments. Statistical significance (*) is indicated where $p<0.05$.

Syncollin does not adversely affect insulin production – One possible explanation of the inhibitory effect of syncollin expression on secretagogue-induced insulin secretion is that insulin production in islet β-cells is adversely affected. In Adv-GFP, Adv-Sync-Met1 and -Met2 infected islets, proinsulin biosynthesis was increased approximately ten fold in response to glucose as seen previously (Alarcon, Leahy et al. 1995). Translational regulation of glucose-induced proinsulin biosynthesis was similar in both Adv-GFP and Adv-Sync-Met1 and -Met2 infected islets (Figure 3.8A) suggesting proinsulin production was unaffected by syncollin expression, as also indicated by the observation that there was no difference in insulin content in Adv-Sync-Met1 ($62^{\pm}7$ ng/islet; n=4) and Adv-Sync-Met2 ($67^{\pm}11$ ng/islet; n=6) infected islets compared to control Adv-GFP infected islets ($66^{\pm}11$ ng/islet; n=6; Figure 3.8B). Total protein synthesis was also normal in Adv-Sync-Met1 and -Met2 infected islets compared to control Adv-GFP infected islets (Figure 3.8C). These data indicated that the inhibition of regulated insulin secretion in syncollin-infected islets was not due to any adverse affects on insulin production or general protein synthesis.

Syncollin expression does not affect β-cell constitutive secretion – Adenovirally-mediated expression of syncollin-Met1 and -Met2 in β-granules (Figure 3.3) of β-cells indicated that as a secretory pathway protein it would traverse the ER-Golgi network prior to localization in β-granules. However, at the trans-Golgi network newly synthesized syncollin could be sorted to either the constitutive or regulated secretory pathways (Arvan and Castle 1998). Consequently, it was examined whether adenoviral-mediated expression of syncollin-Met2 in rat pancreatic islets might also affect the

constitutive secretory pathway. In order to examine constitutive versus regulated secretion in pancreatic β-cells, secreted alkaline phosphatase (sAP) was used as an artificial marker of constitutive secretion as previously described (Molinete, Lilla et al. 2000). Isolated rat islets were co-infected with Adv-sAP and either Adv-GFP (as a control) or Adv-Sync-Met2, and the amount of alkaline phosphatase secreted over a 1-hour incubation period was measured in parallel with glucose-stimulated insulin secretion in the same islets. The same amount of sAP activity was secreted (15-16% of content) at basal or stimulatory glucose concentrations, indicating that sAP was acting as a suitable marker of constitutive secretion (Table 3.1). In Adv-Sync-Met2 infected islets, glucose-induced insulin secretion was significantly inhibited to $62^{\pm}8.8\%$ ($p<0.05$, $n=5$) of control Adv-GFP infected islets (Table 3.1). In contrast, sAP constitutive secretion was unaffected in Adv-Sync infected islets compared to Adv-GFP control infected islets (Table 3.1). These data demonstrate that syncollin specifically inhibited regulated insulin secretion, but not constitutive secretion in isolated rat islets emphasizing the specific targeting of syncollin to β-granules in islet β-cells.

A. Proinsulin Biosynthesis

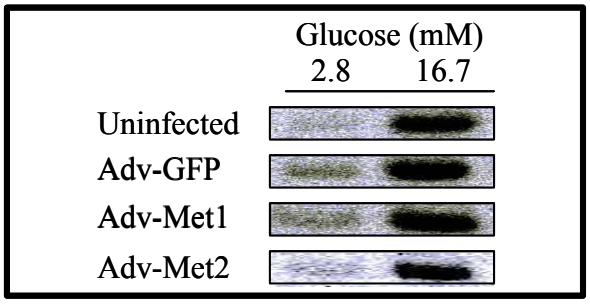

B. Insulin Content

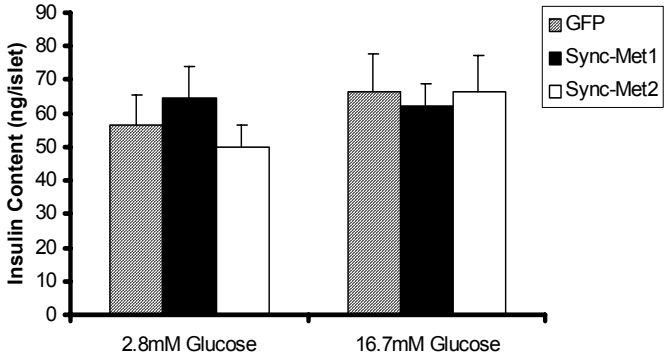

C. Protein Synthesis

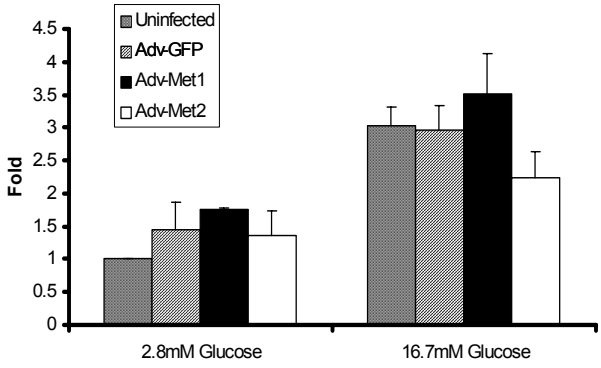

Figure 3.8: Advenoviral expressed syncollin does not affect A. proinsulin biosynthesis B. insulin content or C. total protein synthesis.

	Regulated Secretion		Constitutive Secretion	
	Insulin Secretion (% content)		sAP Secretion (% content)	
Glucose (mM)	2.8	16.7	2.8	16.7
Adv-GFP	0.20±0.1	1.63±0.25	15.1±1.9	16.3±2.2
Adv-Syncollin-Met2	0.08±0.1	0.83±0.12*	15.1±1.7	16.4±2.0

Table 3.1: Overexpression of syncollin affects regulated insulin secretion, but not constitutive secretion in β-cells. (* indicates statistical significant difference compared to control Adv-GFP infected islets, where $p<0.05$, n=3)

3.4. Discussion

In this study it has been ascertained that syncollin is not endogenously expressed in primary pancreatic ß-cells, due to the lack of syncollin expression in INS-1 cells and insulinoma tissues, which represent a predominantly homogenous β-cell population (Chick, Warren et al. 1977; Hutton 1989). Syncollin was identified in isolated islets at the mRNA and protein level; however, the apparent expression of syncollin in islets is possibly due to acinar cell contamination of the islet preparations, since syncollin expression is high in acinar cells (Tan and Hooi 2000) and obtaining a completely pure population of islets without acinar cells is problematical (Lacy and Kostianovsky 1967). It is possible; however, that other non-β-cell components of the islet, such as α-cells, δ-cells, pancreatic polypeptide, or ε-cells, could express syncollin. RT-PCR or immunoblot analysis of homogenous α-cell, δ-cell, ε-cell, or pancreatic polypeptide containing cell lines (i.e. α-TC1-9 cell line for α-cells) would examine whether syncollin is expressed in these other cell types. Additionally, isolated islets can be dispersed and sorted by a FACS sorter, utilizing cell-type specific markers, and subsequent RT-PCR or Northern blot analysis would also characterize syncollin expression in these cells.

Identification of an additional 10Kd band in an enriched β-granule subcellular fraction detected by the anti-syncollin polyclonal antibody and RT-PCR identification of a second smaller band in islets, INS-1 cells, and insulinoma tissue, suggests that a syncollin isoform may exist in β-cells. Until a syncollin isoform has been identified and characterized in β-cells; however, it is important to exercise caution in interpreting these results. Although the possibility of other 'syncollin-like' proteins present in the β-cell is intriguing, no known syncollin isoforms have been identified to date. Despite the lack of

syncollin isoforms currently in the database, other syncollin family members, that share a particular domain with syncollin, could still be expressed in the β-cell. The enriched β-granule fraction is not pure and likely contains only ~75-80% β-granules. The other 20-25% consists of plasma membrane, RER micelles, as well as minor mitochondrial membrane fractions (Rhodes and Halban 1987), which would introduce other non-β-granule membrane proteins perhaps containing homologous domains potentially recognized by the anti-syncollin polyclonal antibody. Identification and characterization of putative syncollin family members is a logical next step for follow-up studies and discussed in Chapter 5.

Using recombinant adenoviruses, syncollin (Met1 and Met2) was specifically targeted to ß-granules. Both forms of syncollin (Met1 and Met2) were proteolytically cleaved from their predicted 16kD and 15kD respective precursor forms to the same 14kD mature form. This implied that the N-terminal hydrophobic leader sequence of both syncollin isoforms was acting as a signal peptide that would place mature syncollin in the lumen of the rough endoplasmic reticulum (RER) in ß-cells during translation and, as with proinsulin trafficking, traverse from the *cis* to *trans* Golgi, where it would ultimately be sorted to the lumen of the ß-granule. This was also found for a chimeric protein consisting of GFP fused to the C-terminus of syncollin. The sorting of proinsulin to ß-granules is >99% efficient with structural features that are important in sorting (Rhodes 2000), as described in Cheaper 1. Likewise, sorting of syncollin to ß-granules was very efficient, not leaky. Therefore, syncollin likely contains a primary or secondary structure or even biological characteristics to sort it specifically to ß-granules, similar to that of proinsulin. Hence, these data reaffirm the observation that syncollin is packaged

into immature secretory granules in a homotypic manner and retained during granule maturation of neuroendocrine cells (Hodel and Edwardson 2000).

Intriguingly, mature syncollin (derived from either syncollin-Met1 or -Met2 precursors) inhibited secretagogue induced insulin secretion from primary ß-cells without affecting basal insulin secretion. This was a specific effect since translational control of proinsulin biosynthesis, general protein synthesis, islet insulin content, and constitutive secretion was all unaffected in Adv-Sync infected cells. Hence, syncollin appears to affect the regulated secretory pathway in pancreatic ß-cells downstream of the RER and Golgi apparatus, in secretory compartments, consistent with its restricted localization to ß-granules. For pancreatic ß-cells, this is the first example of a soluble factor located within a ß-granule capable of inhibiting insulin secretion, and implies that ß-granule elements and/or the intragranular environment are important contributing aspects to the mechanism of regulated insulin exocytosis. The syncollin-mediated inhibition of insulin secretion did not appear to be at the level of generating secondary signals necessary to evoke exocytosis, since syncollin significantly inhibited insulin secretion induced by both GLP-1 and glyburide. The rise in $[Ca2+]_i$ caused by either glucose or KCl depolarization and was also unaffected in Adv-Sync infected islet β-cells, suggesting that syncollin was inhibiting insulin secretion at the level of exocytosis (data not shown; in collaboration with Dr. Louis H. Philipson, University of Chicago). Under normal basal conditions there are several thousand ß-granules per pancreatic ß-cell existing mostly in a cytosolic storage compartment, with only around 50-100 docked at the plasma membrane in a so-called readily-releasable pool (Easom 2000; Rorsman and Renstrom 2003). The biphasic nature of glucose-stimulated insulin secretion is thought to reflect the initial release of ß-

granules in the readily-releasable pool (first phase) followed by ß-granules being brought in to replenish that pool and subsequently undergo exocytosis (second phase) (Daniel, Noda et al. 1999; Bratanova-Tochkova, Cheng et al. 2002). This second phase of secretion is longer and reflective of the additional transport, pre-docking, and docking steps in the exocytosis mechanism (Figure 1.2). In perifused Adv-Sync-Met1 and Adv-Sync-Met2 infected islet ß-cells, the first phase of glucose-induced insulin secretion was significantly inhibited relative to second phase. This suggested that the inhibitory effect of syncollin is likely mediated at the distal stages of the insulin exocytotic mechanism, probably at the level of docked β-granules in the readily-releasable pool.

The mechanism of insulin exocytosis is complex, involving interplay between several ß-granule, cytosolic and plasma membrane proteins. There are several stages to the mechanism including ß-granule transport, docking, priming, and membrane fusion events, each one of which has rate-limiting and regulatory aspects (Easom 2000). Moreover, it is currently unclear whether the final step in insulin exocytosis is actually fusion between the ß-granule and plasma membranes *per se*, or the transient formation of an exocytotic fusion pore, as originally proposed by Orci (Orci, Perrelet et al. 1977), for which some evidence has been recently uncovered (Takahashi, Kishimoto et al. 2002) and the kinetics of exocytosis would support (Olofsson, Gopel et al. 2002). However, for the ß-cell, the components of such a putative exocytosis fusion pore are unknown. Analogous to other neuroendocrine cell types, certain synaptotagmin and syntaxin isoforms (Hua and Scheller 2001; Wang, Grishanin et al. 2001), as well as syncollin oligomerization in pancreatic exocrine cells (Hodel, An et al. 2001; Geisse, Wasle et al. 2002), have been suggested as potential components of an exocytotic fusion pore.

Although the mechanism by which syncollin functions to inhibit insulin exocytosis is undetermined, it is worthwhile speculating on possible scenarios with which intragranular syncollin could affect insulin exocytosis. Interestingly, expression of the syncollin-GFP chimera, although efficiently targeted to β-granules, had no effect on glucose-stimulated insulin secretion implying the intrinsic secondary structure of syncollin is important in the mechanism of syncollin inhibition in β-cells. It is undetermined; however, whether the GFP portion of the chimera prevents syncollin homo-oligomerization, which is likely an important aspect of syncollin function. Direct evidence of homo-oligomerization in β-cells could be assessed by deoxycholate sucrose gradients of INS-1 lysates as described (An, Hansen et al. 2000). Nonetheless, native syncollin expression in pancreatic β-cells significantly inhibits secretagogue-induced insulin secretion. This raises the possibility that introduction of syncollin to β-cells is interfering with the function of an endogenous 'syncollin-like' protein that, in turn, impedes the insulin exocytotic mechanism, and that this ability is lost within a different structural conformation of syncollin when expressed as a syncollin-GFP chimera.

Another possibility for syncollin inhibition of insulin secretion could be that syncollin reduces the number of competent granules available for secretion. Recent data suggests that syncollin expression in erythrocytes resulted in lysis of erythrocytes *in vitro*. Furthermore, syncollin overexpression in AtT20 cells reduced the number of LDCV in the active zones for secretion in AtT20 cells, ultimately inhibiting adrenocorticotrophic hormone (ACTH) secretion. Together these data suggest that syncollin may function in the destruction of LDCV in neuroendocrine cells prior to stimulated secretion (Waesle, Hays et al. 2004). However, these studies did not examine

secretory protein transport through pulse chase analysis; therefore, it is unknown whether the decrease in ACTH secretion was due to defects in secretory granule protein transport from the Golgi to LDCV. Previous studies with syncollin null mice displayed defects in secretory protein transport, suggesting the lack of secretion seen in the AtT20 cells, INS-1 cells, and isolated islets may be due to improper secretory hormone transport to LDCV (Antonin, Wagner et al. 2002). Pulse chase experiments analyzing proinsulin and other secretory protein transport, such as PC2 or carboxypeptidase H, in Adv-GFP and Adv-syncollin infected cells would determine whether defects in secretory protein transport could explain the inhibition of insulin secretion. Furthermore, electron microscopy of stimulated and unstimulated INS-1 cells could examine the number of β-granules localized to active zones of secretion or possibly determine whether there is a decrease in the amount of granules in the readily-releasable pool of granules.

Alternatively, syncollin could be inhibiting insulin secretion by chelating low molecular weight ions or factors involved in insulin exocytosis. Syncollin was originally identified as a calcium-dependent syntaxin binding-protein (Edwardson, An et al. 1997), suggesting syncollin could chelate intragranular calcium ions. It is hypothesized that intragranular calcium and maintenance of the proton gradient is important in priming the ß-granules for exocytosis (Barg, Huang et al. 2001; Mitchell, Lai et al. 2003). However, intragranular calcium and acidic pH are important in proinsulin processing (Hutton 1982). If syncollin chelated calcium or disrupted the proton gradient in β-granules, proinsulin conversion may be inhibited.

Regardless of the means by which syncollin inhibits regulated insulin secretion, the evidence outlined in this study provide a novel insight into the mechanism of insulin

exocytosis where a soluble factor located within the lumen of a ß-granule can inhibit secretagogue-induced insulin secretion. It has been previously proposed that only ß-granule membrane proteins that have domains exposed on the cytosolic surface (*e.g.* VAMP-2 (Hua and Scheller 2001), synaptogamin-III and -VII (Gao, Reavey-Cantwell et al. 2000), rab3A (Yaekura, Julyan et al. 2003)) transiently interact with certain cytosolic and plasma membrane proteins to promote insulin exocytosis. However, intragranular proteins and/or other factors within the ß-granule environment (*e.g.* intragranular [Ca2+] (Mitchell, Pinton et al. 2001)) should now also be considered to make a contribution to the control of insulin exocytosis.

CHAPTER FOUR

Syncollin-GFP and Syncollin-dsRFP: β-granule Specific Markers to Examine the Dynamics of Insulin Exocytosis

4.1. Introduction

Recent technological advances have enabled scientists to examine the spatiotemporal dynamics of insulin β-granule exocytosis in greater detail than previously possible. Initially, measurement of insulin exocytosis was limited to biochemical analysis of insulin release into the extracellular milieu by radioimmunoassay (RIA) and ELISA or by secondary amperometric or capacitance techniques, which may or may not detect β-granule exocytosis *per se*. Although a useful tool to compare differences in insulin secretion due to experimental manipulation of the cells (i.e. via pharmacological agents, modification of protein expression, etc), the temporal resolution of the biochemical assay to directly measure insulin release is limited to minutes, much slower than membrane fusion in β-cells is thought to occur (Rorsman and Renstrom 2003). Electrophysiological analysis of membrane capacitance enhanced the temporal resolution to milliseconds, by measuring changes to the surface area of the cell (Barg, Ma et al. 2001). However, this approach measures the net change to the surface area and cannot distinguish β-granule exocytosis from other events, which may alter the β-cell surface area, such as endocytosis or exocytosis of GABA-containing synaptic-like vesicles present in the β-cell. Furthermore, both capacitance measurements and biochemical secretion assays indicate exocytosis has occurred, but cannot reveal any pre- or post-exocytotic mechanistic details, such as pore formation. This limitation is overcome

utilizing optical microscopy in combination with novel fluorescent probes. Laser scanning confocal microscopy allows for examination of thin sections in the XYZ planes with minimal background interference from the remainder of the cell, thereby permitting visualization of individual exocytotic events (Rorsman and Renstrom 2003). Evanescent wave (or total internal reflective fluorescent - TIRF), microscopy limits the excitation of the fluorophore to within 100nm of the coverslip, ensuring only emitted fluorescence from granules in the vicinity of the plasma membrane are visualized (Sako and Yanagida 2003). These optical techniques are dependent on fluorescent markers that allow discrimination of β-granules from other cellular components.

Fluorescent labeling of cellular compartments in live cells is achieved through either fluorescent dyes or protein chimeras with fluorescent tags (Rorsman and Renstrom 2003). Takahashi *et al* examined fusion pore dynamics by two-photon confocal microscopy with sulforhodamine B (SRB), a fluid phase tracer that resulted in transient SRB spot formation and ultimate disappearance of the spot adjacent to the plasma membrane upon stimulation (Takahashi, Kishimoto et al. 2002). Although this study provided insights into membrane fusion, the use of fluorescent dyes in this manner does not allow for analysis of other exocytotic stages prior to membrane fusion. Several other studies have evaluated these pre-fusion events as well as membrane fusion with β-granule specific protein chimeras, (including synaptotagmin III, VAMP-2, proinsulin, IAPP, and phogrin) containing fluorescent tags, such as green fluorescent protein (GFP) (Pouli, Emmanouilidou et al. 1998; Tsuboi, Zhao et al. 2000; Rorsman and Renstrom 2003; Tsuboi and Rutter 2003; Tsuboi and Rutter 2003). However, these proteins are all endogenous components of the β-granule. Some of which are involved directly in the

exocytotic machinery (e.g. synaptotagamin III, VAMP-2) and consequently may have effects that reduces exocytosis introducing additional complexity in the analysis of these studies (Rorsman and Renstrom 2003). Others are not as efficiently targeted to β-granules (e.g. proinsulin-GFP and IAPP-GFP) and may detect other vesicular trafficking events (Pouli, Emmanouilidou et al. 1998). Some are even cytotoxic to islet β-cells, as with phogrin-GFP (Hutton, personal communication). Since syncollin-GFP was very efficiently targeted to β-granules, did not adversely affect insulin secretion, and syncollin is not endogenously expressed in β-cells (as discussed in detail in Chapter 3), syncollin-GFP could be an ideal β-granule specific marker for examination of spatiotemporal exocytotic dynamics in live β-cells.

4.2. Materials and Methods

Real-time Laser Scanning Confocal Microscopy – INS-1 cells were grown on Delta T (0.17mm) circular black dishes designed for the Delta T heated stage and infected with $5X10^{10}$ pfu/plate of Adv-sync-GFP adenovirus for four hours. Cells were then allowed to express syncollin-GFP for twenty-four hours prior to visualization. Cells were incubated for one hour in 2.8mM glucose KRB and transferred to a Delta T heated stage/objective setup where temperature was kept at 35°C throughout imaging. Confocal microscopy was performed with an Olympus FV500 equipped with Fluoview software using a 60X UPLAPO objective on an Olympus IX81 inverted microscope. Continual XY scans over ten minutes with a multi-argon laser was used to excite EGFP at 488nm and emission at 507nm. Compression of the images into .AVI format was done with Microsoft VidEdit software.

Syncollin-dsRFP adenovirus construction – Syncollin was tagged with *Discosoma sp.* red fluorescent protein (dsRFP) by subcloning dsRFP into pBluescript-syncollin between SmaI and NotI resulting in seven amino acid linker region at the C-terminus of syncollin. Syncollin-dsRFP was then introduced into pShuttle-CMV between SalI and NotI. The PNRI Viral Vector Core performed cloning, recombination, and adenovirus purification of syncollin-dsRFP.

4.3. Results

Syncollin-GFP as a β-granule marker for real-time confocal imaging – It was previously demonstrated that syncollin-GFP is localized to β-granules; however, glucose stimulated insulin secretion was unaffected compared to control Adv-GFP infected cells (Chapter 3). These data suggest that syncollin-GFP can be utilized as a β-granule specific marker to follow β-granule movement in real-time by confocal microscopy. Live INS-1 [832/13] cells infected with Adv-Sync-GFP were stimulated with glucose and visualized by confocal microscopy by continual XY scans occurring approximately every seven seconds over a twenty-six minute period. Individual images were merged into a .mov file allowing visualization of consecutive events (Movie Sgglu). Individual β-granules underwent small directional motions from the interior of the cell to the plasma membrane. Sequential images magnifying the same area captured one β-granule progressing towards the plasma membrane and eventual exocytosis as indicated by changes in β-granule position followed by loss of fluorescence at the plasma membrane at 15min 31sec (Figure 4.1A). Other β-granules in the interior of the cells underwent random or directional movement; however, those at the plasma membrane were

immobile, suggesting the β-granules were morphologically docked at the plasma membrane. These data suggest that sustained insulin secretion includes β-granule transport from storage pools within the interior of the cell.

In addition, most β-granules underwent a transient loss of fluorescence during stimulation with glucose, as demonstrated by the reemergence of the β-granule highlighted by the arrow (Figure 4.1A). However, occasionally β-granules were detected with a complete loss of fluorescence, suggesting total membrane fusion and release of intragranule cargo (Figure 4.1B). These data indicate that both transient and total membrane fusion occur in β-cells and that first phase secretion is largely due to release of morphologically docked β-granules at the plasma membrane.

Syncollin-dsRFP infection following initial syncollin-GFP infection of INS-1 cells labels distinct pools of β-granules – Syncollin was tagged with dsRFP, which has a different excitation and emission spectra than GFP, to enhance the analysis of β-granule trafficking and exocytosis. Although dsRFP requires an additional autocatalytic modification, the maturation and folding process of GFP and dsRFP undergo similar slow kinetics to yield the fluorescent probes (Miyawaki, Sawano et al. 2003). Therefore, it was hypothesized that variation in the time of dual infection, might result in localization of syncollin-GFP and syncollin-dsRFP to different β-granule populations on the basis of granule age. Initial evaluation of syncollin-dsRFP compared to syncollin-GFP over the same infection time period in different cells identified small, punctate spots approximately 0.5μm in size indicative of β-granule localization throughout the intracellular space (Figure 4.2). Simultaneous co-infection of INS-1 cells with Adv-

Sync-GFP and Adv-Sync-dsRFP co-localized to the same β-granules throughout the intracellular space; however, overall, fewer β-granules contained syncollin-dsRFP in these cells, which was likely due to decreased syncollin-dsRFP levels compared to syncollin-GFP (Figure 4.3A). Delayed infection of Adv-Sync-dsRFP by twenty-four hours post Adv-Sync-GFP infection seemed to label distinct pools of β-granules, localized primarily in the perinuclear region of the cell, suggesting localization to β-granules newly derived from the Golgi apparatus; whereas, syncollin-GFP labeled β-granules were distributed throughout the intracellular space (Figure 4.3B). The transfection efficiency of the same cell containing both adenoviruses was approximately 10-15% when administered consecutively, suggesting an exclusionary effect once cells were infected with adenovirus (data not shown). These data indicate syncollin-dsRFP is also a useful β-granule marker, which can be used in conjunction with syncollin-GFP to distinguish newly synthesized β-granules.

A.

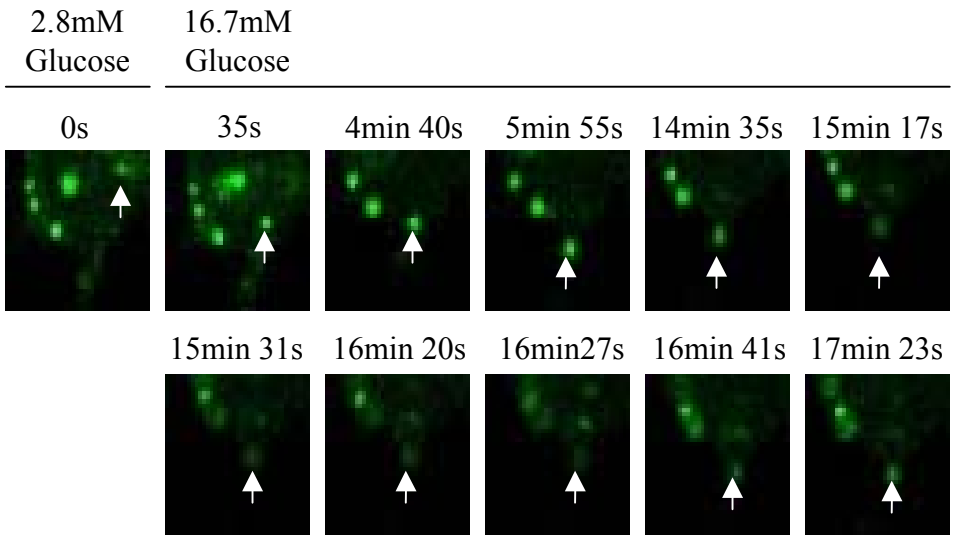

B.

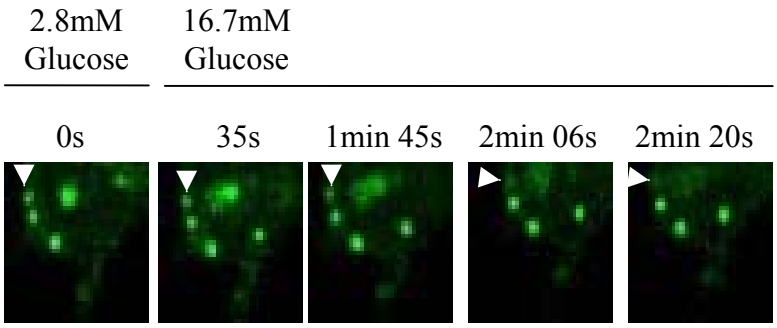

Figure 4.1: Captured frames from syncollin-GFP movie highlighting individual β-granule movement and exocytosis. A. Arrow indicates β-granule transport overtime and eventual exocytosis. Notice that exocytosis of the transported β-granule occurs during the 2nd phase of insulin secretion. B. Example of complete membrane fusion. Punctate spot fluorescence decreases over time indicative of exocytosis.

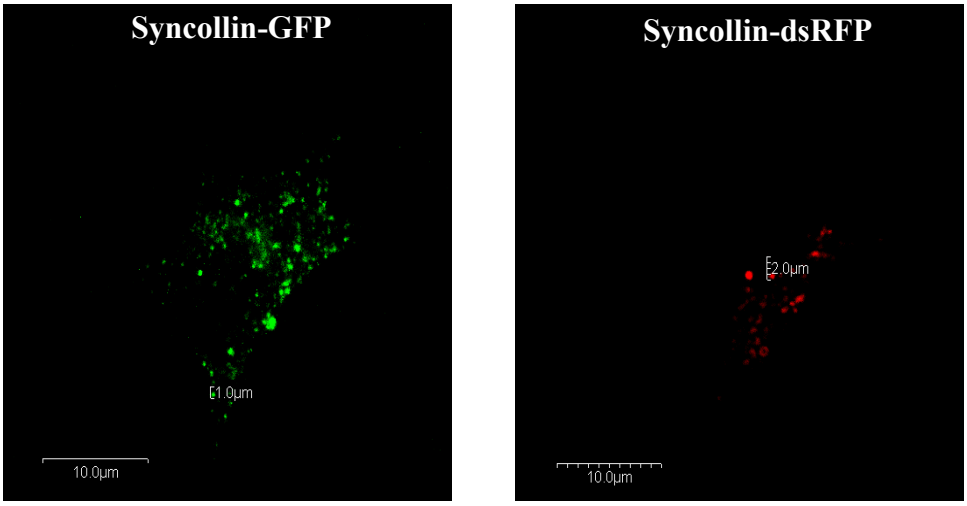

Figure 4.2: Syncollin-GFP and syncollin-dsRFP label β-granules. Syncollin-GFP (green) and syncollin-dsRFP (red) individually infected INS-1 cells display punctate spots of ~0.5µm in size.

A.

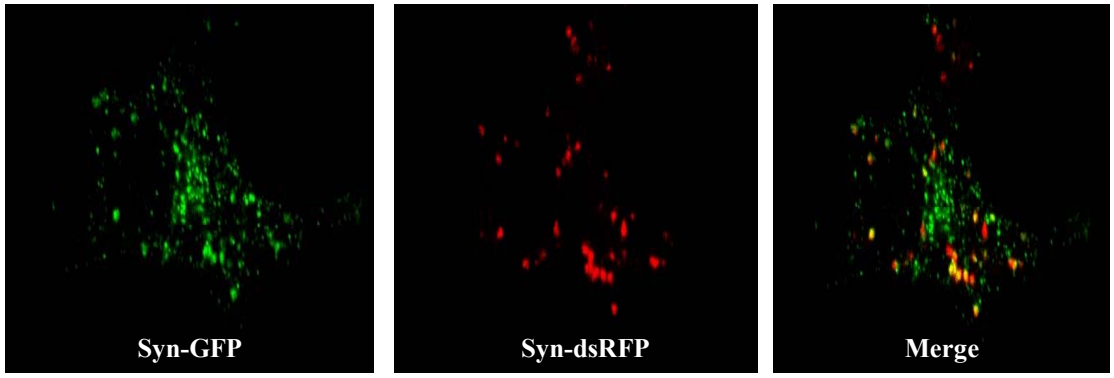

B..

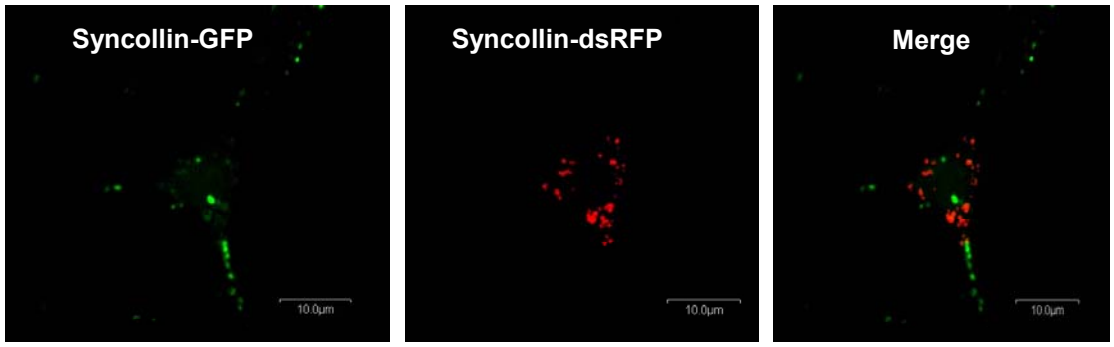

Figure 4.3: Syncollin-GFP co-infection with syncollin-dsRFP labels distinct pools of β-grnaules. A. Simultaneous co-infection of syncollin-GFP and syncollin-dsRFP depicting colocalization within the some of the same β-granules (yellow, Merge). B. Infection with syncollin-dsRFP occurs 24 hours after infection with syncollin-GFP. Syncollin-dsRFP containing β-granules occur in the perinuclear region of the cell, indicative of early β-granules.

4.4. Discussion

The data presented reveals initial evidence supporting technological applications of syncollin fluorescent fusion proteins, which were based on the conclusions reached through the examination of syncollin in β-cells (Chapter 3). This research begins to provide evidence that syncollin-GFP and syncollin-dsRFP can be successfully utilized in advanced optical applications to examine the spatiotemporal dynamics of pre-exocytotic events in the β-cell. Not surprisingly, fusion of syncollin with different fluorophores other than GFP still results in β-granule localization. It is further probable that syncollin-dsRFP would also function similar to syncollin-GFP, although syncollin-dsRFP was not analyzed for effects on insulin secretion. That being said, dsRFP is a large, tetrameric protein implying any steric hindrance GFP introduces to prohibit syncollin inhibition of insulin exocytosis likely applies to syncollin-dsRFP as well (Miyawaki, Sawano et al. 2003). Regardless, further characterization of syncollin-dsRFP co-localization with insulin by immunofluorescence and examination of insulin secretion in cells infected with Adv-sync-dsRFP would be necessary to adequately characterize this marker.

Several studies in the literature indicate both transient and complete membrane fusion occur in β-cells (as discussed in Chapter 1). The data presented here confirms the presence of both transient and total membrane fusion in β-cells validating the use of syncollin-GFP as a tool in the optical confocal analysis of the dynamics of insulin exocytosis. However, caution must be used in analyzing the preliminary real-time confocal data presented in this study. One of the difficulties in interpretation of this data is that the confocal imaging with this procedure was limited to continual XY scans, so disappearance of β-granule fluorescence, especially in the interior of the cell, could imply

movement into the Z plane, which would not be visualized. A more comprehensive confocal method to elucidate movement into the Z plane would be to utilize continual XYZ scans requiring more sophisticated computer software to compile the images into a format for analysis. Other comprehensive data validates the use of syncollin-GFP and provides insight into the dynamics of membrane fusion. Collaboration with Dr. Lou Philipson (University of Chicago) has demonstrated with syncollin-GFP using both laser scanning confocal and TIRF microscopy that β-granules which are released predominantly undergo complete membrane fusion (Ma, Bindokas et al. 2003 Submitted). Alternatively, Tsuboi and Rutter proposed that multiple forms of transient exocytosis are predominant in β-cells; however, these studies utilized VAMP2-GFP and phogrin-GFP, components in the exocytotic machinery, which may affect the results (Tsuboi and Rutter 2003). The dynamics of membrane fusion, albeit transient or complete, is still unresolved aspect of insulin exocytosis; however, the use of syncollin-GFP, although still in the initial phase of characterization, may resolve these issues in the future.

Preliminary data from this study indicates most β-granule movement occurs in the interior of the cell either directionally or in a random pattern, while β-granules at the plasma membrane appears immobile. Evidence from Duncan *et al* also observed LDCV movement in chromaffin cells undergo directional transport to the plasma membrane, movement in a random pattern, or are immobile at the plasma membrane (Duncan, Greaves et al. 2003) further validating syncollin-GFP in examination of insulin exocytotic mechanisms.

The use of syncollin-GFP alone is unable to determine whether newly synthesized or older β-granules were preferentially secreted. To analyze which population of β-granules were preferentially secreted, it was hypothesized that co-infection with syncollin-dsRFP after initial syncollin-GFP infection could be used. Indeed, syncollin-dsRFP β-granules appears to be localized exclusively to a perinuclear region deeper inside the β-cell, suggesting newly derived β-granules from the *trans* Golgi network. In contrast syncollin-GFP β-granules were localized to the distal areas of the β-cell near the plasma membrane. However, localization to this region of the cell is not necessarily direct evidence of β-granule age. Furthermore, due to low co-infection efficiency following delayed infection, syncollin-dsRFP and syncollin-GFP provide limited value to study preferential secretion of β-granules. An alternative solution to studying β-granule age is by constructing syncollin-dsRFP-E5, a red fluorescent protein derivative that changes from green to red over time and can more accurately distinguish β-granule populations by age as demonstrated by Duncan *et al* in chromaffin cells (Duncan, Greaves et al. 2003).

Regardless, the preliminary data with sequentially infected syncollin-GFP and syncollin-dsRFP does reveal some interesting aspects of insulin exocytosis. It has previously been shown that newly synthesized β-granules are preferentially secreted (Rhodes and Halban 1987). Based on the data presented in this study, new β-granules were localized deeper in the β-cell implying the importance of β-granule transport in the exocytotic mechanism for preferential release of the newly synthesized insulin. Interestingly, syncollin-GFP labeled β-granules were primarily directed to the tips of INS-1 cells, which is where active secretion was previously hypothesized to occur (Rivas

and Moore 1989). However, syncollin-dsRFP labeled β-granules were directed to other regions of the plasma membrane, not the tips. Supposing newly synthesized β-granules are preferentially secreted, this data implicates other regions of the plasma membrane not the tips are the active sites for hormone secretion.

In summary the data in this chapter, although preliminary, provide sufficient evidence that syncollin-GFP (and presumably syncollin-dsRFP) provide useful tools for the emerging technology of optical confocal and evanescent imaging to analyze the spatiotemporal dynamics of insulin exocytosis without the complexity of syncollin involvement in exocytosis. The efficient targeting to β-granules, the lack of endogenous syncollin expression and syncollin-GFP functional effects in β-cells, the adenoviral technology to infect primary cells, and the advantages over existing β-granule markers, as discussed previously, makes syncollin-GFP one of the best available β-granule cargo markers to date.

CHAPTER FIVE

FXYD6 is Expressed in Pancreatic β-cells and Influences β-granule Transport

5.1. Introduction

The FXYD family of proteins is a newly classified family of proteins, as discussed in Chapter 1.6.2, of which little is known about the functional significance in a physiological context (Geering, Beguin et al. 2003). Expression data for several FXYD proteins indicate that most have limited expression to certain tissues; suggesting functional roles of each FXYD protein may result in different physiological consequences for the cells (Sweadner and Rael 2000; Geering, Beguin et al. 2003). The tissue expression pattern and function of FXYD6, which has become the focus of this research, is largely unknown, although there is a concentrated expression in the hippocampus giving it the alternative name phosphohippolin (Yamaguchi, Yamaguchi et al. 2001; Geering, Beguin et al. 2003). Considering other members of the FXYD family are putative modulators of Na^+/K^+ ATPase activity it has been examined if FXYD6 has such activity when reconstituted in *Xenopus* oocytes; however, no modulation of the ATPase was seen and essentially its function is unknown (Yamaguchi, Yamaguchi et al. 2001). Based on the activity of other FXYD isoforms, as discussed in Chapter 1.6.2, it is possible that FXYD6 may play a role in insulin exocytosis. FXYD1, which has 48% homology to FXYD6 (Yamaguchi, Yamaguchi et al. 2001), was implicated in GLUT4 translocation in adipocytes, suggesting a possible role for FXYD proteins in granule transport (Walaas, Horn et al. 1999). Additionally, FXYD2 has been demonstrated to form 5nm pore structures in the plasma membrane, large enough to allow passage of

inulin (Sha, Lansbery et al. 2001). It has been observed that pore-like structures exist on the plasma membrane of β-cells, although their composition and possible role in insulin exocytosis remains unresolved (Orci, Perrelet et al. 1977; Takahashi, Kishimoto et al. 2002). Here characterization of FXYD6 endogenous expression in β-cells, as well as determination of a putative effect of FXYD6 on insulin secretion will be presented.

5.2. Materials and Methods

FXYD6-Myc, FXYD6-siRNA, and scrambled control (Neg) siRNA adenovirus construction –Cloning, recombination, and adenoviral purification techniques for Adv-FXYD6-Myc, Adv-FXYD6-siRNA, and Adv-Neg-siRNA were performed as described in Chapter2. Adv-FXYD6-Myc contained a Myc tag (EQKLISEEDL) on the C-terminus and was cloned between BglII and XbaI in the pShuttle-CMV adenoviral vector by the PNRI adenoviral vector core facility. Adenoviral MOI was evaluated by immunoblot with an anti-Myc antibody and no obvious effects on cell viability were seen at the levels of adenovirus used in these experiments. FXYD6-siRNA target sequence design was based on the protocol of Tuschl (Elbashir, Harborth et al. 2001). FXYD6 siRNA oligos contained the target sequence 5' AAGTCGCAGGTGCAAGTGCAGTT 3'. Neg-siRNA was a random computer-based scramble of the FXYD6 target sequence to which the sequence was 5' AATGTACGGAGACGGAGTCGCTT 3'. BLAST search revealed no significant homology to known proteins for either FXYD6-siRNA or Neg-siRNA. Adenoviral vector modification of pShuttle was designed based on the strategy by Shen *et al* (Shen, Buck et al. 2003). The CMV promoter and multi-cloning region was replaced with an H1 RNA promoter and multi-cloning stuffer region. Cloning of FXYD6-siRNA and Neg-siRNA target sequences was performed by annealing sense and

anti-sense 64mer oligonucleotides and inserting into the modified pShuttle-H1RNA vector between Bgl II and Hind III to create Adv-FXYD6-siRNA and Adv-Neg-siRNA vectors. Thorough determination of adenoviral MOI and expression length was evaluated for both siRNA vectors at the mRNA and protein level. No obvious effects on cell viability were seen at the conditions chosen for the siRNA experiments presented. Conditions used in these experiments utilized $6X10^9$ pfu/well of purified adenovirus infected for 16 hours. Following adenoviral infection, INS-1 media was replaced with fresh media and siRNA-mediated effects were allowed an additional 24 hours prior to experimentation.

Immunofluorescence –Immunofluorescence and staining were performed as described in Chapter 2. The lipophilic tracer, dialkylcarbocyanine or DiD (excitation 644nm; emission 665nm) was added for 30 seconds to fixed INS-1 cells after staining with primary and secondary antibodies. All cells utilized in immunofluorescence were incubated prior to fixation at 5.6mM glucose.

Sucrose Gradient – INS-1 cells were infected with $6X10^9$ pfu purified Adv-FXYD6-Myc for 16-18 hours then lysed in lysis buffer (50 mM HEPES (pH 7.5), 2mM Sodium Vanadate, 4mM EDTA, 1μM leupeptin, 10μg/ml aprotinin, and 1% deoxycholate) and sonicated on ice (10 seconds, 15 watts). 400 μg of protein was layered onto 7-15% or 0-7% continuous sucrose density gradients (50mM HEPES, 1% deoxycholate, and either 7-15% or 0-7% sucrose) and centrifuged at 125,000Xg for 16 hours. 200μl fractions were removed from the lower to upper portions of the gradient and concentrated with

Microcon YM 3,000 concentrators. Every other fraction was then analyzed by immunoblot with an anti-Myc antibody. The apparent MW of the fractions was determined with 100 μg of purified cytochrome c (12Kd) on sucrose gradients and analyzed by Coomassie blue staining.

5.3. Results

FXYD6 is specifically expressed in β-cells – It has been hypothesized that there may be a 'syncollin-like' protein in pancreatic β-cells (Chapter 3). RT-PCR analysis with conserved syncollin-specific primers revealed a 150bp band (Chapter 3), which when sequenced corresponded to rat FXYD6. Comparison of the FXYD6 nucleotide sequence with syncollin revealed only a 47% identity within the PCR product and a 31% identity overall between the two nucleotide sequences. However, the overall similarity between syncollin and FXYD6 at the amino acid level was only 19%; nonetheless, distinct domains including the 'DPFXYD domain', a signal peptide, and a small portion of a hydrophobic domain had significant homology (Figure 5.1). Examination of the protein primary structure suggested various similarities between the two proteins. FXYD6 has a predicted molecular weight of 10Kd, which corresponded to the molecular weight of the unidentified band present in immunoblot analysis with the anti-syncollin polyclonal antibody (Chapter 3; Figure 3.1). Sequence in the C-terminal end of the hydrophobic region of FXYD6 had significant similarity to syncollin, which is also a putative epitope recognition site for the anti-syncollin polyclonal antibody. Interestingly, the syncollin gene locus is located on human chromosome 19 immediately adjacent to other FXYD proteins (FXYD5, FXYD7, FXYD1, syncollin, and FXYD3). Based on these similarities, it was likely that FXYD6 may correspond to the unidentified 'syncollin-like'

protein alluded to in Chapter 3, as well as syncollin being an associate, evolutionarily-related member of the FXYD protein family.

FXYD6 (phosphohippolin) was originally cloned from a rat hippocampal cDNA library and expression of FXYD6 had been reported in heart, brain, lung, liver, kidney, and testis by Northern blot analysis (Yamaguchi, Yamaguchi et al. 2001). However, expression of FXYD6 had not been evaluated experimentally in pancreatic tissues. Human and mouse dEST search revealed FXYD6 expression in pancreatic islets, as well as normal mammary gland and fetal brain (Yamaguchi, Yamaguchi et al. 2001). Confirmation of FXYD6 endogenous expression in pancreatic islets and determination of islet cell-type expression, specifically whether expression of FXYD6 was unique to β-cells, was examined by RT-PCR with conserved primers corresponding to FXYD6. A 300bp band was identified in INS-1, islet and brain tissues, which when sequenced was identified as FXYD6 (Figure 5.2A). Thorough comparison of the sequence data from multiple sequence analyses revealed a single base mutation, which resulted in the amino acid, Ser_{41}, in islets instead of Leu_{41}, which was conserved in brain, INS-1 and the published phosphohippolin sequences from rat, mouse, and human (Figure 5.2B). It is likely that this alteration in the islet sequence was a result of an introduced mutation by Taq polymerase during the initial RT-PCR. Further comparison of FXYD6 sequence data to previously cloned rat phosphohippolin, revealed consistently that brain, islet, and INS-1 cells contain the amino acid Asn_{65} instead of Ser_{65}, as published in the rat phosphohippolin sequence. Conservation of Asn_{65} within the published mouse and human sequence for phosphohippolin suggests the likely amino acid in this position of the primary sequence is actually asparagine.

Other FXYD family members were also evaluated for expression by RT-PCR analysis with isoform-specific FXYD primers in a variety of tissues including brain, kidney, heart, human mammary tumor tissue, pancreatic rat islets, INS-1, and αTC1-9 cells. Expression for FXYD1 in heart and brain, as well as FXYD2 and FXYD 4 expression in kidney were consistent with previous publications in the literature (Figure 5.2) (Sweadner and Rael 2000). However, these isoforms were not expressed in either pancreatic islets or the clonal β-cell line, INS-1, suggesting that FXYD1, 2 and 4 are not expressed in β-cells (Figure 5.2). FXYD3 is typically ubiquitously expressed with enhanced expression also identified in mammary tumor (Sweadner and Rael 2000). Expression of FXYD3 was identified in heart, kidney, brain, INS-1 and αTC1-9 cells, with no expression in isolated islets (Figure 5.2). FXYD3 was not detected in mammary tumor tissue; however this may be indicative of this individual tumor cell line and not representative of published tumor expression data. Identification of FXYD3 in INS-1 and αTC1-9 cells is consistent with the expression of FXYD3 in immortalized cells and is probably not indicative of α- or β-cell expression, since no FXYD3 expression was detected in islet tissue. Previously, no published expression data has been determined for FXYD5 (Sweadner and Rael 2000), which was identified only in kidney and brain tissues, but not islet cells in this study (Figure 5.2). Interestingly, FXYD7 was expressed in heart, brain, islets, and αTC1-9 cells, but not INS-1 cells suggesting expression in islets is limited to α-cells (Figure 5.2). Expression of FXYD6 was confirmed in brain, INS-1, and islet tissues; however, no appreciable expression was detected in heart and kidney as previously reported. Regardless, these data suggest that FXYD6 is the only FXYD isoform endogenously expressed in β-cells.

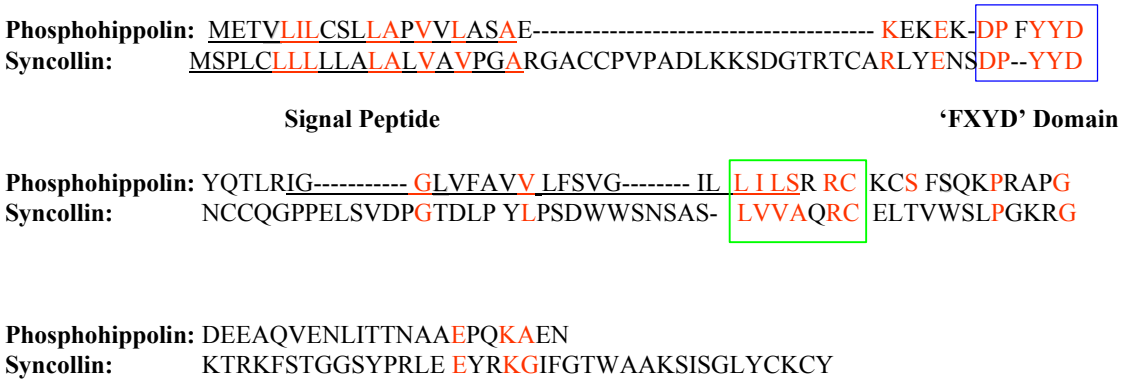

Figure 5.1: Amino acid comparison between syncollin and FXYD6 primary protein sequences. Conserved amino acids are indicated in red. Hydrophobic regions of each protein are underlined. DPFXYD domain is boxed in blue and putative anti-syncollin polyclonal epitope is in green.

A.

RT-PCR:

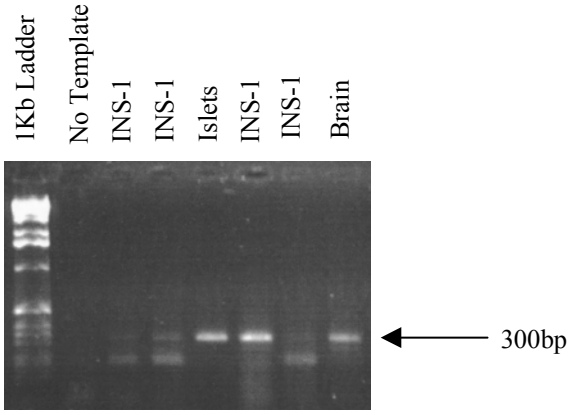

FXYD6-specific primers

B.

Phosphohippolin:	METVLILCSLLAPVVLASA--EKEKEKDPFYYDYQTLRIGGLVFAVV
Brain:	METVLILCSLLAPVVLASAAEKEKEKDPFYYDYQTLRIGGLVFAVV
Islets:	METVLILCSLLAPVVLASAAEKEKEKDPFYYDYQTLRIGGSVFAVV
INS-1:	METVLILCSLLAPVVLASA--EKEKEKDPFYYDYQTLRIGGLVFAVV
	Signal Peptide **'FXYD' Domain**

Phosphohippolin:	LFSVG ILLILSRRCK CSFSQKPRAPGDEEAQVENLITTNAAEPQKAEN
Brain:	LFSVG ILLILSRRCK CSFNQKPRAPGDEEAQVENLITTNAAEPQKAEN
Islets:	LFSVG ILLILSRRCK CSFNQKPRAPGDEEAQVENLITTNAAEPQKAEN
INS-1:	LFSVG ILLILSRRCK CSFNQKPRAPGDEEAQVENLITTNAAEPQKAEN

Figure 5.2: FXYD6 is endogenously expressed in endocrine cells. A. RT-PCR analysis of INS-1 cell, isolated rat islet, and brain cDNA with FXYD6 specific primers. B. Sequnce comparison of RT-PCR products from brain, islets, and INS-1 cells compared to published phosphohippolin (FXYD6). Hydrophobic regions are underlined. Amino acid differences between sequences are highlighted in red.

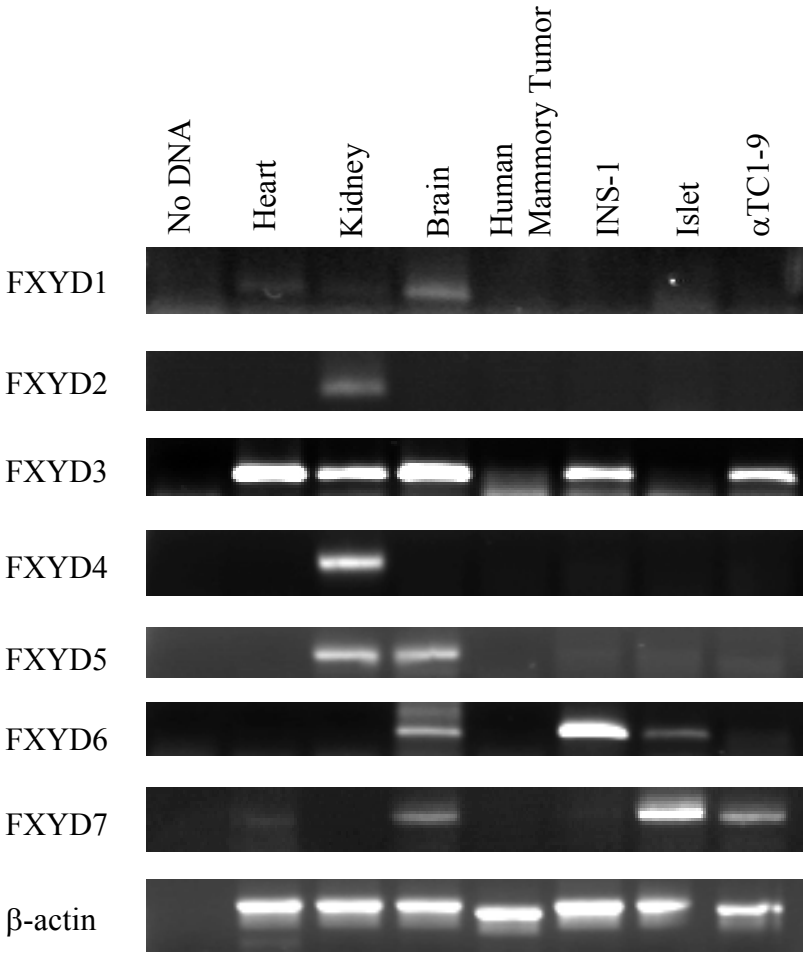

Figure 5.3: FXYD6 is the only isoform endogenously expressed in β-cells. FXYD7 is endogenously expressed in α-cells. A. RT-PCR analysis of heart, kidney, brain, human mammory tumor, INS-1 cell, isolated rat islet, and αTC1-9 cell cDNA with FXYD isoform-specific primers.

FXYD6 is localized to the plasma membrane – FXYD6 contains a hydrophobic domain, consistent with a putative trans-membrane region, from Ile_{38} to Ser_{57}, suggesting localization of FXYD6 to membrane compartments (Yamaguchi, Yamaguchi et al. 2001). Subcellular fractionation of INS-1 cells confirmed endogenous FXYD6 was localized to the membrane fraction consistent with the putative hydrophobic transmembrane domain predicted in the primary structure of FXYD6. Further characterization with enriched insulinoma subcellular fractions from cytosol, synaptic-like vesicles, and β-granules did not detect FXYD6, suggesting that the membrane localization of FXYD6 was in non-granule components of the β-cell (Figure 5.3). Detection of munc18/nSec1 in membrane and cytosolic fractions was consistent with published data confirming the integrity of the subcellular fractionation (Katagiri, Terasaki et al. 1995)(Figure 5.3), as previously indicated by enzyme markers for the different compartments (Chapter 2). Since available anti-FXYD6 antibodies were not appropriate for immunofluorescence techniques, evaluation of FXYD6 localization was examined by expression of adenoviral-mediated FXYD6 with a C-terminal Myc-tag allowing for immunofluorescence using anti-Myc antibodies. In these studies, FXYD6-Myc (green) localized to distinct regions of the plasma membrane with the lipophilic tracer DiD (red), used to identify the plasma membrane (Figure 5.4). These data indicate FXYD6 was localized to discrete patches of the plasma membrane.

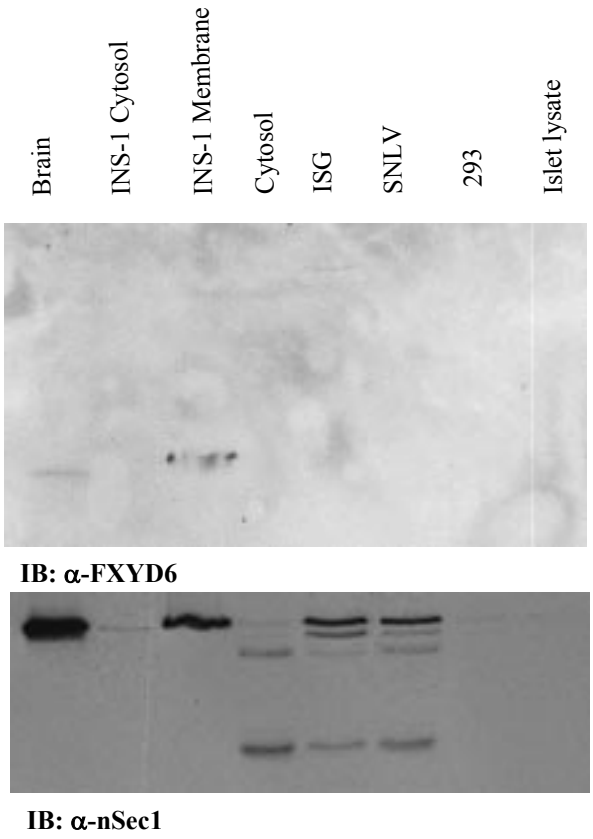

Figure 5.4: FXYD6 is localized to the plasma membrane. Differential centifugation of INS-1 cytosol and membrane fractions. SNLV, β-granule, and cytosol fractions are from insulinoma tumor subcellular fractionation. Immunoblot analysis with α-FXYD6 antibody recognizes FXYD6 in the INS-1 membrane fraction, but not in the other membrane fractions.

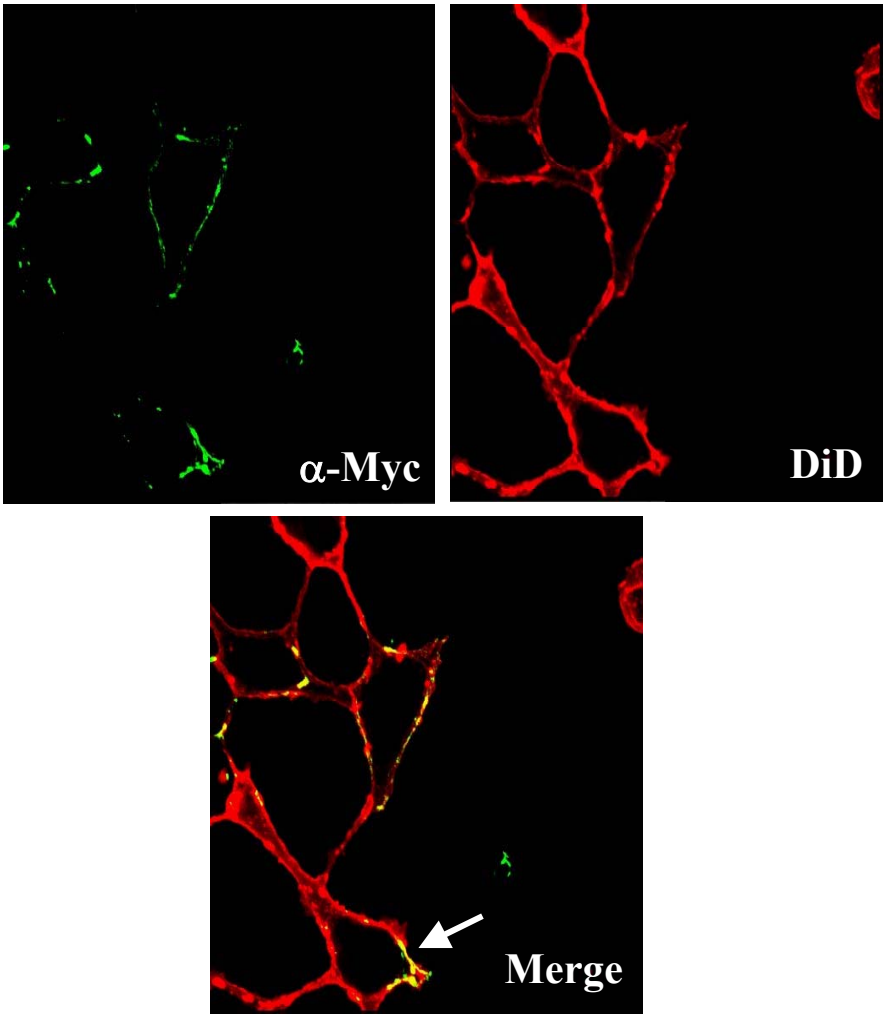

Figure 5.5: FXYD6-Myc is localized to distinct regions of the plasma membrane. Immunofluorescent confocal microscopy of INS-1 cells infected with Adv-FXYD6-Myc. Did=lipophilic tracer, dialkylcarbocyanine labels the plasma membrane. Co-localization of FXYD6 with the plasma membrane in INS-1 cells is depicted by arrow in the merged image (yellow).

FXYD6 influences β-granule distribution at the plasma membrane –Most β-granules are maintained in a cytosolic storage pool, with only ~1-5% morphologically associated with the plasma membrane in the readily-releasable pool (Rorsman and Renstrom 2003). Examination of β-granule distribution in INS-1 cells overexpressing FXYD6-Myc revealed most β-granules targeted to distinct regions of the cell and several morphologically associated with the plasma membrane compared to Adv-luciferase infected control INS-1 cells (Figure 5.6). To evaluate whether β-granule distribution correlated with localization of FXYD6, the expression of FXYD-Myc was reduced to $1X10^7$ pfu/well effectively decreasing the amount of FXYD6-Myc, which was previously revealed to localize to distinct regions of the plasma membrane (Figure 5.5). The β-granules (red) in cells expressing lower levels of FXYD6-Myc (green) seemed to be attracted to distinct regions of the plasma membrane FXYD6-Myc expression was concentrated (yellow) (Figure 5.6C). Control cells infected with Adv-luciferase displayed β-granule distribution (red) throughout the cytosol with few morphologically docked at the plasma membrane, indicative of normal β-granule distribution prior to glucose stimulation (Figure 5.6).

An approach to elucidate the function of proteins at the cellular level is achieved through RNA interference (RNAi), which accomplishes gene-specific reduction in protein levels via small-interfering RNA molecules (siRNA) directed against the protein of interest (Elbashir, Harborth et al. 2001). SiRNA-mediated reduction in FXYD6 expression was achieved in INS-1 cells at both the mRNA and protein level by FXYD6-siRNA adenoviral-mediated delivery (Figure 5.7). However, FXYD6 protein levels were also reduced, albeit to a lesser extent, with a scrambled FXYD6 control siRNA

adenovirus (Figure 5.7). Neither β-actin at the mRNA level nor β-catenin at the protein level were decreased in either Adv-FXYD6-siRNA or Adv-Neg-siRNA infected INS-1 cells compared to uninfected cells (Figure 5.7). These data indicate siRNA-mediated reduction in FXYD6 levels through RNAi methods. Analysis of β-granule distribution by immunofluorescence revealed no obvious differences in β-granule distribution in Adv-FXYD6-siRNA infected INS-1 cells compared to uninfected and Adv-Neg-siRNA infected INS-1 cells (Figure 5.8). Enhancement of FXYD6 protein levels altered β-granule distribution in INS-1 cells, implicating a role for FXYD6 in the influence of β-granule transport and/or docking at the plasma membrane.

Real-time confocal microscopy using syncollin-GFP labeled β-granules allows analysis of β-granule movement during glucose stimulation (Chapter 5). Overexpression of FXYD6-Myc resulted in β-granule localization to distinct regions of the plasma membrane as previously observed; however, minute granule movement was observed upon glucose stimulation (Movie Fxyd6). Based on these results, it was hypothesized that reduction in FXYD6 expression would affect β-granule transport to the plasma membrane. Indeed, Adv-FXYD6-siRNA infected INS-1 cells displayed erratic and misdirected β-granule movements in the interior of the cell over the ten-minute stimulation period (Movie Fsirna). In comparison, Adv-Neg-siRNA infected INS-1 cells display less β-granule movement (Movie Neg), which was comparable to that previously demonstrated by real-time confocal imaging in syncollin-GFP infected INS-1 cells (Chapter 4). These observations suggest FXYD6 functions as a molecular beacon directing β-granule transport to the plasma membrane.

A.

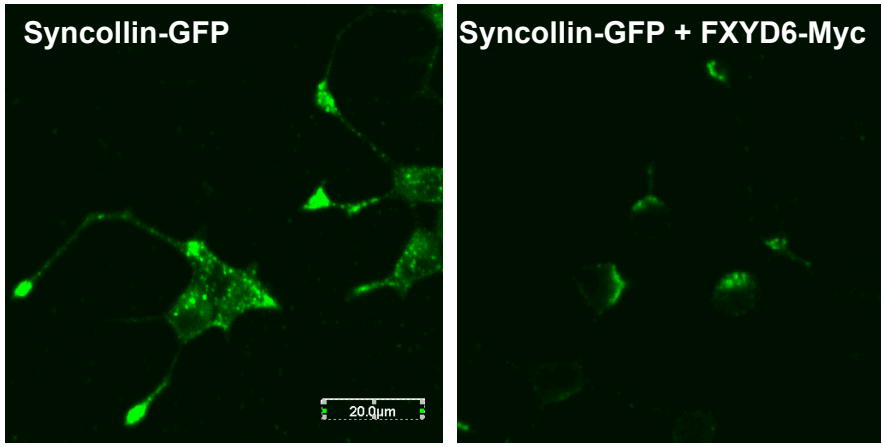

B.

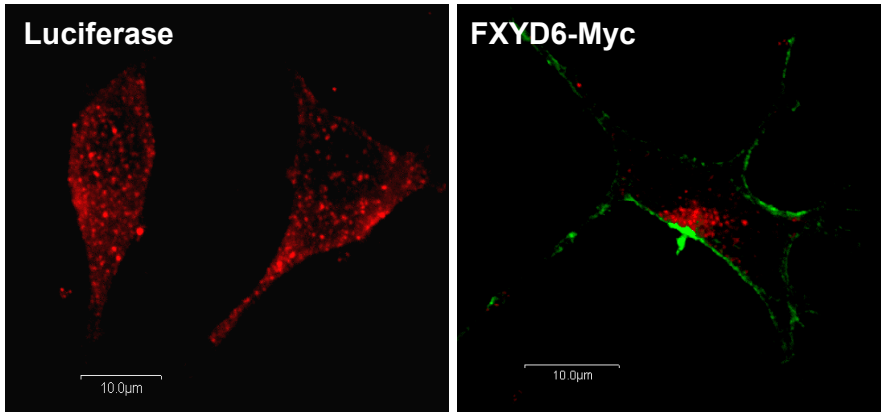

C.

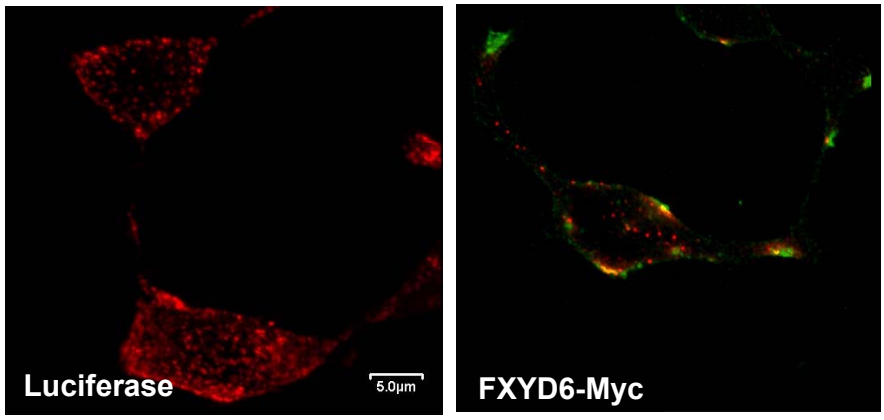

Figure 5.6: Insulin secretory granules are localized to distinct regions of INS-1 cell expressing FXYD6-Myc. A. Images are XY scans at 180X of syncollin-GFP infected INS-1 cells with or without Adv-FXYD6-Myc at $6X10^9$ pfu/well. B. Images are XY scans at 300X. Immunofluorescence of α-insulin (red), α-Myc (green), and merged images (yellow). Confocal microscopy of INS-1 cells infected with Adv-FXYD6-Myc at $6X10^9$ pfu/well. C. Confocal microscopy as in B. with INS-1 cells infected with Adv-FXYD6-Myc at $2X10^9$ pfu/well.

A. RT-PCR

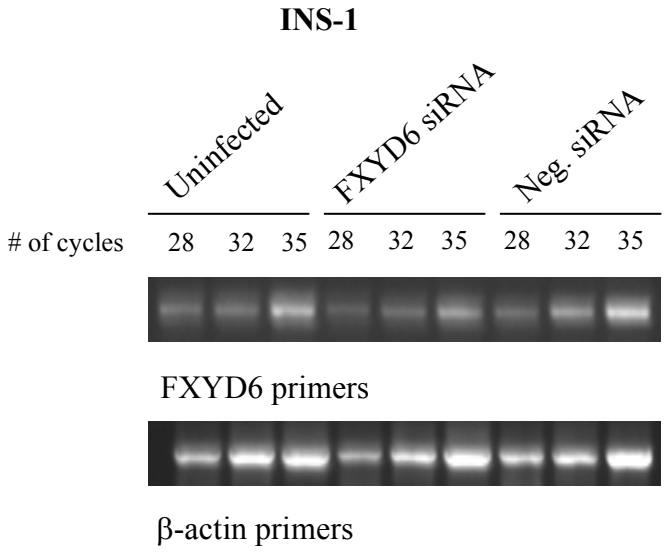

B. Immunoblot

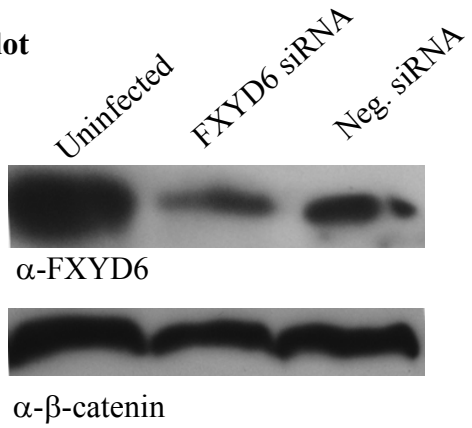

Figure 5.7: siRNA-mediated inhibition of FXYD6 mRNA and protein expression after 48 hours. A. RT-PCR with FXYD6 primers (or control: β-actin primers) on uninfected, scrambled (Neg) siRNA, and FXYD6 siRNA cDNA from INS-1 cells ($6X10^9$ pfu/well) . B. Immunoblot with α-FXYD6 antibody or α-β-catenin (control) on INS-1 lysates.

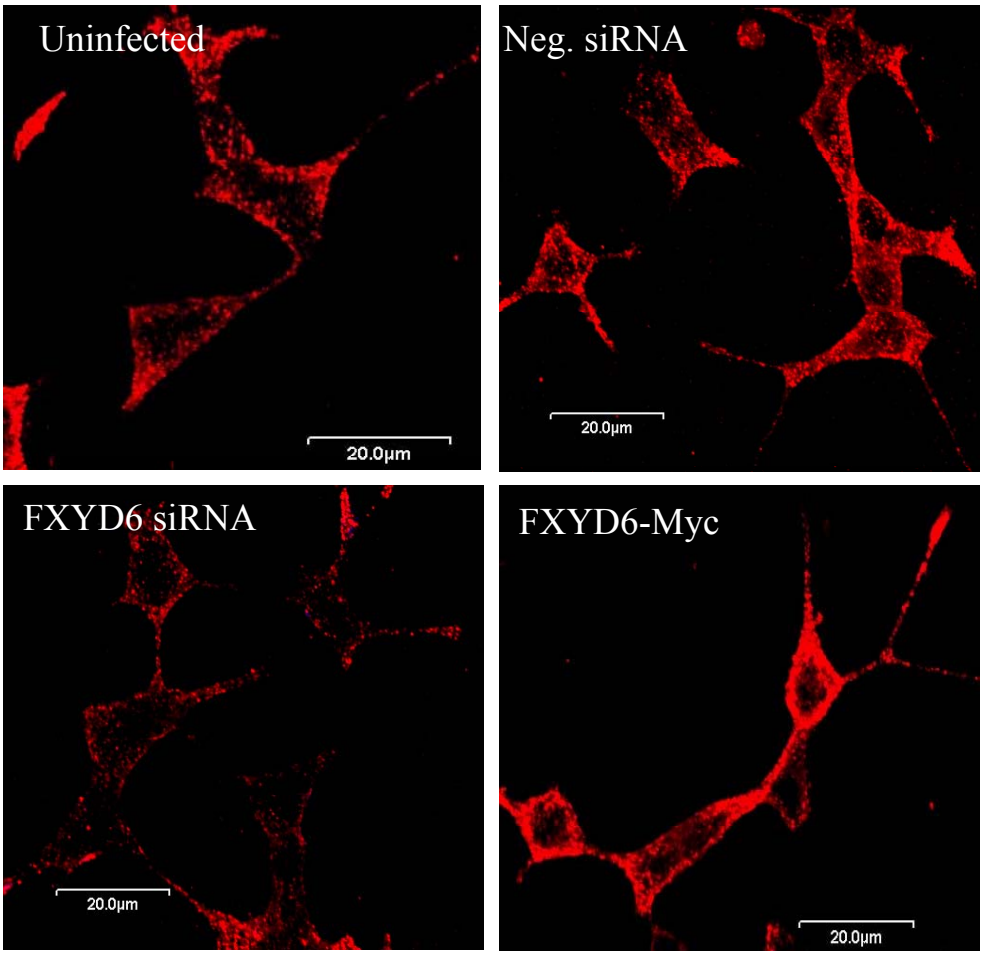

Figure 5.8: FXYD6-siRNA influences β-granule localization. Confocal microscopy of INS-1 cells stained with α-insulin (red) at 5.6mM glucose. Images are digitally compressed XYZ scans at 180X.

Oligomerization/Modification of FXYD6 is glucose-dependent –Several FXYD proteins, including FXYD2, homo-oligomerize in the plasma membrane, although the functional significance of oligomerization is unknown (Geering, Beguin et al. 2003). Other FXYD proteins within the family, including FXYD6, have putative phosphorylation sequences, although FXYD1 is the only family member demonstrated experimentally to be phosphorylated *in vitro* (Walaas, Horn et al. 1999; Sweadner and Rael 2000). To elucidate whether FXYD6 is modified and/or has an oligomeric quaternary structure in response to glucose, sucrose gradients of INS-1 lysates infected with FXYD6-Myc were analyzed by immunoblot such that any density shifts in FXYD6 mobility would indicate either oligomerization and/or protein modification. Indeed, in both high and low percentage density sucrose gradients, a shift to the more dense fractions was identified in response to glucose (Figure 5.9). Cytochrome c, a 12 Kd protein, was identified in the same upper fractions as FXYD6 on high percentage density sucrose gradients, consistent with the monomeric molecular weight of FXYD6 (Figure 5.9A). However, in lower percentage density sucrose gradients, the more dense fractions of the gradient did not contain cytochrome c (Figure 5.9B). It is difficult to assess the precise molecular weight of these dense fractions in the lower percentage gradients, since all higher molecular weight proteins would migrate in these fractions. Regardless, these data suggest that modification of FXYD6, whether oligomerization and/or perhaps another protein modification, occurs in INS-1 cells in response to glucose stimulation.

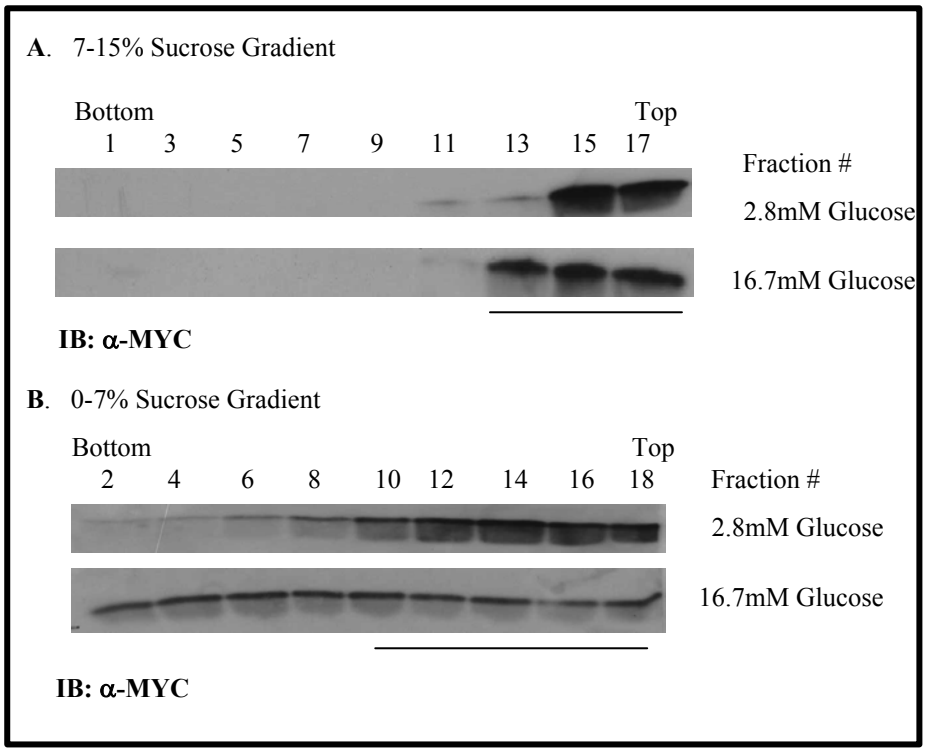

Figure 5.9: Glucose-dependent modification of FXYD6-Myc. Immunoblot analysis with an anti-Myc antibody of fractions from A. (7-15%) and B. (0-7%) sucrose density gradients of INS-1 lysate overexpressing FXYD6-Myc. Fractions were removed from the bottom to top of the gradient following centrifugation. Representative immunoblots from (n=3) experiments. Underlined fractions represent cytochrome c, 12 Kd, density association.

FXYD6-Myc overexpression does not significantly affect GSIS –β-granule transport involves the mobilization of β-granules from a cytosolic storage pool and is a stage of exocytosis that likely influences insulin secretion (Easom 2000). It was hypothesized that since FXYD6-Myc resulted in increased β-granule translocalization to the plasma membrane that glucose-stimulated insulin secretion might be enhanced. Evaluation of insulin secretion after 1 hour either by glucose dose-response or stimulation with 16.7mM glucose did not reveal any differences in total insulin secretion in FXYD6-Myc overexpressing islets compared to Adv-GFP control infected islets (Figure 5.10). It is hypothesized that second phase insulin secretion involves β-granule transport; therefore, kinetic analysis via perifusion of isolated islets may reveal subtle differences not detected through static evaluation of insulin secretion (Straub and Sharp 2002). Adv-GFP and Adv-FXYD6-Myc infected islets both exhibited a typical biphasic response to stimulatory glucose concentration as demonstrated previously (Figure 5.11) (Michael 2003; Yaekura, Julyan et al. 2003). No differences in first phase insulin secretion were evident in FXYD6-Myc infected islets compared to Adv-GFP control islets, which is consistent with β-granule transport involvement during second phase and release of the readily-releasable pool during the first phase (Figure 5.11). Interestingly, second phase insulin secretion displayed a modest enhancement of second phase insulin secretion compared to control Adv-GFP infected islets (Figure 5.11). Although the difference in second phase secretion was not statistically significant, additional experiments may decrease the variability in the percentage of insulin released translating in tighter standard error and possibly statical significance. Regardless, this data supports preliminary evidence of FXYD6 involvement in insulin secretion.

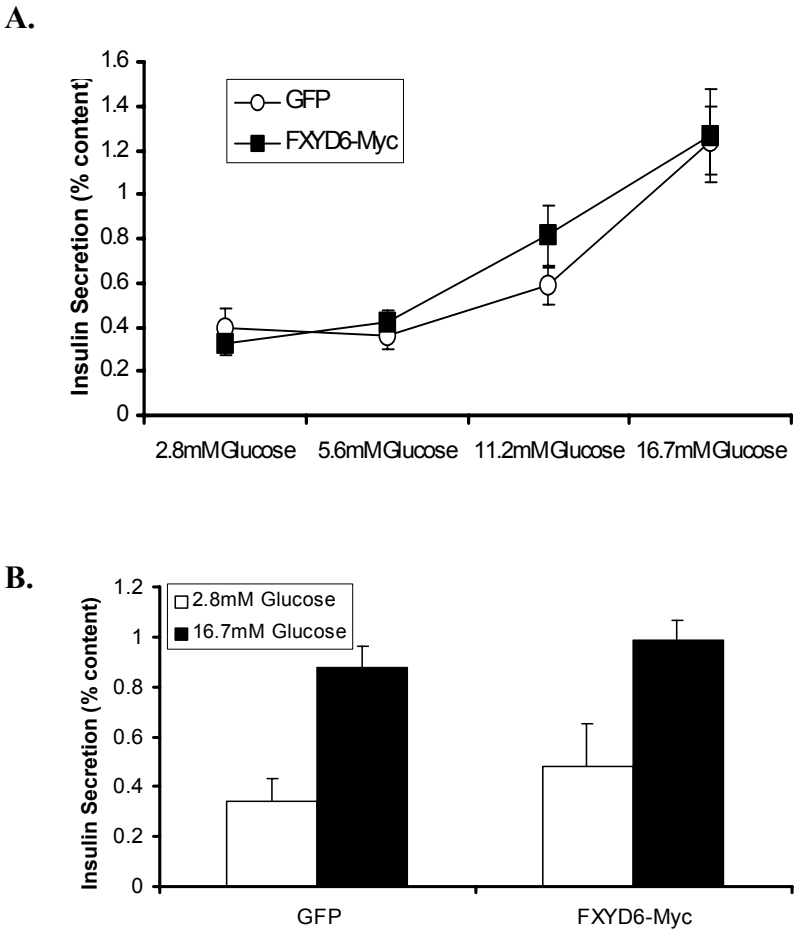

Figure 5.10: FXYD6-Myc overexpression does not affect insulin secretion. Static secretion in isolated islets stimulated with glucose A. Glucose dose response (n=9) B. Basal (2.8mM) and stimulated (16.7mM) glucose (n=5)

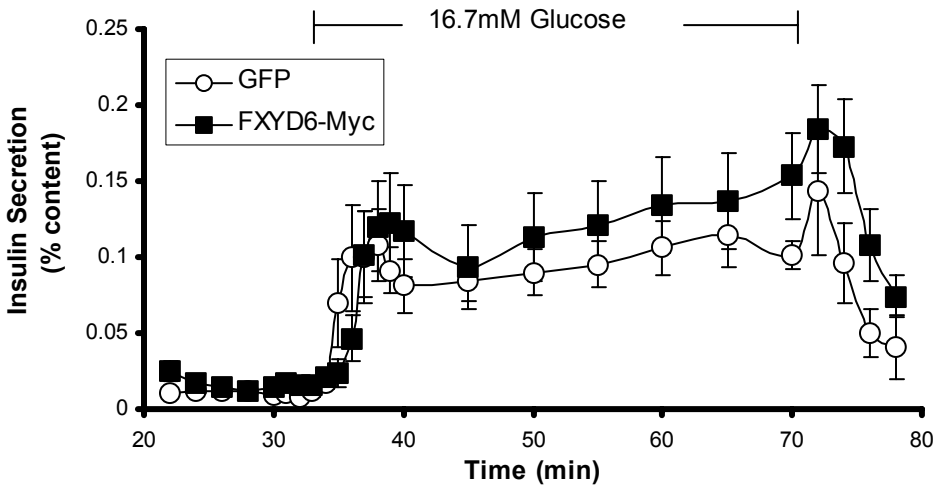

Figure 5.11: FXYD6-Myc overexpression may influence 2nd phase insulin secretion in isolated islets stimulated with glucose. Perifusion analysis of isolated islets infected with Adv-GFP or Adv-FXYD6-Myc and stimulated with 16.7mM glucose (n=6)

5.4. Discussion

RT-PCR analysis identified FXYD6, a member of the FXYD family of proteins, to be specifically expressed in pancreatic β-cells. No other FXYD family members were identified in β-cells, which is in agreement with the tissue-specific distribution of most FXYD proteins (Sweadner and Rael 2000). Interestingly, FXYD7 was identified in α-cells of pancreatic islets. It is also important to note that both FXYD6 and FXYD7, along with FXYD1, were also identified in the brain. As discussed earlier (Chapter 3), some similarities between synaptic vesicle exocytosis in brain and β-granule exocytosis in islets implicate analogous proteins involved in the exocytotic machinery, such as the v- and t-SNARE proteins. Therefore, it is possible FXYD-1, 6, and 7 isoforms may be functionally conserved in neurons and islets.

Despite some lack of sequence identity between syncollin and FXYD6, these two proteins share several similarities in their protein structure. The existence of a signal peptide on both proteins suggests that they are translated and processed through the RER placing them in the secretory pathway (Gorr and Darling 1995). The 'DPFXYD domain' of FXYD6, which is the hallmark identification of FXYD family members (Sweadner and Rael 2000) and is located within the primary amino acid sequence N-terminal to the trans-membrane domain, was similar in syncollin (DPYYD). However, the functional role of this domain is undetermined (Sweadner and Rael 2000). Regardless, functional significance of this domain can be assessed through mutational analysis. Another structural feature of FXYD proteins is a large hydrophobic region, consistent with a trans-membrane domain. Although syncollin lacks a hydrophobic region, syncollin is known to tightly associate with the luminal membrane of zymogen granules in a

cholesterol-dependent manner (Hodel, An et al. 2001). The structural components responsible for mediation of this membrane attachment have not been examined. The C-terminal portion of this hydrophobic region of FXYD6 shares significant homology with syncollin and could be the region of anti-syncollin polyclonal antibody recognition. It is also interesting to note that the syncollin gene is located in the same vicinity within the human genome as other FXYD proteins, indicating an evolutionarily correlation. Based on the structural evidence, it is likely that syncollin represents a 'pseudo family member' of the FXYD proteins.

Assessment of FXYD6 intracellular localization in INS-1 cells via confocal imaging indicated that FXYD6 was concentrated to certain regions of the plasma membrane. The localization of FXYD6 to the plasma membrane is unlike syncollin, which was targeted to the lumen of β-granules. However, within zymogen granules syncollin associates with the luminal membrane in cholesterol-rich regions (Hodel, An et al. 2001). It is well established that distinct regions of the plasma membrane that correspond to secretion are typically associated with lipid rafts, which are regions of the plasma membrane rich in cholesterol or sphingolipid composition (Rhodes and Halban 1987). Analysis of the lipid/protein composition of the plasma membrane associated with FXYD6 could assess whether FXYD6 is uniquely targeted to a particular lipid composition.

β-granule localization in uninfected INS-1 cells was randomly distributed throughout the cytosol; whereas, FXYD6 overexpression resulted in β-granule association with distinct regions of the plasma membrane where FXYD6 was concentrated. These data support that FXYD6 is capable of directing β-granules to the plasma membrane by acting

as an attractant or beacon, honing β-granules to the FXYD6-rich patches on the plasma membrane. In contrast, siRNA-mediated FXYD6 deficiency demonstrated no obvious changes in β-granule distribution compared to control uninfected cells. However, stimulation with glucose resulted in erratic and misdirected β-granule movement. Interestingly, there was no perceivable effect of FXYD6 overexpression on glucose-stimulated insulin secretion, although perifusion experiments with Adv-FXYD6-Myc infected islets revealed a slight, albeit not statistically significant, increase in second phase secretion, which is consistent with a role for FXYD6 in β-granule transport.

The idea that FXYD6 may be involved in directional β-granule movement to the plasma membrane is supported by data implicating FXYD1 involvement in GLUT4 translocation in adipocytes. It is established that GLUT4 is mobilized in response to insulin in adipocytes from intracellular storage pools to the plasma membrane where it increases cellular glucose uptake (Simpson, Whitehead et al. 2001). Walaas *et al* demonstrated anti-FXYD1 antibodies inhibited insulin-dependent GLUT4 translocation to the membrane and incubation of permeabilized adipocytes with an FXYD1 peptide also inhibited GLUT4 translocation (Walaas, Horn et al. 1999).

In β-cells, the data accumulated to date indicate that FXYD6 likely functions as a molecular beacon directing β-granule movement to the plasma membrane; thereby, enhancing the efficiency of β-granule transport to the site of exocytosis. The initiation of β-granule transport from an intracellular storage pool involves the calcium/calmodulin-dependent activation of kinesin through PP2B-mediated dephosphorylation involving attachment of β-granules to microtubules and kinesin motor activity for increased β-granule transport to the plasma membrane (Easom 2000; Rhodes 2000; Donelan, Morfini

et al. 2002). Due to the location of FXYD6 on the plasma membrane, it likely operates downstream of the initiation of ß-granule transport and kinesin activation, which occurs deeper inside the ß-cell. In this regard, FXYD-6 expression in ß-cells appears to be concentrated to specific areas of the plasma membrane to which ß-granules are attracted. It is established that the pancreatic ß-cell is polarized, requiring ß-granule transport to particular regions of the plasma membrane that are active areas for exocytosis allowing efficient regulated insulin secretion (Bonner-Weir 1988). FXYD6 appears to function in the ß-cell by providing direction to ß-granule transport towards active zones of insulin secretion. Interestingly, these active zones of secretion were previously hypothesized to exist predominantly in the tips of INS-1 cells (Rivas and Moore 1989). However, FXYD6 and insulin immunofluorescence data presented in this study suggest these active regions of secretion may occur in distinct areas within the main body of the INS-1 cells. Although increased FXYD6 expression can markedly increase the number of ß-granules located at the ß-cell plasma membrane, that are presumably active areas of exocytosis, this does not significantly enhance glucose-induced insulin secretion. This implies that FXYD6 operates upstream of the docking, priming and fusion steps in the insulin exocytosis mechanism and emphasizing the importance of regulation at these more distal steps, especially priming and membrane fusion, which is required to trigger insulin exocytosis.

Considering most β-granule transport in β-cells is glucose regulated (Easom 2000) it follows that the role of FXYD6 as a beacon to which β-granules migrate might also be glucose regulated. Data presented in this study suggest that oligomerization and/or modification of FXYD6 occurs in β-cells in a glucose-dependent manner.

Oligomerization of FXYD6 is consistent with the structure of other members of the FXYD family (e.g. FXYD2) (Sweadner and Rael 2000). Alternatively, motif comparison of FXYD6 with known domains revealed that FXYD6 contains a conserved PKC phosphorylation site, implicating the density shift observed in the sucrose gradient may be due to phosphorylation of FXYD6. Future experimentation will consolidate these possible mechanisms and relate it to the putative functional role of FXYD6 in directing β-granule transport to active sites of insulin exocytosis in the β-cell. However, considering what little is known about the family of FXYD proteins, one must still postulate other alternatives as to the functional role of FXYD6 in pancreatic β-cells. Some FXYD proteins are capable of pore formation and it should be considered whether FXYD6 participates in membrane fusion through pore formation in β-cells. The possibility that FXYD6 forms an oligomeric structure in response to glucose exists. Indeed, examination by atomic force microscopy of syncollin reconstitution in *Xenopus* oocytes revealed a pore-like homo-oligomeric structure within the membrane (Geisse, Wasle et al. 2002). Precedence for FXYD protein pore formation was demonstrated by FXYD2 reconstitution in *Xenopus* oocytes, which resulted in the formation of a 5nm diameter pore capable of passing inulin, a 5 Kd protein (Sha, Lansbery et al. 2001). However from the data accumulated to date, it is unlikely that FXYD6 influences membrane fusion via pore formation in the mechanism of insulin exocytosis since abundant FXYD6 expression did not markedly enhance insulin secretion.

Other FXYD family members have been implicated in modulating Na^+/K^+ ATPase activity, but FXYD6 reconstitution in *Xenopus* oocytes did not show any effect of ATPase activity (Yamaguchi, Yamaguchi et al. 2001; Geering, Beguin et al. 2003). It

is important to note that although FXYD proteins modulate Na^+/K^+ ATPase activity, function of the pump does not require FXYD protein modulation (Therien and Blostein 2000). However, it is unknown whether FXYD6 modulates the Na^+/K^+ ATPase in β-cells and further experiments will be needed to eliminate the possibility. For the moment, modulation of the Na^+/K^+ ATPase in β-cells by FXYD6 cannot be ruled out as a possible mechanism contributing to the facilitation of β-granule movement.

Notwithstanding, prior to this research no FXYD proteins had been experimentally evaluated for expression in pancreatic islet endocrine cells. RT-PCR analysis of the different FXYD isoforms revealed specific FXYD6 expression in islet β-cells and specific FXYD7 expression in islet α-cells. My data provide evidence that FXYD6 influences directed β-granule transport to specific locations on the β-cell plasma membrane, perhaps the active areas of exocytosis, and implicates a novel protein, FXYD6, in the insulin exocytotic mechanism.

CHAPTER SIX

General Discussion

6.1. Discussion

Insulin secretion is a complex, highly regulated process involving numerous exocytotic proteins that coordinate with various metabolic signals to elicit a precisely controlled release of insulin, as discussed in Chapter 1 (Lang 1999). The aim of this study was to analyze other proteins (including the FXYD protein family and an associated family member, syncollin) implicated in exocytosis for their expression and functional relevance in regulated insulin exocytosis. In this research adenoviral-mediated expression of syncollin significantly inhibited insulin secretion at the distal stages of insulin exocytosis downstream of glucose metabolism without altering insulin production, providing the first evidence that an intraluminal β-granule protein can influence insulin secretion. The mechanism of this inhibition of insulin secretion by adenoviral-mediated syncollin expression is unresolved; however, possible scenarios include inhibition of endogenous pore formation, reduction in the number of fusion competent β-granules, chelating low molecular weight ions or factors within the β-granule, potentially inhibiting proinsulin processing (Hutton and Rhodes 1991), or other possible mechanisms. Although syncollin was not endogenously expressed in β-cells, a smaller 10 Kd 'syncollin-like' protein was recognized. Sequence analysis indicated the identity of this 10 Kd protein was likely FXYD6. Indeed, FXYD6 endogenous expression was identified in β-cells. Comparison of the amino acid primary sequence of

syncollin and FXYD6 indicated multiple conserved motifs suggesting syncollin may be an evolutionarily associated member of the FXYD family.

Syncollin and syncollin-GFP were both sorted to β-granules with high efficiency, making syncollin-GFP a useful β-granule specific marker. The mechanisms responsible for sorting secretory granule proteins, including proinsulin, from the *trans* Golgi network in β-cells is unresolved; however, it is hypothesized that aggregation of the secretory proteins may involve cholesterol-rich lipid microdomains (Rhodes 2000; Tooze, Martens et al. 2001). Indeed, syncollin homo-oligomers associated with the zymogen granule membrane in cholesterol-rich regions (Hodel, An et al. 2001). In AtT20 cells, syncollin was efficiently sorted in a homotypic manner and retained during granule maturation, suggesting that the sorting mechanism for syncollin is cell-type independent (Hodel and Edwardson 2000) and such a mechanism of sorting is likely present in β-cells. Therefore, it is possible that the efficiency of syncollin sorting in β-cells occurs as a result of aggregation and association of syncollin to cholesterol-rich microdomains of the β-granule membrane and is retained during β-granule maturation. However, there is no direct evidence in β-cells to suggest that this mechanism is responsible for the efficiency of syncollin sorting to β-granules.

The data presented in this study identifies a novel protein, FXYD6, in β-cells, which appears to be involved in insulin exocytosis by directing β-granule transport to the plasma membrane. A hypothetical model summarizing adenoviral-mediated syncollin inhibition of insulin secretion and FXYD6 function in β-cells is depicted in Figure 6.1. It is hypothesized that FXYD6 acts as a molecular beacon directing β-granules from the cytosolic storage pool to its location in restricted regions of the plasma membrane that

may represent active zones of secretion. Notwithstanding, the question arises as to how FXYD6 might direct ß-granule transport mechanistically. Obviously this requires further experimentation. However, one possibility may be that FXYD6 tethers the end of the cytoskeletal network to specific locations in the ß-cell plasma membrane to direct microtubule/microfilament-mediated ß-granule transport to those specific locations hypothesized to be active sites of exocytosis. This, in turn, implies that FXYD6 needs to be located to certain regions of the ß-cell plasma membrane that, as with syncollin and other members of the FXYD family, could be influenced by local lipid composition in patches of the plasma membrane. In addition, if these are active zones of exocytosis in the polarized ß-cell it would be predicted that FXYD6 associates with proteins specifically involved in the latter stages of the insulin exocytosis, such as components of the L-type Ca^{2+} channel, t-SNARES and synaptotagamin isoforms 3 or –7. In this regard it should be noted that SNARE proteins involved in regulated exocytosis are often located in cholesterol-dependent clusters in lipid rafts that define docking and fusion sites for exocytosis (Chamberlain, Burgoyne et al. 2001; Lang, Bruns et al. 2001).

To consolidate this hypothetical model, additional studies would be aimed at elucidating the mechanism of FXYD6 action and extent to which insulin secretion is affected. Among future studies it will be examined whether FXYD6 is located to plasma membrane lipid rafts in the ß-cell, as well as any interactions with microtubules/microfilaments and co-localization with late stage exocytotic proteins, such as L-type calcium channels and t-SNARE proteins. Together these experiments would provide evidence to enhance the argument for FXYD6 directed targeting of β-granules to active zones of secretion. Despite the apparent involvement of FXYD6 in insulin

exocytosis, only modest effects were observed on glucose-stimulated secretion in islets overexpressing FXYD6. This implicates distal docking, priming, and membrane fusion stages of exocytosis as pivotal areas of regulation for insulin secretion with the function of FXYD6 directed β-granule transport enhancing the efficiency of exocytosis. However, sustained insulin secretion requires β-granule transport (Rorsman and Renstrom 2003); therefore, analysis of insulin secretion in FXYD6 deficient pancreatic islets would elucidate whether FXYD6 is necessary for regulated insulin exocytosis. This will consolidate these early findings that implicate a role for FXYD6 in the mechanism of insulin exocytosis.

It is hypothesized that β-cell defects contribute to the pathophysiology of type-2 diabetes and that a hallmark characteristic of the disease is impaired insulin secretion (Bergman, Finegood et al. 2002), which may result from defects in the exocytotic machinery, as discussed in Chapter 1.1.2 . It is well established that β-granule transport is a putative regulatory stage for insulin secretion and is crucial for sustained insulin secretion (Takahashi, Kadowaki et al. 1997; Easom 2000; Rorsman and Renstrom 2003). Based the apparent role of FXYD6 in β-granule transport, it would be predicted that FXYD6 null mice may develop glucose intolerance due to β-cell dysfunction from inefficient β-granule transport resulting in reduced insulin secretion similar to rab3A null mice (Yaekura, Julyan et al. 2003). Regardless, FXYD6 represents a novel candidate protein involved in the activation/regulation of insulin secretion giving a better insight into the mechanism of insulin exocytosis that, in turn, could lead to therapeutic approaches to improve the efficiency of glucose-stimulated insulin secretion in type-2 diabetes.

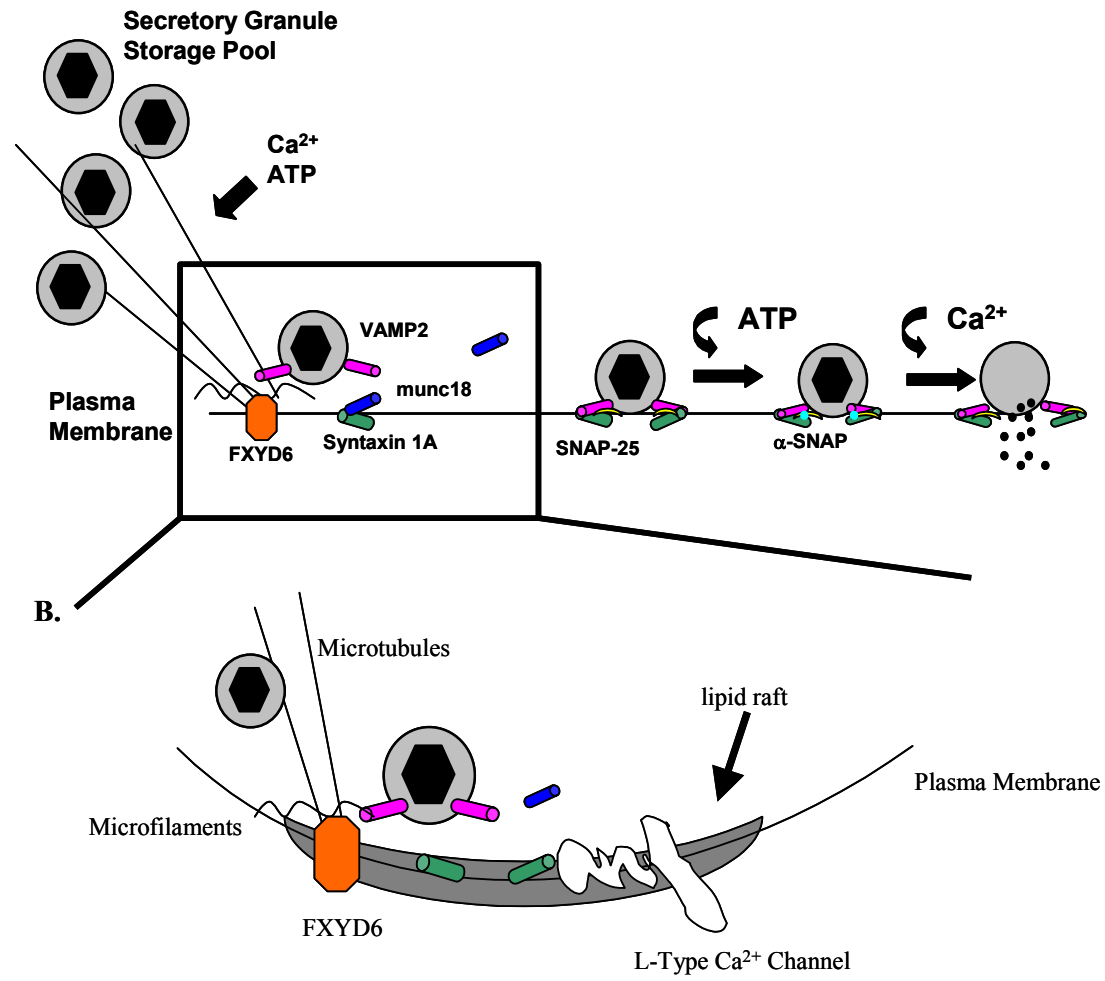

Figure 6.1: Hypothetical model depicting FXYD6 function in insulin secretion. A. FXYD6 functions as a beacon directing β-granules to the plasma membrane to "active zones of secretion". B. FXYD6 may associate with the cytoskeletal network directing β-granules to lipid rafts.

APPENDIX

Supplemental Data

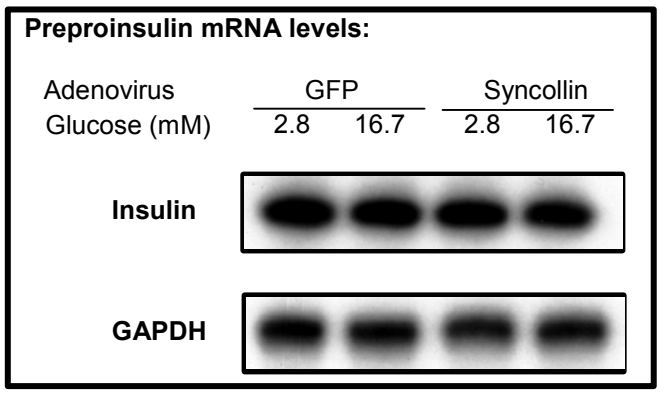

Appendix A.1: Preproinsulin mRNA levels are normal in syncollin infected islets compared to control GFP infected islets. RNAse protection assay over a 1-hour stimulation period with basal and stimulatory glucose concentrations. RNAse protection assay was performed by a postdoctoral fellow in the lab; whereas, islet isolation and subsequent incubation with glucose was performed by me.

BIBLIOGRAPHY

Alarcon, C., J. L. Leahy, et al. (1995). "Increased secretory demand rather than a defect in the proinsulin conversion mechanism causes hyperproinsulinemia in a glucose-infusion rat model of non-insulin-dependent diabetes mellitus." J Clin Invest **95**(3): 1032-9.

Alarcon, C., B. Wicksteed, et al. (2002). "Succinate is a preferential metabolic stimulus-coupling signal for glucose-induced proinsulin biosynthesis translation." Diabetes **51**(8): 2496-504.

An, S. J., N. J. Hansen, et al. (2000). "Analysis of the association of syncollin with the membrane of the pancreatic zymogen granule." J Biol Chem **275**(15): 11306-11.
Antonin, W., M. Wagner, et al. (2002). "Loss of the zymogen granule protein syncollin affects pancreatic protein synthesis and transport but not secretion." Mol Cell Biol **22**(5): 1545-54.

Arvan, P. and D. Castle (1998). "Sorting and storage during secretory granule biogenesis: looking backward and looking forward." Biochem J **332 (Pt 3)**: 593-610.

Arvan, P. and P. A. Halban (2004). "Sorting ourselves out: seeking consensus on trafficking in the Beta-cell." Traffic **5**(1): 53-61.

Barg, S. (2003). "Mechanisms of exocytosis in insulin-secreting B-cells and glucagon-secreting A-cells." Pharmacol Toxicol **92**(1): 3-13.

Barg, S., P. Huang, et al. (2001). "Priming of insulin granules for exocytosis by granular Cl(-) uptake and acidification." J Cell Sci **114**(Pt 11): 2145-54.

Barg, S., X. Ma, et al. (2001). "Fast exocytosis with few Ca(2+) channels in insulin-secreting mouse pancreatic B cells." Biophys J **81**(6): 3308-23.

Bauerfeind, R. and W. B. Huttner (1993). "Biogenesis of constitutive secretory vesicles, secretory granules and synaptic vesicles." Curr Opin Cell Biol **5**(4): 628-35.

Bell, G. I., W. F. Swain, et al. (1979). "Nucleotide sequence of a cDNA clone encoding human preproinsulin." Nature **282**(5738): 525-7.

Bennett, P. H., T. A. Burch, et al. (1971). "Diabetes mellitus in American (Pima) Indians." Lancet **2**(7716): 125-8.

Bergman, R. N., D. T. Finegood, et al. (2002). "The evolution of beta-cell dysfunction and insulin resistance in type 2 diabetes." Eur J Clin Invest **32 Suppl 3**: 35-45.

Bergsten, P., E. Grapengiesser, et al. (1994). "Synchronous oscillations of cytoplasmic Ca2+ and insulin release in glucose-stimulated pancreatic islets." J Biol Chem **269**(12): 8749-53.

Bjorklund, A., G. Yaney, et al. (1997). "Fatty acids and beta-cell function." Diabetologia **40 Suppl 3**: B21-6.

Blachier, F., A. Mourtada, et al. (1989). "Stimulus-secretion coupling of arginine-induced insulin release. Uptake of metabolized and nonmetabolized cationic amino acids by pancreatic islets." Endocrinology **124**(1): 134-41.

Bonner-Weir, S. (1988). "Morphological evidence for pancreatic polarity of beta-cell within islets of Langerhans." Diabetes **37**(5): 616-21.

Boyd, A. E., 3rd, L. Aguilar-Bryan, et al. (1991). "Sulfonylurea signal transduction." Recent Prog Horm Res **47**: 299-316; discussion 316-7.

Boyd, R. S., M. J. Duggan, et al. (1995). "The effect of botulinum neurotoxins on the release of insulin from the insulinoma cell lines HIT-15 and RINm5F." J Biol Chem **270**(31): 18216-8.

Bratanova-Tochkova, T. K., H. Cheng, et al. (2002). "Triggering and augmentation mechanisms, granule pools, and biphasic insulin secretion." Diabetes **51 Suppl 1**: S83-90.

Brown, G. K. (2000). "Glucose transporters: structure, function and consequences of deficiency." J Inherit Metab Dis **23**(3): 237-46.

Bryan, J. a. A.-B., L. (2000). Sulfonylurea Receptors, ATP-Sensitive Potassium Channels and Insulin Secretion. Diabetes Mellitus: A Fundamental and Clinical Text. D. LeToith, Taylor, S., and Olefsky, J.M. Philadelphia, Lippincott. Williams, and Wilkins. **2:** 61-77.

Burgoyne, R. D. and A. Morgan (2003). "Secretory granule exocytosis." Physiol Rev **83**(2): 581-632.

Chamberlain, L. H., R. D. Burgoyne, et al. (2001). "SNARE proteins are highly enriched in lipid rafts in PC12 cells: implications for the spatial control of exocytosis." Proc Natl Acad Sci U S A **98**(10): 5619-24.

Chey, W. Y. and T. Chang (2001). "Neural hormonal regulation of exocrine pancreatic secretion." Pancreatology **1**(4): 320-35.

Chick, W. L., S. Warren, et al. (1977). "A transplantable insulinoma in the rat." Proc Natl Acad Sci U S A **74**(2): 628-32.

Chizmadzhev, Y. A., P. I. Kuzmin, et al. (2000). "Dynamics of fusion pores connecting membranes of different tensions." Biophys J **78**(5): 2241-56.

Cho, S. J., A. S. Quinn, et al. (2002). "Structure and dynamics of the fusion pore in live cells." Cell Biol Int **26**(1): 35-42.

Cunningham, B. A., J. T. Deeney, et al. (1996). "Glucose-induced oscillatory insulin secretion in perifused rat pancreatic islets and clonal beta-cells (HIT)." Am J Physiol **271**(4 Pt 1): E702-10.

Daniel, S., M. Noda, et al. (1999). "Identification of the docked granule pool responsible for the first phase of glucose-stimulated insulin secretion." Diabetes **48**(9): 1686-90.

Deeney, J. T., J. Gromada, et al. (2000). "Acute stimulation with long chain acyl-CoA enhances exocytosis in insulin-secreting cells (HIT T-15 and NMRI beta-cells)." J Biol Chem **275**(13): 9363-8.

Deeney, J. T., M. Kohler, et al. (2001). "Glucose-induced metabolic oscillations parallel those of Ca(2+) and insulin release in clonal insulin-secreting cells. A multiwell approach to oscillatory cell behavior." J Biol Chem **276**(40): 36946-50.

Dentler, W. L. and K. A. Suprenant (1986). "Isolation of microtubule-secretory granule complexes from the anglerfish endocrine pancreas." Ann N Y Acad Sci **466**: 813-31.

Dickson, L. M. a. R., C.J. (In press). "Pancreatic beta-cell Growth and Survival in the onset of Type-2 Diabetes: A Role for Protein Kinase-B in the Akt?" American Journal of Physiology.

Docherty, K. and A. R. Clark (1994). "Nutrient regulation of insulin gene expression." Faseb J **8**(1): 20-7.

Donelan, M. J., G. Morfini, et al. (2002). "Ca2+-dependent dephosphorylation of kinesin heavy chain on beta-granules in pancreatic beta-cells. Implications for regulated beta-granule transport and insulin exocytosis." J Biol Chem **277**(27): 24232-42.

Doyle, M. E. and J. M. Egan (2003). "Pharmacological agents that directly modulate insulin secretion." Pharmacol Rev **55**(1): 105-31.

Duncan, R. R., J. Greaves, et al. (2003). "Functional and spatial segregation of secretory vesicle pools according to vesicle age." Nature **422**(6928): 176-80.

Easom, R. A. (2000). "Beta-granule transport and exocytosis." Semin Cell Dev Biol **11**(4): 253-66.

Edwardson, J. M., S. An, et al. (1997). "The secretory granule protein syncollin binds to syntaxin in a Ca2(+)-sensitive manner." Cell **90**(2): 325-33.

Elbashir, S. M., J. Harborth, et al. (2001). "Duplexes of 21-nucleotide RNAs mediate RNA interference in cultured mammalian cells." Nature **411**(6836): 494-8.

Eliasson, L., E. Renstrom, et al. (1997). "Rapid ATP-dependent priming of secretory granules precedes Ca(2+)-induced exocytosis in mouse pancreatic B-cells." J Physiol **503 (Pt 2)**: 399-412.

Fahien, L. A., M. J. MacDonald, et al. (1988). "Regulation of insulin release by factors that also modify glutamate dehydrogenase." J Biol Chem **263**(27): 13610-4.

Farman, N., M. Fay, et al. (2003). "Cell-specific expression of three members of the FXYD family along the renal tubule." Ann N Y Acad Sci **986**: 428-36.

Foster, D. (1998). Diabetes Mellitus. Harrison's Principles of Internal Medicine. A. Fauci, Braunwald, E., Isselbacher, K., Wilson, J., Martin, J., Kasper, D., Hauser, S., and Longo, D. **14:** 2060-2081.

Fridlyand, L. E., N. Tamarina, et al. (2003). "Modeling of Ca2+ flux in pancreatic beta-cells: role of the plasma membrane and intracellular stores." Am J Physiol Endocrinol Metab **285**(1): E138-54.

Fukuda, M. and K. Mikoshiba (2000). "Distinct self-oligomerization activities of synaptotagmin family. Unique calcium-dependent oligomerization properties of synaptotagmin VII." J Biol Chem **275**(36): 28180-5.

Gao, Z., J. Reavey-Cantwell, et al. (2000). "Synaptotagmin III/VII isoforms mediate Ca2+-induced insulin secretion in pancreatic islet beta -cells." J Biol Chem **275**(46): 36079-85.

Geering, K., P. Beguin, et al. (2003). "FXYD proteins: new tissue- and isoform-specific regulators of Na,K-ATPase." Ann N Y Acad Sci **986**: 388-94.

Geisse, N. A., B. Wasle, et al. (2002). "Syncollin homo-oligomers associate with lipid bilayers in the form of doughnut-shaped structures." J Membr Biol **189**(2): 83-92.

Gerich, J. E. (2003). "Contributions of insulin-resistance and insulin-secretory defects to the pathogenesis of type 2 diabetes mellitus." Mayo Clin Proc **78**(4): 447-56.

Goodge, K. A. and J. C. Hutton (2000). "Translational regulation of proinsulin biosynthesis and proinsulin conversion in the pancreatic beta-cell." Semin Cell Dev Biol **11**(4): 235-42.

Gorr, S. U. and D. S. Darling (1995). "An N-terminal hydrophobic peak is the sorting signal of regulated secretory proteins." FEBS Lett **361**(1): 8-12.

Gotte, M. and G. F. von Mollard (1998). "A new beat for the SNARE drum." Trends Cell Biol **8**(6): 215-8.

Gylfe, E., M. Ahmed, et al. (2000). "Signaling underlying pulsatile insulin secretion." Ups J Med Sci **105**(2): 35-51.

Halban, P. A., C. B. Wollheim, et al. (1982). "The possible importance of contact between pancreatic islet cells for the control of insulin release." Endocrinology **111**(1): 86-94.

He, T. C., S. Zhou, et al. (1998). "A simplified system for generating recombinant adenoviruses." Proc Natl Acad Sci U S A **95**(5): 2509-14.

Heidelberger, R., C. Heinemann, et al. (1994). "Calcium dependence of the rate of exocytosis in a synaptic terminal." Nature **371**(6497): 513-5.

Hodel, A., S. J. An, et al. (2001). "Cholesterol-dependent interaction of syncollin with the membrane of the pancreatic zymogen granule." Biochem J **356**(Pt 3): 843-50.

Hodel, A. and J. M. Edwardson (2000). "Targeting of the zymogen-granule protein syncollin in AR42J and AtT-20 cells." Biochem J **350 Pt 3**: 637-43.

Hohmeier, H. E., H. Mulder, et al. (2000). "Isolation of INS-1-derived cell lines with robust ATP-sensitive K+ channel-dependent and -independent glucose-stimulated insulin secretion." Diabetes **49**(3): 424-30.

Holz, G. G. t., W. M. Kuhtreiber, et al. (1993). "Pancreatic beta-cells are rendered glucose-competent by the insulinotropic hormone glucagon-like peptide-1(7-37)." Nature **361**(6410): 362-5.

Hu, C., M. Ahmed, et al. (2003). "Fusion of cells by flipped SNAREs." Science **300**(5626): 1745-9.

Hua, Y. and R. H. Scheller (2001). "Three SNARE complexes cooperate to mediate membrane fusion." Proc Natl Acad Sci U S A **98**(14): 8065-70.

Hutton, J. C. (1982). "The internal pH and membrane potential of the insulin-secretory granule." Biochem J **204**(1): 171-8.

Hutton, J. C. (1989). "The insulin secretory granule." Diabetologia **32**(5): 271-81.

Hutton, J. C. and C. J. Rhodes (1991). "The enzymology of proinsulin conversion." Cell Biophys **19**(1-3): 57-62.

Irminger, J. C., C. B. Verchere, et al. (1997). "Proinsulin targeting to the regulated pathway is not impaired in carboxypeptidase E-deficient Cpefat/Cpefat mice." J Biol Chem **272**(44): 27532-4.

Jahn, R., T. Lang, et al. (2003). "Membrane fusion." Cell **112**(4): 519-33.

Jena, B. P. (2003). "Fusion pore or porosome: structure and dynamics." J Endocrinol **176**(2): 169-74.

Jena, B. P., S. J. Cho, et al. (2003). "Structure and composition of the fusion pore." Biophys J **84**(2 Pt 1): 1337-43.

Kahn, C. R., D. Vicent, et al. (1996). "Genetics of non-insulin-dependent (type-II) diabetes mellitus." Annu Rev Med **47**: 509-31.

Kahn, S. E. (2003). "The relative contributions of insulin resistance and beta-cell dysfunction to the pathophysiology of Type 2 diabetes." Diabetologia **46**(1): 3-19.

Kajio, H., S. Olszewski, et al. (2001). "A low-affinity Ca2+-dependent association of calmodulin with the Rab3A effector domain inversely correlates with insulin exocytosis." Diabetes **50**(9): 2029-39.

Katagiri, H., J. Terasaki, et al. (1995). "A novel isoform of syntaxin-binding protein homologous to yeast Sec1 expressed ubiquitously in mammalian cells." J Biol Chem **270**(10): 4963-6.

Kirchgessner, A. L. and M. D. Gershon (1991). "Innervation and regulation of the pancreas by neurons in the gut." Z Gastroenterol Verh **26**: 230-3.

Klenchin, V. A. and T. F. Martin (2000). "Priming in exocytosis: attaining fusion-competence after vesicle docking." Biochimie **82**(5): 399-407.

Konturek, S. J., R. Zabielski, et al. (2003). "Neuroendocrinology of the pancreas; role of brain-gut axis in pancreatic secretion." Eur J Pharmacol **481**(1): 1-14.

Kuliawat, R. and P. Arvan (1994). "Distinct molecular mechanisms for protein sorting within immature secretory granules of pancreatic beta-cells." J Cell Biol **126**(1): 77-86.

Lacy, P. E. (1967). "The pancreatic beta cell. Structure and function." N Engl J Med **276**(4): 187-95.

Lacy, P. E. and M. Kostianovsky (1967). "Method for the isolation of intact islets of Langerhans from the rat pancreas." Diabetes **16**(1): 35-9.

Lang, J. (1999). "Molecular mechanisms and regulation of insulin exocytosis as a paradigm of endocrine secretion." Eur J Biochem **259**(1-2): 3-17.

Lang, T., D. Bruns, et al. (2001). "SNAREs are concentrated in cholesterol-dependent clusters that define docking and fusion sites for exocytosis." Embo J **20**(9): 2202-13.

Linial, M. (1997). "SNARE proteins--why so many, why so few?" J Neurochem **69**(5): 1781-92.

Liu, Y. M., P. H. Guth, et al. (1993). "Dynamic in vivo observation of rat islet microcirculation." Pancreas **8**(1): 15-21.

Lomedico, P. T., N. Rosenthal, et al. (1980). "The structure of rat preproinsulin genes." Ann N Y Acad Sci **343**: 425-32.

Ma, L., V. P. Bindokas, et al. (2003 Submitted). "Optical discrimination of exocytosis and endocytosis in insulin secreting cells." Nat Neuroscience.

MacDonald, M. J. (1990). "Elusive proximal signals of beta-cells for insulin secretion." Diabetes **39**(12): 1461-6.

MacDonald, P. E., W. El-Kholy, et al. (2002). "The multiple actions of GLP-1 on the process of glucose-stimulated insulin secretion." Diabetes **51 Suppl 3**: S434-42.

Malaisse, W. J., F. Blachier, et al. (1989). "Stimulus-secretion coupling of arginine-induced insulin release. Metabolism of L-arginine and L-ornithine in pancreatic islets." Biochim Biophys Acta **1013**(2): 133-43.

Malaisse, W. J., F. Malaisse-Lagae, et al. (1975). "Role of microtubules in the phasic pattern of insulin release." Ann N Y Acad Sci **253**: 630-52.

Martin, T. F. (2003). "Tuning exocytosis for speed: fast and slow modes." Biochim Biophys Acta **1641**(2-3): 157-65.

Matschinsky, F. M. (2002). "Regulation of pancreatic beta-cell glucokinase: from basics to therapeutics." Diabetes **51 Suppl 3**: S394-404.

Mayo, K. E., L. J. Miller, et al. (2003). "International Union of Pharmacology. XXXV. The glucagon receptor family." Pharmacol Rev **55**(1): 167-94.

Melloul, D., S. Marshak, et al. (2002). "Regulation of insulin gene transcription." Diabetologia **45**(3): 309-26.

Michael, D. a. C., R. (2003). "Glucose-Stimulated, Pulsatile Secretion from Primary Cultured Pancreatic Beta Cells." Diabetes **52**(Suppl. 1): A373.

Mitchell, K. J., F. A. Lai, et al. (2003). "Ryanodine receptor type I and nicotinic acid adenine dinucleotide phosphate receptors mediate Ca2+ release from insulin-containing vesicles in living pancreatic beta-cells (MIN6)." J Biol Chem **278**(13): 11057-64.

Mitchell, K. J., P. Pinton, et al. (2001). "Dense core secretory vesicles revealed as a dynamic Ca(2+) store in neuroendocrine cells with a vesicle-associated membrane protein aequorin chimaera." J Cell Biol **155**(1): 41-51.

Miyawaki, A., A. Sawano, et al. (2003). "Lighting up cells: labelling proteins with fluorophores." Nat Cell Biol **Suppl**: S1-7.

Molinete, M., V. Lilla, et al. (2000). "Trafficking of non-regulated secretory proteins in insulin secreting (INS-1) cells." Diabetologia **43**(9): 1157-64.

Nakazaki, M., A. Crane, et al. (2002). "cAMP-activated protein kinase-independent potentiation of insulin secretion by cAMP is impaired in SUR1 null islets." Diabetes **51**(12): 3440-9.

Ohneda, K., H. Ee, et al. (2000). "Regulation of insulin gene transcription." Semin Cell Dev Biol **11**(4): 227-33.

Olofsson, C. S., S. O. Gopel, et al. (2002). "Fast insulin secretion reflects exocytosis of docked granules in mouse pancreatic B-cells." Pflugers Arch **444**(1-2): 43-51.

Olsen, H. L., M. Hoy, et al. (2003). "Phosphatidylinositol 4-kinase serves as a metabolic sensor and regulates priming of secretory granules in pancreatic beta cells." Proc Natl Acad Sci U S A **100**(9): 5187-92.

Orci, L., A. Perrelet, et al. (1977). "Pore-like structures in biological membranes." J Cell Sci **25**: 157-61.

Orci, L., J. D. Vassalli, et al. (1988). "The insulin factory." Sci Am **259**(3): 85-94.
Owerbach, D., G. I. Bell, et al. (1980). "The insulin gene is located on chromosome 11 in humans." Nature **286**(5768): 82-4.

Padfield, P. J. and N. Panesar (1998). "The two phases of regulated exocytosis in permeabilized pancreatic acini are modulated differently by heterotrimeric G-proteins." Biochem Biophys Res Commun **245**(2): 332-6.

Perin, M. S., V. A. Fried, et al. (1990). "Phospholipid binding by a synaptic vesicle protein homologous to the regulatory region of protein kinase C." Nature **345**(6272): 260-3.

Pouli, A. E., E. Emmanouilidou, et al. (1998). "Secretory-granule dynamics visualized in vivo with a phogrin-green fluorescent protein chimaera." Biochem J **333 (Pt 1)**: 193-9.

Prado, C. L., Pugh-Bernard, A.E., Elghazi, L., Sosa-Pineda,B. and Sussel,L. (2004). "Ghrelin cells replace insulin-producing ß cells in two mouse models of pancreas development." Proc Natl Acad Sci U S A **In press**.

Prentki, M., K. Tornheim, et al. (1997). "Signal transduction mechanisms in nutrient-induced insulin secretion." Diabetologia **40 Suppl 2**: S32-41.

Quinn, D., L. Orci, et al. (1991). "Intracellular transport and sorting of mutant human proinsulins that fail to form hexamers." J Cell Biol **113**(5): 987-96.

Regazzi, R., K. Sadoul, et al. (1996). "Mutational analysis of VAMP domains implicated in Ca2+-induced insulin exocytosis." Embo J **15**(24): 6951-9.

Rhodes, C. J. (2000). Processing of the Insulin Molecule. Diabetes Mellitus: A Fundamental and Clinical Text. D. LeToith, Taylor, S., and Olefsky, J.M. Philadelphia, Lippincott williams and Wilkins. **1:** 20-37.

Rhodes, C. J. and P. A. Halban (1987). "Newly synthesized proinsulin/insulin and stored insulin are released from pancreatic B cells predominantly via a regulated, rather than a constitutive, pathway." J Cell Biol **105**(1): 145-53.

Rivas, R. J. and H. P. Moore (1989). "Spatial segregation of the regulated and constitutive secretory pathways." J Cell Biol **109**(1): 51-60.

Roe, M. W., M. E. Lancaster, et al. (1993). "Voltage-dependent intracellular calcium release from mouse islets stimulated by glucose." J Biol Chem **268**(14): 9953-6.

Rorsman, P. and E. Renstrom (2003). "Insulin granule dynamics in pancreatic beta cells." Diabetologia **46**(8): 1029-45.

Sako, Y. and T. Yanagida (2003). "Single-molecule visualization in cell biology." Nat Rev Mol Cell Biol **Suppl**: SS1-5.

Schmidt, H. H., T. D. Warner, et al. (1992). "Insulin secretion from pancreatic B cells caused by L-arginine-derived nitrogen oxides." Science **255**(5045): 721-3.

Schuit, F. C., P. Huypens, et al. (2001). "Glucose sensing in pancreatic beta-cells: a model for the study of other glucose-regulated cells in gut, pancreas, and hypothalamus." Diabetes **50**(1): 1-11.

Schweizer, F. E., H. Betz, et al. (1995). "From vesicle docking to endocytosis: intermediate reactions of exocytosis." Neuron **14**(4): 689-96.

Seagar, M. and M. Takahashi (1998). "Interactions between presynaptic calcium channels and proteins implicated in synaptic vesicle trafficking and exocytosis." J Bioenerg Biomembr **30**(4): 347-56.

Sha, Q., K. L. Lansbery, et al. (2001). "Heterologous expression of the Na(+),K(+)-ATPase gamma subunit in Xenopus oocytes induces an endogenous, voltage-gated large diameter pore." J Physiol **535**(Pt 2): 407-17.

Shen, C., A. K. Buck, et al. (2003). "Gene silencing by adenovirus-delivered siRNA." FEBS Lett **539**(1-3): 111-4.

Shih, D. Q. and M. Stoffel (2002). "Molecular etiologies of MODY and other early-onset forms of diabetes." Curr Diab Rep **2**(2): 125-34.

Sim, A. T., M. L. Baldwin, et al. (2003). "The role of serine/threonine protein phosphatases in exocytosis." Biochem J **373**(Pt 3): 641-59.

Simpson, F., J. P. Whitehead, et al. (2001). "GLUT4--at the cross roads between membrane trafficking and signal transduction." Traffic **2**(1): 2-11.

Sorensen, J. B., R. Fernandez-Chacon, et al. (2003). "Examining synaptotagmin 1 function in dense core vesicle exocytosis under direct control of Ca2+." J Gen Physiol **122**(3): 265-76.

Spurlin, B. A., R. M. Thomas, et al. (2003). "Insulin resistance in tetracycline-repressible Munc18c transgenic mice." Diabetes **52**(8): 1910-7.

Straub, S. G. and G. W. Sharp (2002). "Glucose-stimulated signaling pathways in biphasic insulin secretion." Diabetes Metab Res Rev **18**(6): 451-63.

Sweadner, K. J. and E. Rael (2000). "The FXYD gene family of small ion transport regulators or channels: cDNA sequence, protein signature sequence, and expression." Genomics **68**(1): 41-56.

Takahashi, N., T. Kadowaki, et al. (1997). "Multiple exocytotic pathways in pancreatic beta cells." J Cell Biol **138**(1): 55-64.

Takahashi, N., T. Kishimoto, et al. (2002). "Fusion pore dynamics and insulin granule exocytosis in the pancreatic islet." Science **297**(5585): 1349-52.

Tan, S. and S. C. Hooi (2000). "Syncollin is differentially expressed in rat proximal small intestine and regulated by feeding behavior." Am J Physiol Gastrointest Liver Physiol **278**(2): G308-20.

Therien, A. G. and R. Blostein (2000). "Mechanisms of sodium pump regulation." Am J Physiol Cell Physiol **279**(3): C541-66.

Todd, J. A., C. Mijovic, et al. (1989). "Identification of susceptibility loci for insulin-dependent diabetes mellitus by trans-racial gene mapping." Nature **338**(6216): 587-9.

Tooze, S. A., G. J. Martens, et al. (2001). "Secretory granule biogenesis: rafting to the SNARE." Trends Cell Biol **11**(3): 116-22.

Tsuboi, T. and G. A. Rutter (2003). "Insulin secretion by 'kiss-and-run' exocytosis in clonal pancreatic islet beta-cells." Biochem Soc Trans **31**(Pt 4): 833-6.

Tsuboi, T. and G. A. Rutter (2003). "Multiple forms of "kiss-and-run" exocytosis revealed by evanescent wave microscopy." Curr Biol **13**(7): 563-7.

Tsuboi, T., C. Zhao, et al. (2000). "Simultaneous evanescent wave imaging of insulin vesicle membrane and cargo during a single exocytotic event." Curr Biol **10**(20): 1307-10.

Waesle, B., L. B. Hays, et al. (2004). "Syncollin inhibits regulated ACTH secretion from AtT-20 cells through a reduction in the secretory vesicle population." Biochem J **Pt**.

Walaas, O., R. S. Horn, et al. (1999). "Inhibition of insulin-stimulated phosphorylation of the intracellular domain of phospholemman decreases insulin-dependent GLUT4 translocation in streptolysin-O-permeabilized adipocytes." Biochem J **343 Pt 1**: 151-7.

Wang, C. T., R. Grishanin, et al. (2001). "Synaptotagmin modulation of fusion pore kinetics in regulated exocytosis of dense-core vesicles." Science **294**(5544): 1111-5.

Wang, C. T., J. C. Lu, et al. (2003). "Different domains of synaptotagmin control the choice between kiss-and-run and full fusion." Nature **424**(6951): 943-7.

Waselle, L., T. Coppola, et al. (2003). "Involvement of the Rab27 binding protein Slac2c/MyRIP in insulin exocytosis." Mol Biol Cell **14**(10): 4103-13.

Wasle, B. and J. M. Edwardson (2002). "The regulation of exocytosis in the pancreatic acinar cell." Cell Signal **14**(3): 191-7.

Wheeler, M. B., L. Sheu, et al. (1996). "Characterization of SNARE protein expression in beta cell lines and pancreatic islets." Endocrinology **137**(4): 1340-8.

Wicksteed, B., T. P. Herbert, et al. (2001). "Cooperativity between the preproinsulin mRNA untranslated regions is necessary for glucose-stimulated translation." J Biol Chem **276**(25): 22553-8.

Wollheim, C. B., J. Lang, et al. (1996). Diabetes Rev. **4**: 276-297.

Xu, T., B. Rammner, et al. (1999). "Inhibition of SNARE complex assembly differentially affects kinetic components of exocytosis." Cell **99**(7): 713-22.

Yaekura, K., R. Julyan, et al. (2003). "Insulin Secretory Deficiency and Glucose Intolerance in Rab3A Null Mice." J Biol Chem **278**(11): 9715-21.

Yamaguchi, F., K. Yamaguchi, et al. (2001). "Molecular cloning and characterization of a novel phospholemman-like protein from rat hippocampus." Brain Res Mol Brain Res **86**(1-2): 189-92.

Yaney, G. C. and B. E. Corkey (2003). "Fatty acid metabolism and insulin secretion in pancreatic beta cells." Diabetologia **46**(10): 1297-312.

Yaney, G. C., H. M. Korchak, et al. (2000). "Long-chain acyl CoA regulation of protein kinase C and fatty acid potentiation of glucose-stimulated insulin secretion in clonal beta-cells." Endocrinology **141**(6): 1989-98.

Yang, B., L. Gonzalez, Jr., et al. (1999). "SNARE interactions are not selective. Implications for membrane fusion specificity." J Biol Chem **274**(9): 5649-53.

Zhang, X. Q., A. Qureshi, et al. (2003). "Phospholemman modulates Na+/Ca2+ exchange in adult rat cardiac myocytes." Am J Physiol Heart Circ Physiol **284**(1): H225-33.

Zhou, H., Tran, P., Yang, S., Zhang, T., LeRoy, E., Oseid, E., and Roberston, RP (In press). ""Switch-off" Hypothesis: Regulation of Alpha Cell Function by the Beta Cell during Hypoglycemia in Wistar Rats." Diabetes.

VITAE

Lori Beth Hays was born in Corpus Christi, Texas, on October 18, 1974, the daughter of Melvin Ronald Shilling and Carol Elizabeth Shilling. After completing her work at Calallen High School, Corpus Christi, Texas in 1993, she entered Texas A&M University at College Station, Texas. During the summer of 1994 she attended DelMar College. She received the degree of Bachelor of Science with a major in molecular and cell biology from Texas A&M University in May, 1997. While at Texas A&M University, she taught supplemental instruction for introductory biology and biochemistry courses. From January 1996-June 1997 she was employed as a technician in the laboratory of Dr. James C. Hu, associate professor in biochemistry. In August 1997, she enrolled in the University of Texas Southwestern Medical Center in Dallas, Texas in the Graduate School of Biomedical Sciences. In 1997, she married Brian Christopher Hays of Coppell, Texas. Her son, Ryne Travis Hays, was born in 2002.

Permanent Address: 21828 Meridian Avenue South
Seattle, WA 98021